Cole's Bayou Marsh Hydrodynamic Modeling Report

LOUISIANA COASTAL PROTECTION AND RESTORATION AUTHORITY
P.O. BOX 44027
BATON ROUGE, LOUISIANA 70804-4027

Cole's Bayou Marsh Restoration Project (TV-63), Vermilion Parish, Louisiana
G.E.C., Inc. Contract No. 2503-12-21
December 2, 2014

DYNAMIC SOLUTIONS, LLC
450 LAUREL STREET, 1060 NORTH TOWER
BATON ROUGE, LA 70801

Table of Contents

LIST OF FIGURES II

LIST OF TABLES IV

EXECUTIVE SUMMARY 1

SECTION 1 INTRODUCTION 3

SECTION 2 DATA COLLECTION AND GAP ANALYSIS 6

2.1 Data Collection 6
2.2 System Characterization 30

SECTION 3 MODEL SETUP 37

3.1 Model Description 37
3.2 Model Domain 39
3.3 Calibration Period 40
3.4 Vermilion Bay Model 40
3.5 Cole's Bayou Marsh Model 49

SECTION 4 MODEL CALIBRATION AND RESULTS 62

4.1 Vermilion Bay 62
4.2 Cole's Bayou Marsh 75

SECTION 5 MODEL SCENARIOS 87

5.1 Scenario 1: Marsh Creation 87
5.2 Scenario 2: Marsh Creation with Culverts 96
5.3 Scenario 3A: Marsh Creation with Additional Culverts 107

SECTION 6 CONCLUSIONS 120

SECTION 7 REFERENCES 122

APPENDICES

Appendix A – Technical Memorandum for Cole's Bayou Data Mining and Gap Analysis
Appendix B – Installation of Data Collection Platforms for Cole's Bayou Marsh Restoration Project (TV-63)
Appendix C – Decommissioning Report for the Coastal Protection and Restoration Authority (CPRA) Cole's Bayou Marsh Restoration Project (TV-63)
Appendix D – Trip Report (April 24 -26, Frontal Event)
Appendix E – Trip Report (July 23 – 25, Summer Conditions)
Appendix F – Trip Report (October 5 - 7, Wind Event)

LIST OF FIGURES

Figure 1 – Cole's Bayou Marsh project area 4
Figure 2 – Regional map showing the Cole's Bayou Marsh and surrounding waters 5
Figure 3 – All survey data collected for the project 7
Figure 4 – Water level and salinity data collection stations 9
Figure 5 – Water level data for station TV63-01 10
Figure 6 – Water level data for station TV63-02 11
Figure 7 – Water level data for station TV63-03 12
Figure 8 – Water level data for station TV63-04 13
Figure 9 – Water level data for station TV63-05 14
Figure 10 – Water level data for station TV63-06 15
Figure 11 – Water level data for all stations 16
Figure 12 – Salinity data for station TV63-01 17
Figure 13 – Salinity data for station TV63-02 18
Figure 14 – Salinity data for station TV63-03 19
Figure 15 – Salinity data for station TV63-04 20
Figure 16 – Salinity data for station TV63-05 21
Figure 17 – Salinity data for station TV63-06 22
Figure 18 – Salinity data for all stations. 23
Figure 19 – Five levee breaches in the Oil Field Canals. 24
Figure 20 – Nutrient and bulk density sampling stations located within the project area 26
Figure 21 – Comparison of water levels at Cypremort Point, CRMS 0541, and TV63-03 32
Figure 22 – View of gap (breach) in the levee surrounding Cole's Bayou Marsh 33
Figure 23 – Typical view of a canal surrounding the Cole's Bayou Marsh 34
Figure 24 – Typical view of primary distributary channel in the marsh. 34
Figure 25 – Typical view of narrow, 8-foot wide, channel in the marsh 35
Figure 26 – Water levels in the Oil Field Canals and in Cole's Bayou Marsh 35
Figure 27 – Non-exceedence probability of water level at TV63-04 36
Figure 28 – Vermilion Bay model mesh 43
Figure 29 – Data stations and boundary conditions for the Vermilion Bay model 44
Figure 30 – Daily maximum and minimum water level for the Vermilion Bay model 46
Figure 31 – Salinity boundary conditions for the Vermilion Bay model 47
Figure 32 – DOQQ images of the project area in (a) 2005 and (b) 2008 50
Figure 33 – Cole's Bayou Marsh model mesh, showing location of Figure 34 in the inset 52
Figure 34 – Smaller scale view of the model mesh, highlighting elements in the Canals and marsh 53
Figure 35 – Detail of Marsh model mesh showing greater resolution in the marsh channel 54
Figure 36 – Location and data series used for boundary conditions of the Cole's Bayou Marsh model 56
Figure 37 – Daily minimum and maximum water levels for the Cole's Bayou Marsh 57
Figure 38 – Material types defined for the marsh model 59
Figure 39 – Cole's Bayou Marsh model calibration stations 61
Figure 40 – Water Level calibration at Cypremort Point 65
Figure 41 – Water Level calibration at Bayou Fearman 66
Figure 42 – Water Level calibration at CRMS0541 67
Figure 43 – Water Level calibration at TV63-03 68
Figure 44 – Water Level calibration at TV63-06 69
Figure 45 – Salinity calibration at Cypremort Point 70
Figure 46 – Salinity calibration at CRMS0541 71

Figure 47 – Salinity calibration at Bayou Fearman 72
Figure 48 – Salinity calibration at TV63-03 73
Figure 49 – Salinity calibration at TV63-06 74
Figure 50 – Stage calibration for station TV63-04, central open water area........ 76
Figure 51 – Stage calibration for station TV63-05, southern open water area 77
Figure 52 – Salinity calibration for station TV63-04, central open water area........ 78
Figure 53 – Salinity calibration for station TV63-05, southern open water area. 79
Figure 54 – Inundation percentages for the calibrated existing conditions model........ 81
Figure 55 – Average flow magnitude at each flow observation point........ 82
Figure 56 – Sensitivity test on model bathymetry 83
Figure 57 – Sensitivity analysis for channel roughness........ 84
Figure 58 – Sensitivity analysis for marsh roughness 85
Figure 59 – Water levels for the calibrated model and for the mesh convergence test 86
Figure 60 – Location of Marsh Creation Zones set to elevation of 1.3 feet (0.396 m), NAVD88 89
Figure 61 – Scenario 1 results for water level at points of interest (POI) in the Cole's Bayou Marsh........ 90
Figure 62 – Inundation percentages for Scenario 1........ 91
Figure 63 – Water levels at TV63-04 for Existing Conditions run and Scenario 1........ 92
Figure 64 – Water levels at TV63-05 for Existing Conditions run and Scenario 1........ 92
Figure 65 – Salinity at TV63-04 for Existing Conditions run and Scenario 1. 93
Figure 66 – Salinity at TV63-05 for Existing Conditions run and Scenario 1. 93
Figure 67 – Flow map for Scenario 1 showing average flow magnitud 94
Figure 68 – Flow map for Scenario 1 showing net flow........ 95
Figure 69 – Scenario 2 specifications including marsh creation areas and inlet and outlet culvert 97
Figure 70 – Discharge as a function of head difference across the culvert for a range of tailwater........ 98
Figure 71 – Discharge as a function of head difference for the inflow culverts (0.56 feet). 99
Figure 72 – Discharge as a function of head difference for the inflow culverts (0.22 feet). 99
Figure 73 – Scenario 2 water level results showing greater periods of inundation in marsh areas........ 101
Figure 74 – Inundation frequency over the entire domain for Scenario 2 102
Figure 75 – Water levels at TV63-04 for Existing Conditions, Scenario 1, and Scenario 2.. 103
Figure 76 – Water levels at TV63-05 for Existing Conditions, Scenario 1, and Scenario 2.. 103
Figure 77 – Salinity at TV63-04 for Existing Conditions run and Scenario 2. 104
Figure 78 – Salinity at TV63-05 for Existing Conditions run and Scenario 2. 104
Figure 79 – Net flow (cfs) and change in flow magnitude compared to Scenario 1. 106
Figure 80 – Scenario 3A specifications........ 108
Figure 81 – Discharge as a function of head difference across the culvert for a range of tailwater........ 109
Figure 82 – Discharge as a function of head difference for the inflow culverts (0.56 feet) 110
Figure 83 – Discharge as a function of head difference for each outflow culvert complex. 110
Figure 84 – Scenario 3A water level results........ 112
Figure 85 – Inundation frequency for Scenario 3A 113
Figure 86 – Water levels at TV63-04 for Existing Conditions, Scenarios 1, 2, and 3A 114
Figure 87 – Water levels at TV63-05 for Existing Conditions, Scenarios 1, 2, and 3A 115
Figure 88 – Water levels at CentW-Marsh for Existing Conditions, Scenarios 1, 2, and 3A 115
Figure 89 – Water levels at E-Marsh for Existing Conditions, Scenarios 1, 2, and 3A 116
Figure 90 – Water levels at SW-Marsh for Existing Conditions, Scenarios 1, 2, and 3A 116
Figure 91 – Salinity at TV63-04 for Existing Conditions run and Scenario 3A........ 117
Figure 92 – Salinity at TV63-05 for Existing Conditions run and Scenario 3A........ 117
Figure 93 – Flow magnitude (cfs) and change compared to Scenario 1. 119

LIST OF TABLES

Table 1 – Values for Total Nitrogen (mg/L) samples 25
Table 2 – Values for Total Phosphorus (mg/L) samples 25
Table 3 – TSS data (mg/L) collected for the April 24 frontal passage event 28
Table 4 – TSS data (mg/L) collected for the July 13 ambient conditions event 29
Table 5 – TSS data (mg/L) collected for the October 5 wind event, Tropical Storm Karen 30
Table 6 – Data station information for those used in the Vermilion Bay model 43
Table 7 – Model parameters for each material type 58
Table 8 – Summary of Vermilion Bay Model calibration results 62
Table 9 – Summary of Cole's Bayou Marsh model calibration results 75
Table 10 – URV parameters for marsh roughness sensitivity test 84
Table 11 – Water level comparison for Scenario 1 and Scenario 2 100
Table 12 – Comparison of flows for Scenario 1 and Scenario 2 105
Table 13 – Water level comparison for Scenario 1, Scenario 2, and Scenario 3A 111
Table 14 – Comparison of flows for Scenario 1, Scenario 2, and Scenario 3A 118
Table 15 – Average inflow, outflow, and net flow for the Cole's Bayou Marsh 120

EXECUTIVE SUMMARY

The Cole's Bayou Marsh Restoration site is located on the Gulf Coast of Louisiana in Vermilion Parish within the Teche/Vermilion Basin, immediately east of Freshwater Bayou Canal. Wetlands in Cole's Bayou are undergoing land loss at -0.42% per year based on 1983 to 2011 USGS data. The specific goals of the project are: 1) create 365 acres of brackish marsh in recently formed shallow open water; 2) nourish 53 acres of existing brackish marsh; and 3) increase freshwater and sediment inflow into interior wetlands by improving project area hydrology. In order to accomplish these objectives a hydrodynamic model of Cole's Bayou and the surrounding waters was created to understand water level, flow, and salinity transport in the system and be able to test how modifications to the system will affect hydrodynamics within the marsh.

Cole's Bayou Marsh is surrounded by a low levee which largely isolates its waters from those surrounding it at normal water levels. It is connected to the outlying waters via six primary gaps in the levee in the Oil Field Canals and one primary opening to the McIlheny Canal in the southeast portion of the marsh. The majority of flow into and out of the marsh is through the breaches in the north. Many of these breaches directly connect to the network of distributary marsh channels which exist in the marsh. These channels are between 20 and 75 feet wide, evident in aerial photographs, and carry much of the flow in the marsh at low water levels. Numerous smaller channels exist; some natural and some caused by pipelines or preferential airboat tracks.

The Adaptive Hydraulics Model (ADH) software was recommended as the hydrodynamic modeling software best suited for the Cole's Bayou Marsh Restoration project because of its ability to handle complex and intricate domains, efficiently handle wetting and drying, and simulate flow through hydraulic structures. A nested modeling approach was utilized. A large-scale hydrodynamic model (the Vermilion Bay Model) was developed to simulate the hydrodynamics in the waters of Freshwater Bayou, Little Vermilion Bay, and Vermilion Bay which surround the Cole's Bayou project area. The large-scale model was used to provide boundary conditions for a higher resolution model of the Cole's Bayou Marsh (the Cole's Bayou Marsh Model) which was developed to simulate finer-scale processes in the project area.

The calibration period encompassed the period of data collection, from April 6 to October 21, 2014. Bathymetric, water level, salinity, and sediment data were collected in the vicinity of the Cole's Bayou Marsh to support development of the hydrodynamic model. The average elevation of the marsh is currently 0.95 ± 0.1 feet (0.29 m). This elevation does not vary greatly with the exception of some high ground at the perimeter of the marsh. The median water level in the center of the marsh is 0.85 feet. Bathymetric data collected for this project were merged with publicly available data from NOAA and rectified with aerial photography to create the most realistic elevation data possible from which to develop the model meshes. Boundary conditions were developed from USGS, CRMS, NOAA, and data collection stations deployed as part of this study. All elevation and water level data was rectified to the NAVD88 datum.

The large-scale Vermilion Bay model was calibrated at five stations with RMS values for water level ranging from 0.09 to 0.31 feet and relative RMS values from 2 to 7%. Salinity RMS values ranged from 1.6 to 4.0 with relative RMS values from 10 to 37%. The Cole's Bayou Marsh model was calibrated at two stations, TV63-04 in the center of the marsh and TV63-05 in the southern part of the marsh. RMS values for water level were 0.14 and 0.19 feet and relative RMS values 6 and 11%, respectively. Salinity RMS values were 0.5 and 0.6 ppt and relative RMS values 7 and 11%, respectively. Relative flow magnitudes within the Cole's Bayou Marsh model are in accordance with those observed during field operations. Model calibration can be considered very good. Testing was performed to ensure the robustness of models to variances in elevation and roughness.

The calibrated model was run for three scenarios so modifications to the calibrated model representing future conditions could be tested to see how hydrodynamics within and around the Cole's Bayou Marsh are affected. These changes included the increase of elevation in marsh creation areas due to the introduction of sediments, closing gaps in the perimeter levee, and placing one-way flap-gated culverts at various locations in the system. The scenarios analyzed were designed by CPRA and NOAA staff and modeled by DSLLC staff. Changes in water level, flow, and salinity within the Cole's Bayou Marsh were analyzed and results are contained herein.

Together the hydrodynamic models are valuable tools to support the Coles Bayou Marsh Restoration Project and other hydrodynamic, water quality, ecological, or shoreline protection studies in and around Vermilion Bay. The Cole's Bayou model provides a representative tool for simulating the physical processes in the system and provides vital insights to the inundation and circulation patterns of water within the marsh. It also allows scientists, engineers and managers to determine the flow and salinity impacts from planned changes to the system as part of marsh restoration efforts.

SECTION 1 INTRODUCTION

The Cole's Bayou Marsh Restoration site is located on the Gulf Coast of Louisiana in Vermilion Parish within the Teche/Vermilion Basin, immediately east of Freshwater Bayou Canal (**Figure 1** and **Figure 2**). Wetlands in Cole's Bayou are undergoing land loss at -0.42% per year based on 1983 to 2011 USGS data from the extended boundary. Wetland loss processes in this area include subsidence, sediment deficit, interior ponding and pond enlargement, and storm impacts resulting in rapid episodic losses. Additionally, significant interior marsh loss has resulted from salt water intrusion and hydrologic changes associated with increasing tidal influence. As hydrology in this area has been modified, habitats have shifted to more of a floatant marsh type, resulting in increased vulnerability to tidal energy and storm damages. Habitat shifts and hydrologic stress reduce marsh productivity, a critical component of vertical accretion in wetlands.

The specific goals of the project are: 1) create 365 acres of brackish marsh in recently formed shallow open water; 2) nourish 53 acres of existing brackish marsh; and 3) increase freshwater and sediment inflow into interior wetlands by improving project area hydrology.

In order to accomplish these objectives a hydrodynamic model of Cole's Bayou and the surrounding waters was created to understand water level, flow, and salinity transport in the system and be able to test how modifications to the system will affect hydrodynamics within the marsh. The scenarios will enable engineers and managers to make appropriate changes to the system to accomplish the stated goals of hydrologic and marsh restoration.

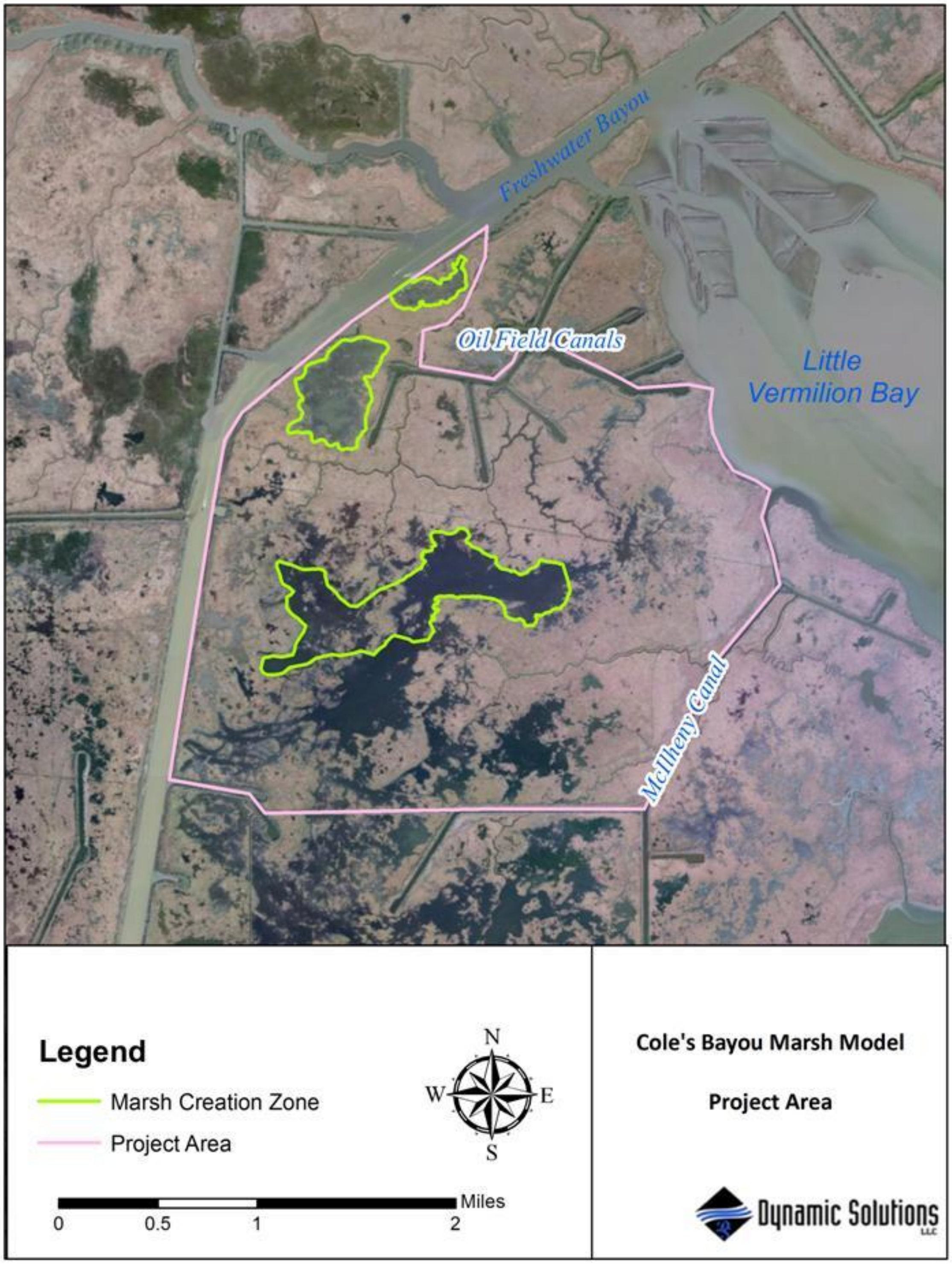

Figure 1 – Cole's Bayou Marsh project area

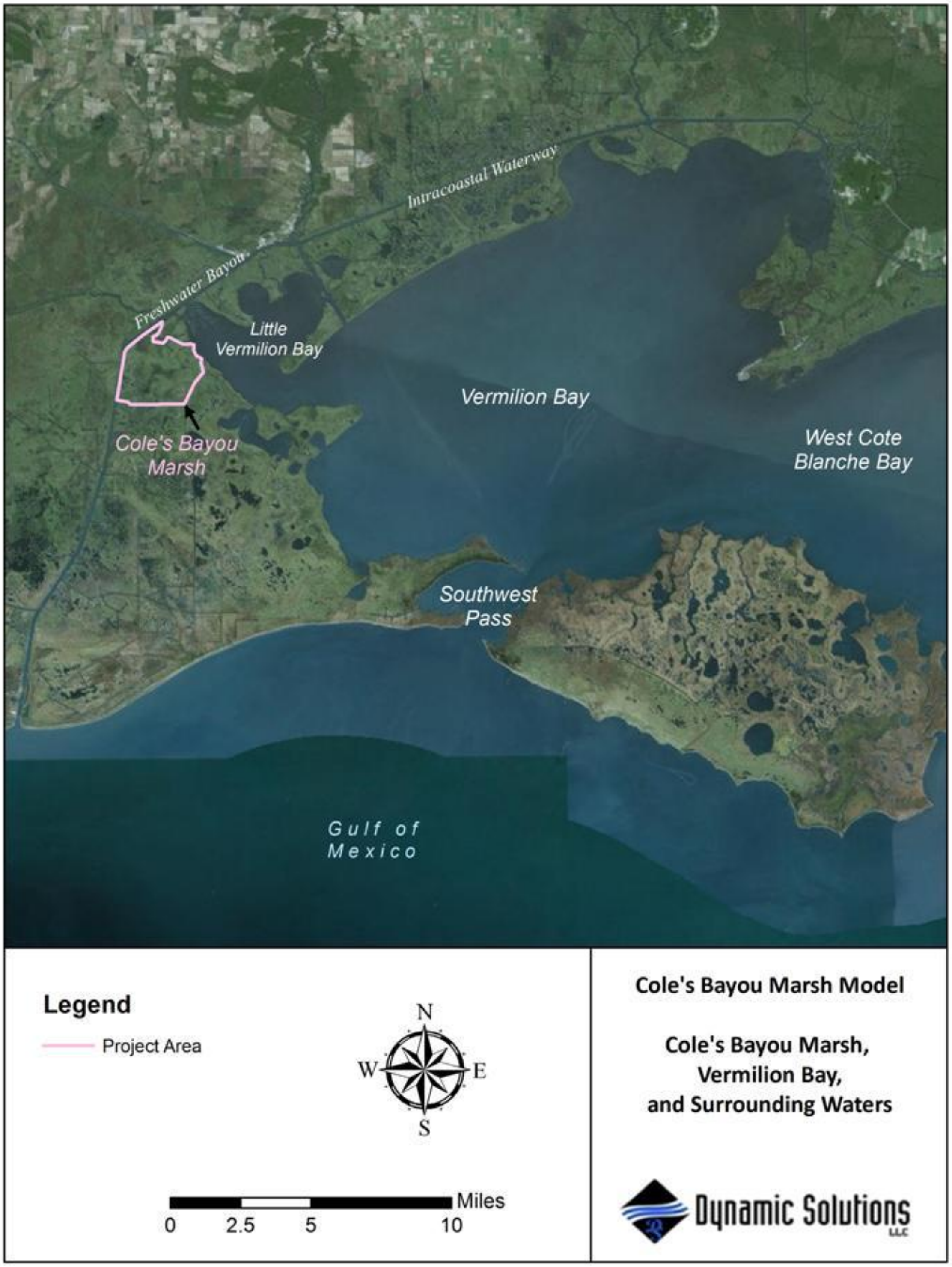

Figure 2 – Regional map showing the Cole's Bayou Marsh and surrounding waters

SECTION 2 DATA COLLECTION AND GAP ANALYSIS

Prior to conducting the modeling study, a "Data Mining and Gap Analysis" was conducted to:

- Identify available water level, salinity, sediment, and nutrient data within the area of interest,
- Recommend a hydrodynamic modeling tool for the project,
- Identify the gaps in available data, and
- Describe the type and location of additional data necessary to support the hydrodynamic modeling effort.

Additionally, the ADaptive Hydraulics Model (ADH) was selected as the appropriate tool for this modeling study.

The "Data Collection and Gap Analysis" report has been placed in **Appendix A**. Some figures and text will be duplicated in the body of this report for ease of review.

2.1 Data Collection

2.1.1 Survey Data

DSLLC worked with CPRA staff to generate locations for survey data collection. The main areas of interest were the Oil Field Canals, McIlheny Canal, major channels within the marsh, and the main open water areas within the marsh. These initial surveys were completed between 3/25 and 5/1/13. HydroTerra Technologies, LLC collected all survey data. It was conveyed in coordinates of Louisiana State Plane, Southern Zone, in feet with a vertical datum of NAVD88. For use in mapping and modeling purposes all survey data was converted to UTM Zone 15, meters, vertical datum of NAVD88.

After beginning work on the large-scale Vermilion Bay model it was determined that additional bathymetry in the areas responsible for most flow through Little Vermilion Bay into the Oil Field Canals was necessary. These areas were surveyed on 5/13 and 5/16/2013.

The boundary survey of the Cole's Bayou Marsh was completed by HydroTerra on 9/6/13. The Cole's Bayou Marsh has a perimeter levee which largely prohibits the exchange of water from the surrounding waters into and out of the marsh. This survey identified gaps in the levee where significant exchange of surface water exists.

After beginning work on the small-scale Cole's Bayou Marsh model, a need for additional surveys of network of distributary channels within the marsh was identified. DSLLC Staff accompanied HydroTerra staff to the field and performed additional surveys and flow measurements in the major marsh channels. Top of marsh elevations were also taken at representative locations. Figure 3 shows the entirety of the data collection effort.

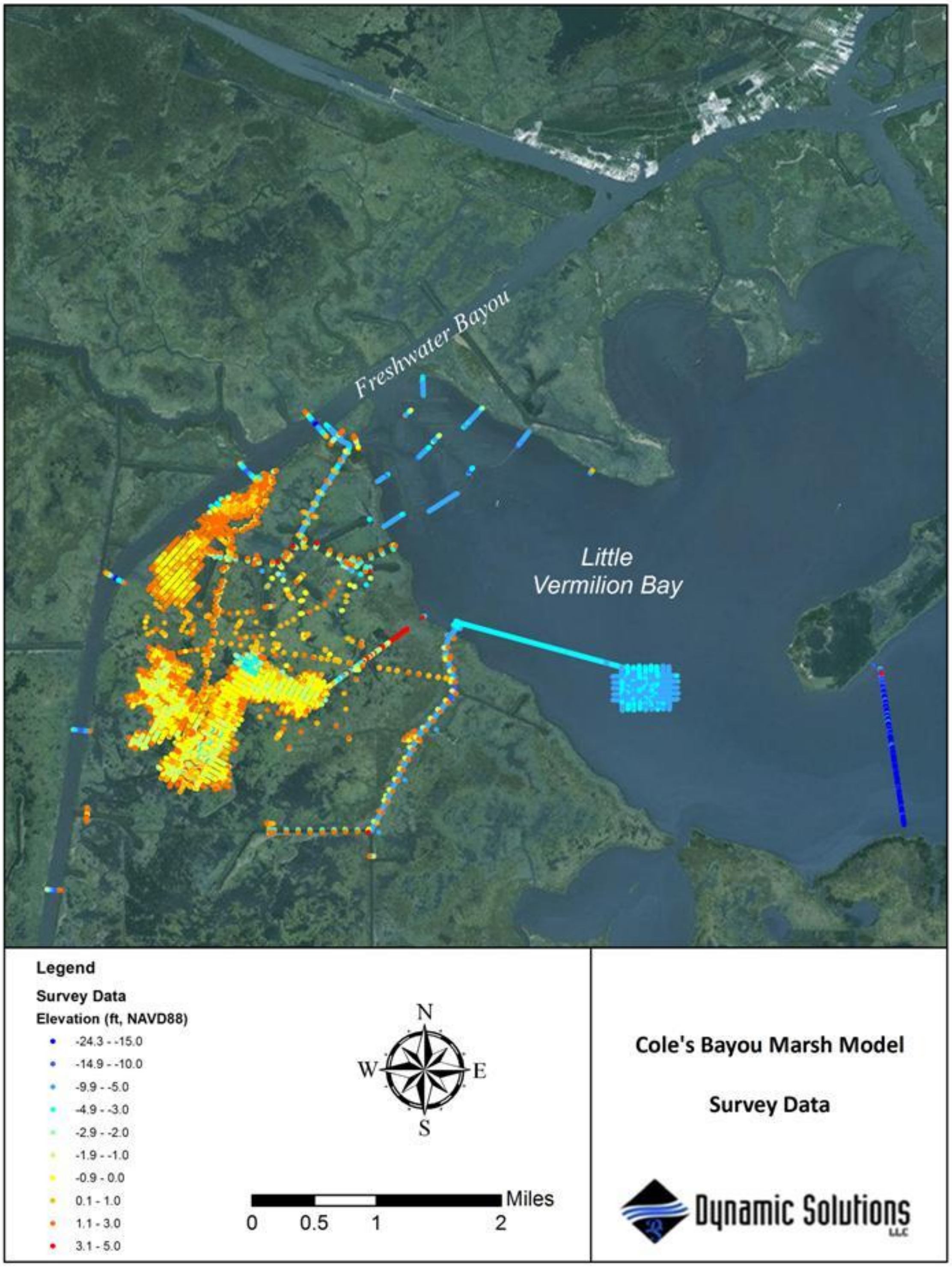

Figure 3 – All survey data collected for the project

2.1.2 Water Level/Salinity

As set forth in the "Data Mining and Gap Analysis" report, six data stations were installed by ENCOS to collect continuous, hourly, water level and salinity values (**Figure 4**). Each station was surveyed to the NAVD88 vertical datum used by HydroTerra throughout the bathymetric surveys. The stations collected data between 4/5/13 and 10/24/13. The installation report submitted by ENCOS is contained in **Appendix B**.

Stations were visited each month to download data, perform maintenance, and check the calibration. Salinity is measured in specific conductance and converted to parts per thousand. When the difference between the dirty specific conductivity readings from the calibrated instrument and the dirty water-quality sonde readings are less than the 5% threshold, data are not shifted. If the difference is greater than 5% a linear shift is applied to the raw data. The corrected (shifted) data was used in the model. The Decommissioning report is contained in **Appendix C**. **Figure 5** through **Figure 10** show the water level data for each station and **Figure 11** shows all stations on the same chart. **Figure 12** through **Figure 17** show the shifted salinity data for each station and **Figure 18** shows all stations on the same chart.

2.1.3 Flow Data

During the December field visit, DSLLC staff took flow measurements at each levee breach site, and where each channel connects to the central open water area in an effort to better understand the magnitude of flow in the major marsh distributary channels. The data taken, and more importantly the observations made, regarding flow, flow direction, and the connectivity of open waters and channels were critically important to visually validate marsh model function.

On December 5 during a rising tide, flow measurements at the five levee breaches in the Oil Field Canals were measured between 9:00 am and 10:15 am. The magnitude of the flows ranged from zero to 68 cfs (shown on **Figure 19**) and water surface elevations at location ranged from 0.45 to 0.65 feet. On December 6, between 9:00 am and 11:00 am during a rising tide with higher water levels as the result of an incoming storm, flow measurements were taken in the interior of the marsh where the major distributary channels connect with the central open water area and at the southeastern levee breach/culvert. Water level at the eastern most breach in the oil field canals at 7:54 am was 1.15 feet. Water levels at the perimeter of the central open water area ranged from 0.82 to 0.96 feet. Discharges into the central open water area ranged from 5 to 84 cfs (shown on Figure 19). Water flowed out of the culvert/breach system in the southeast corner of the marsh at a rate of 45 cfs.

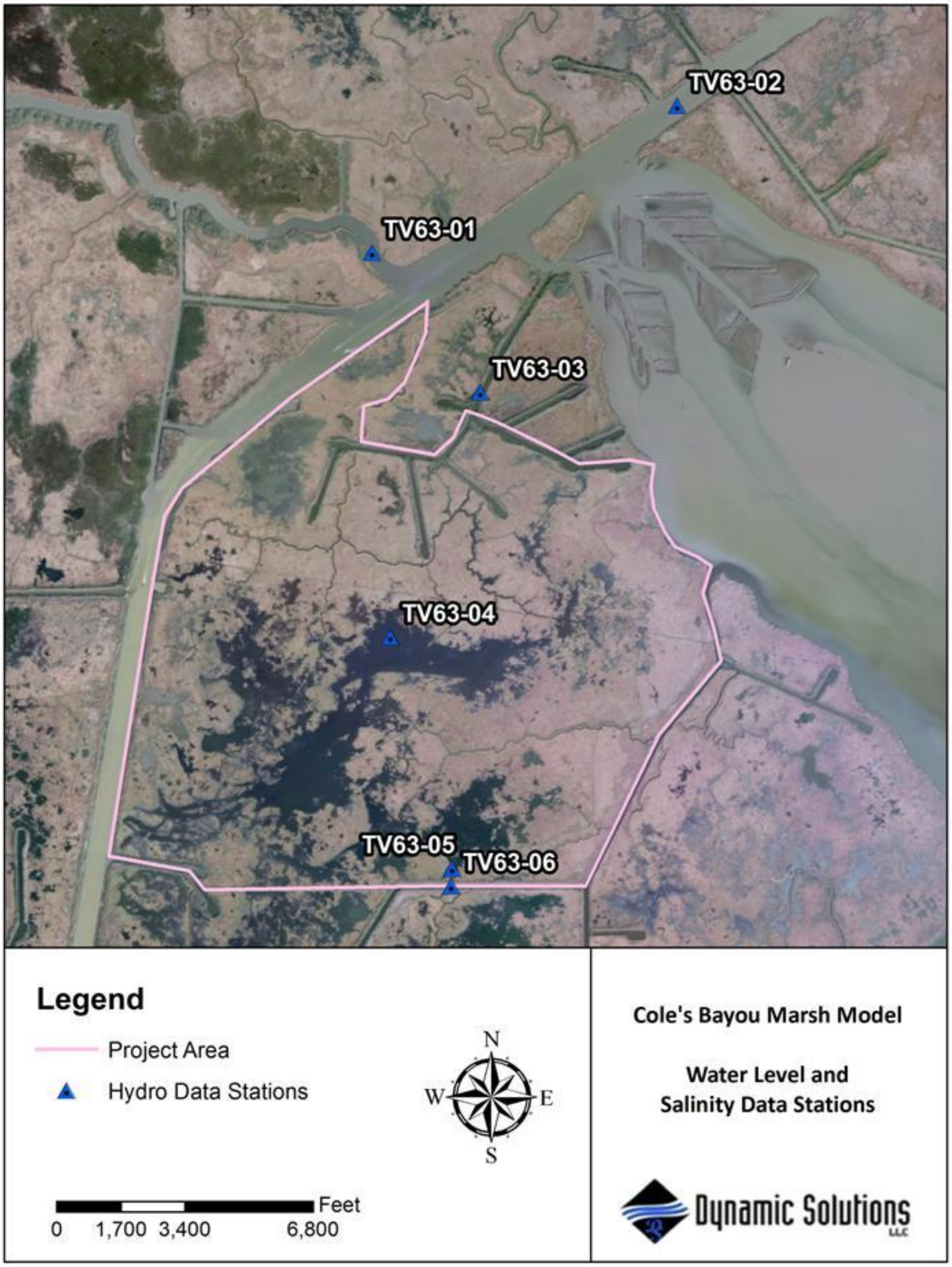

Figure 4 – Water level and salinity data collection stations

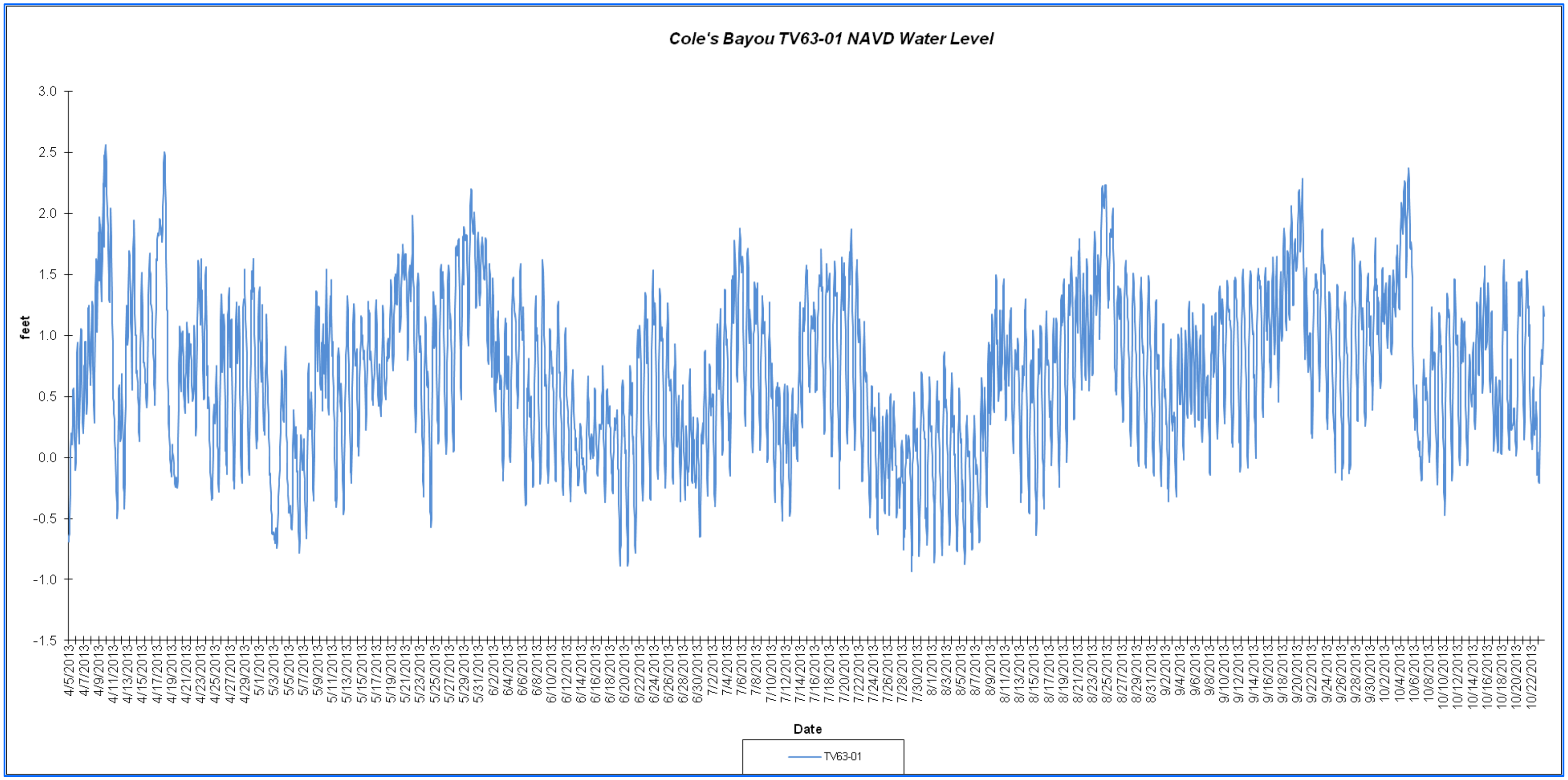

Figure 5 – Water level data for station TV63-01

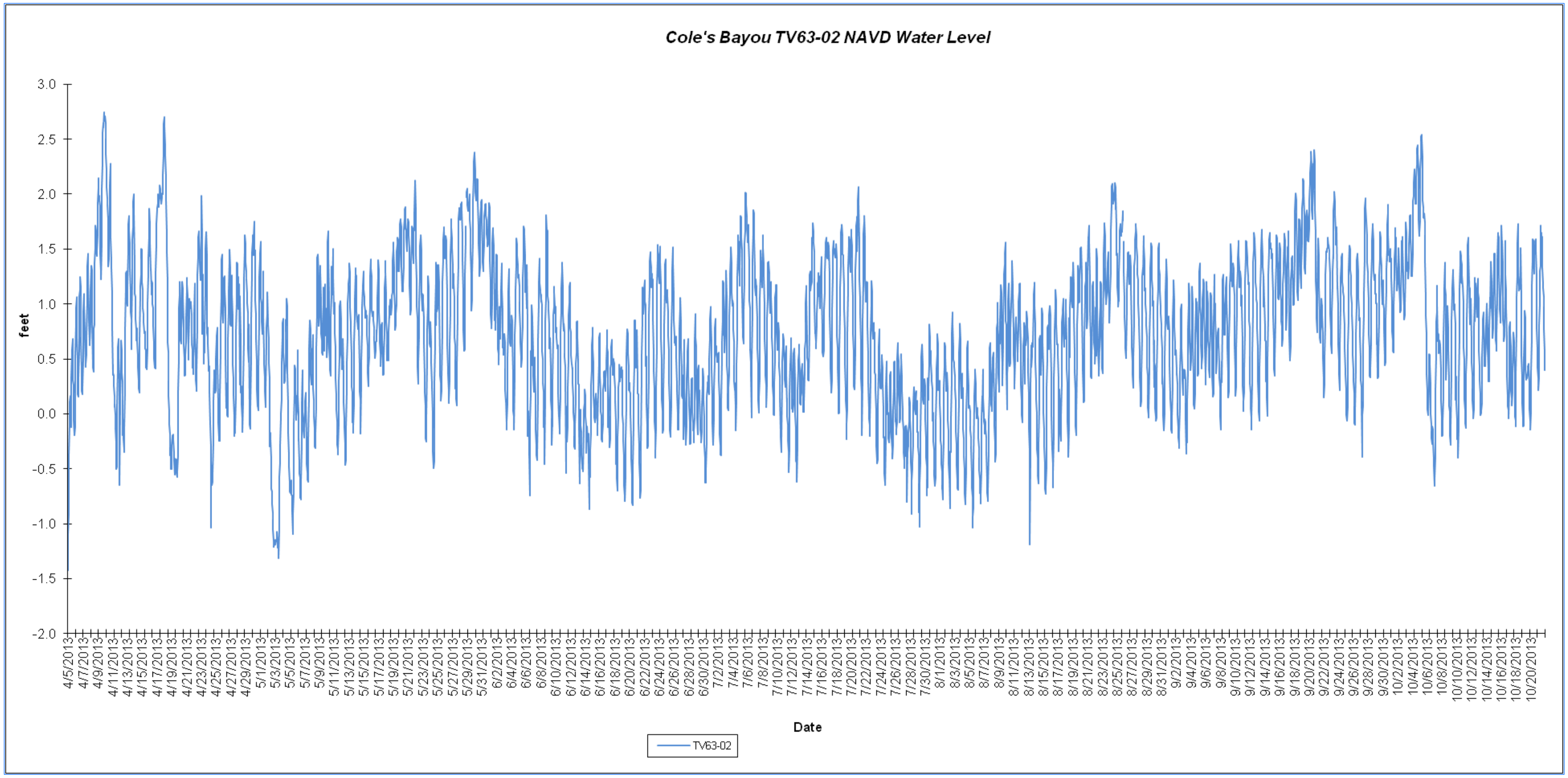

Figure 6 – Water level data for station TV63-02

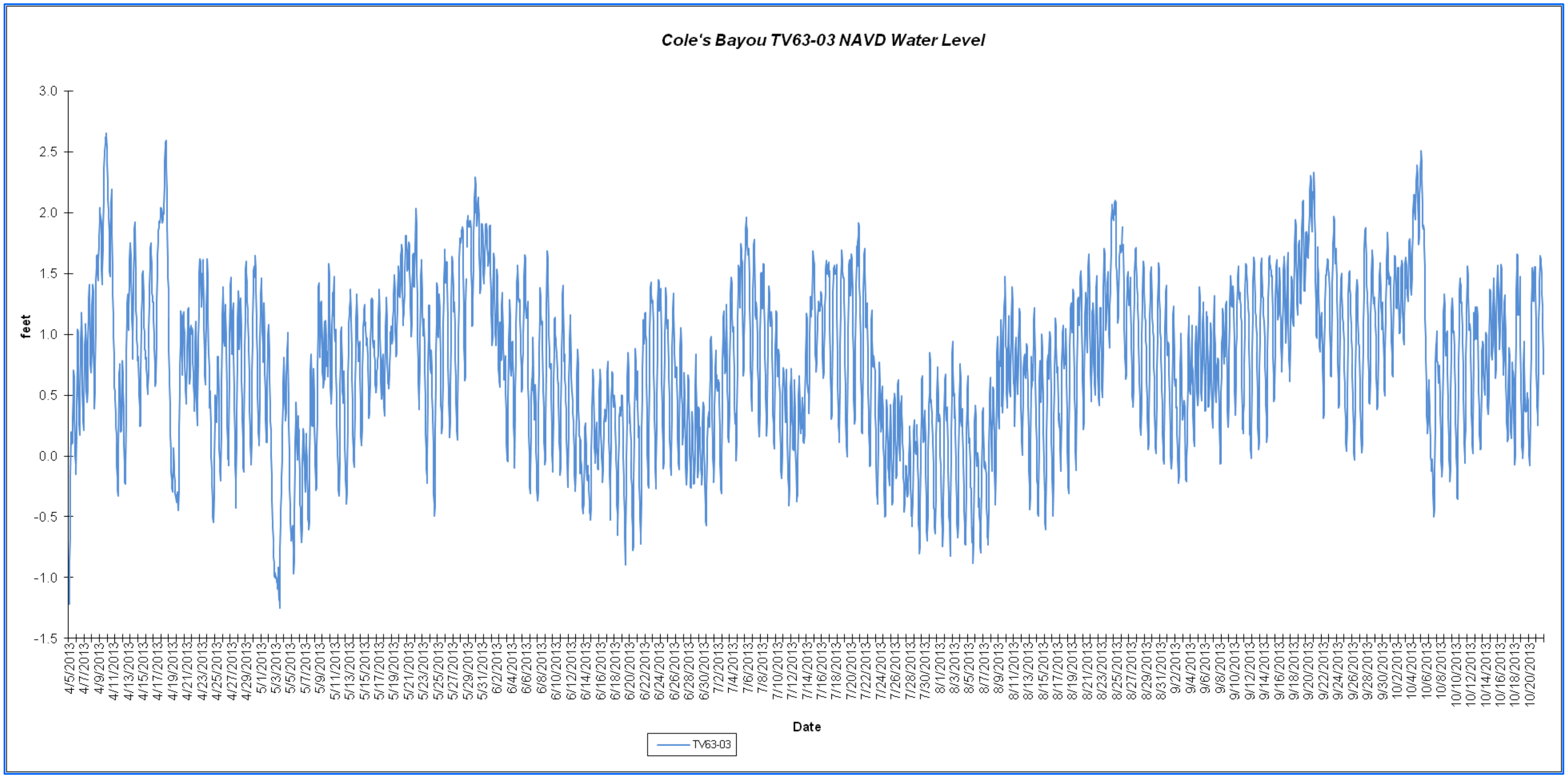

Figure 7 – Water level data for station TV63-03

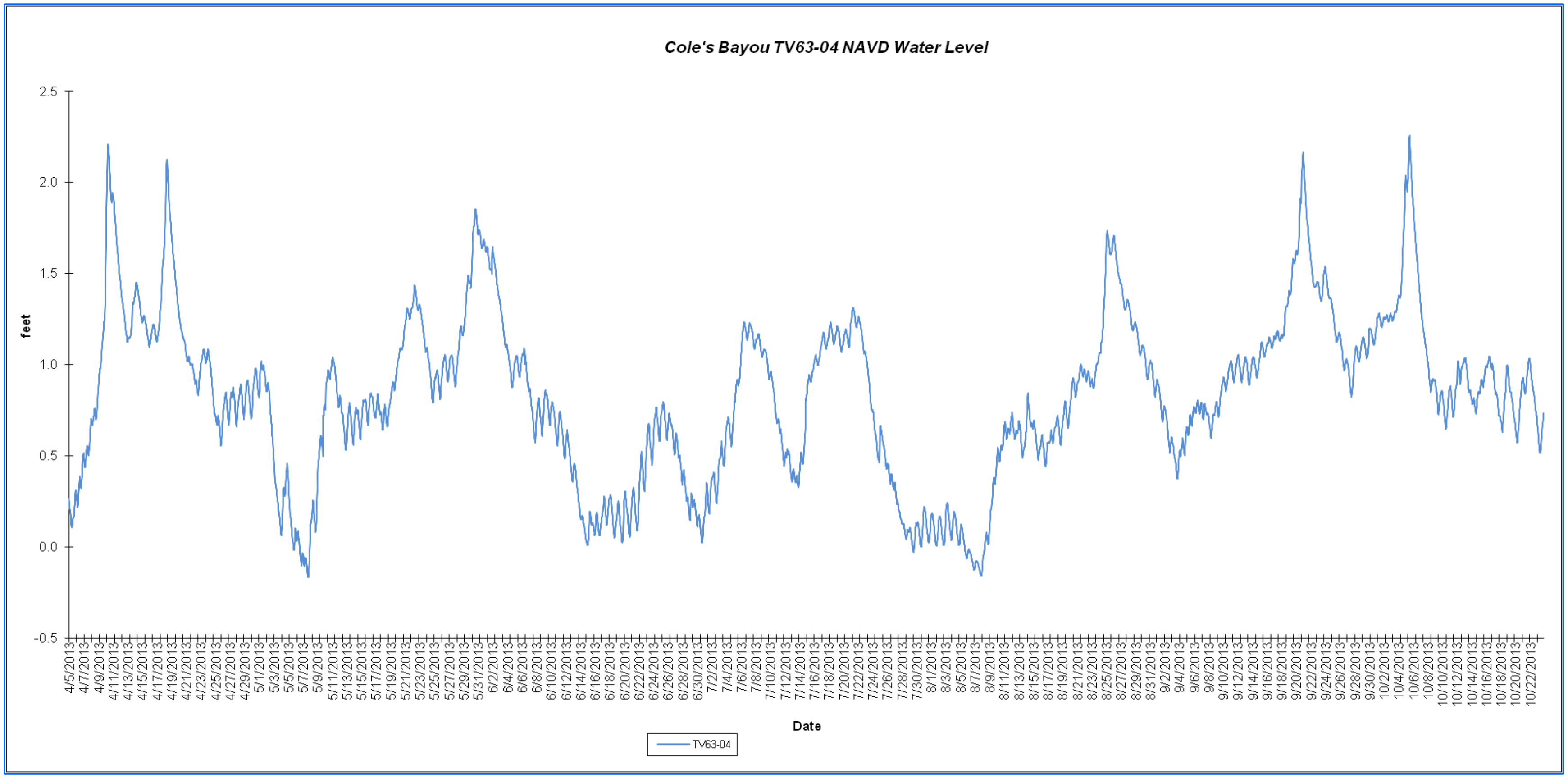

Figure 8 – Water level data for station TV63-04

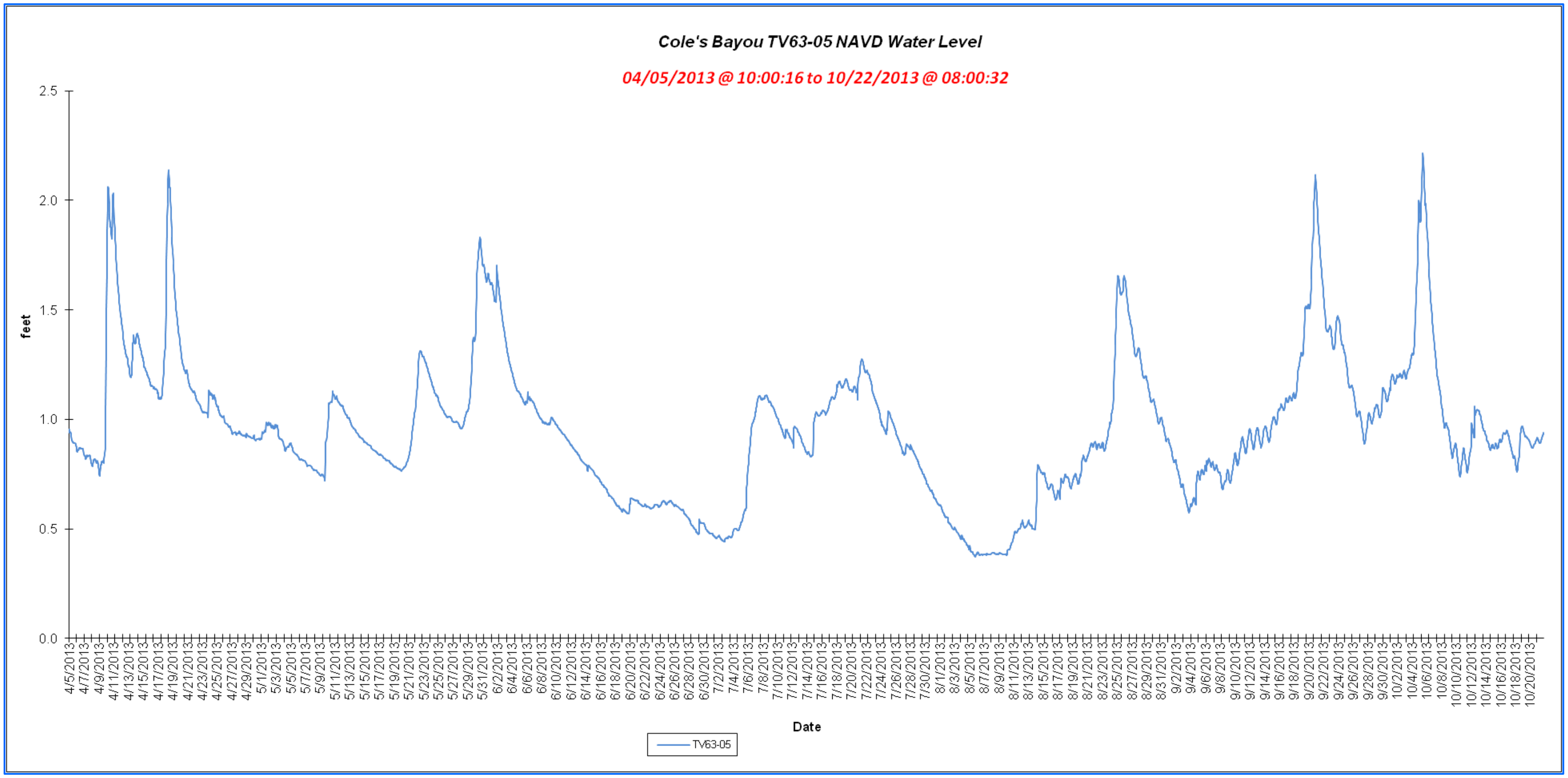

Figure 9 – Water level data for station TV63-05

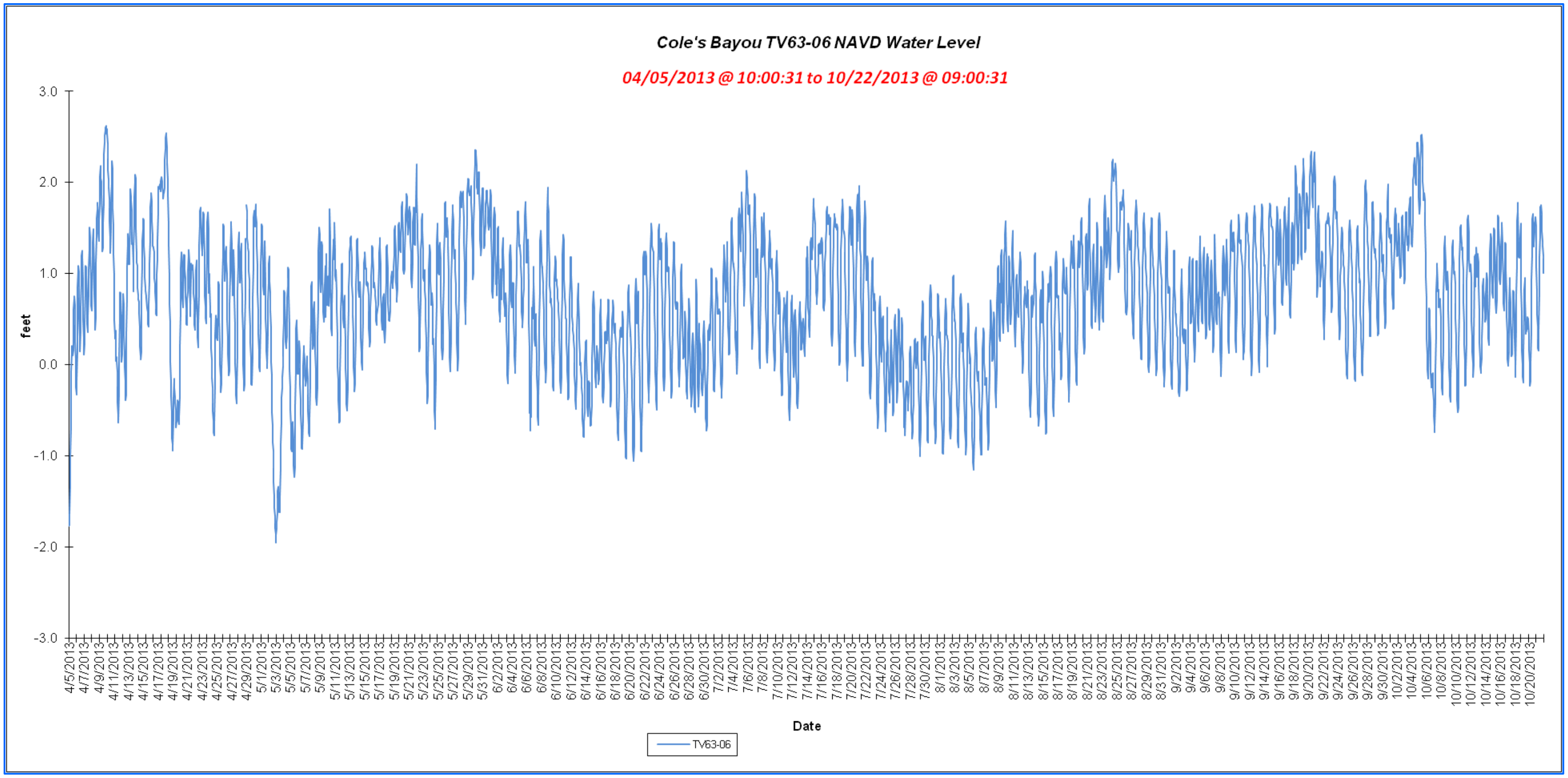

Figure 10 – Water level data for station TV63-06

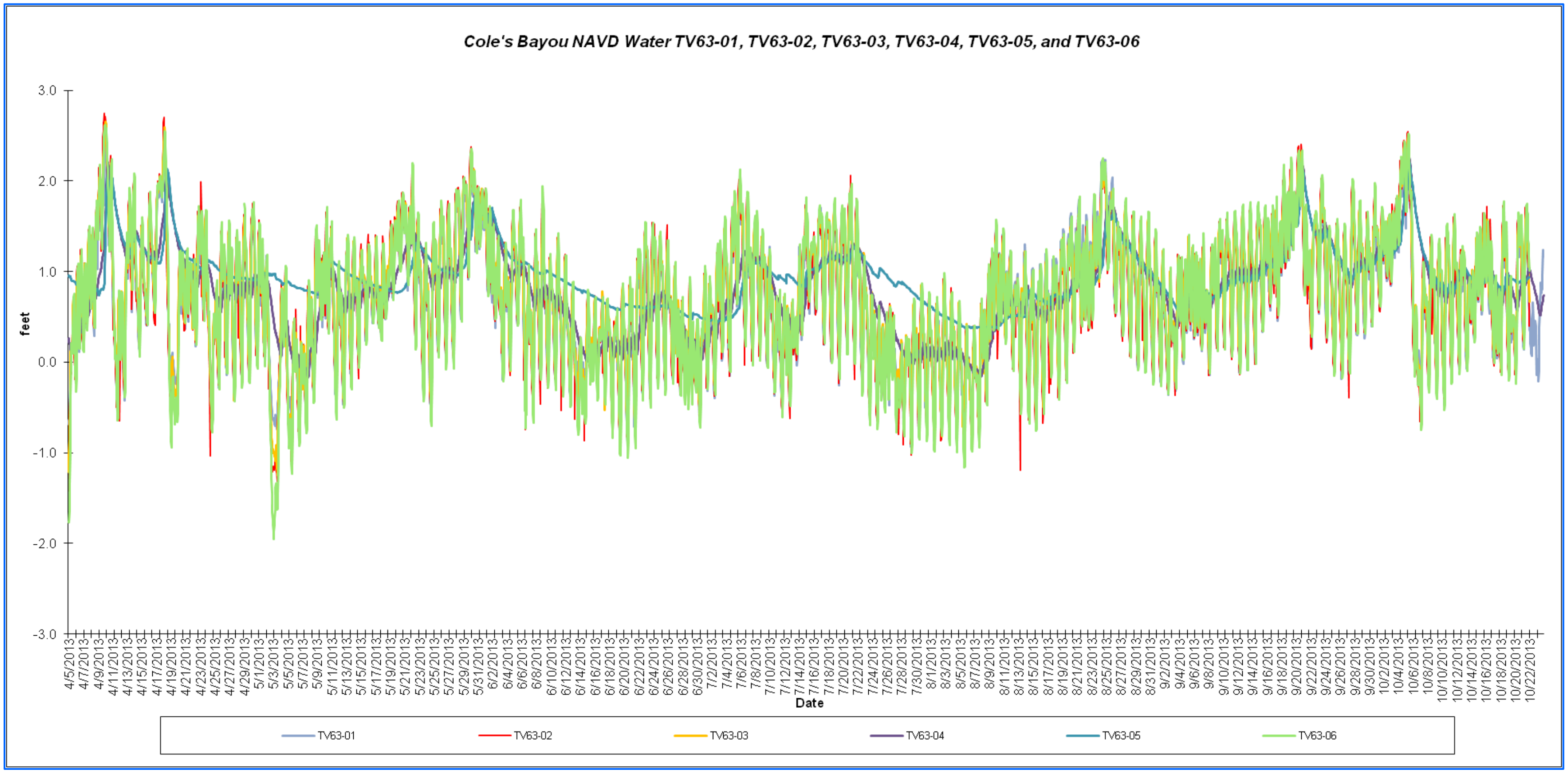

Figure 11 – Water level data for all stations

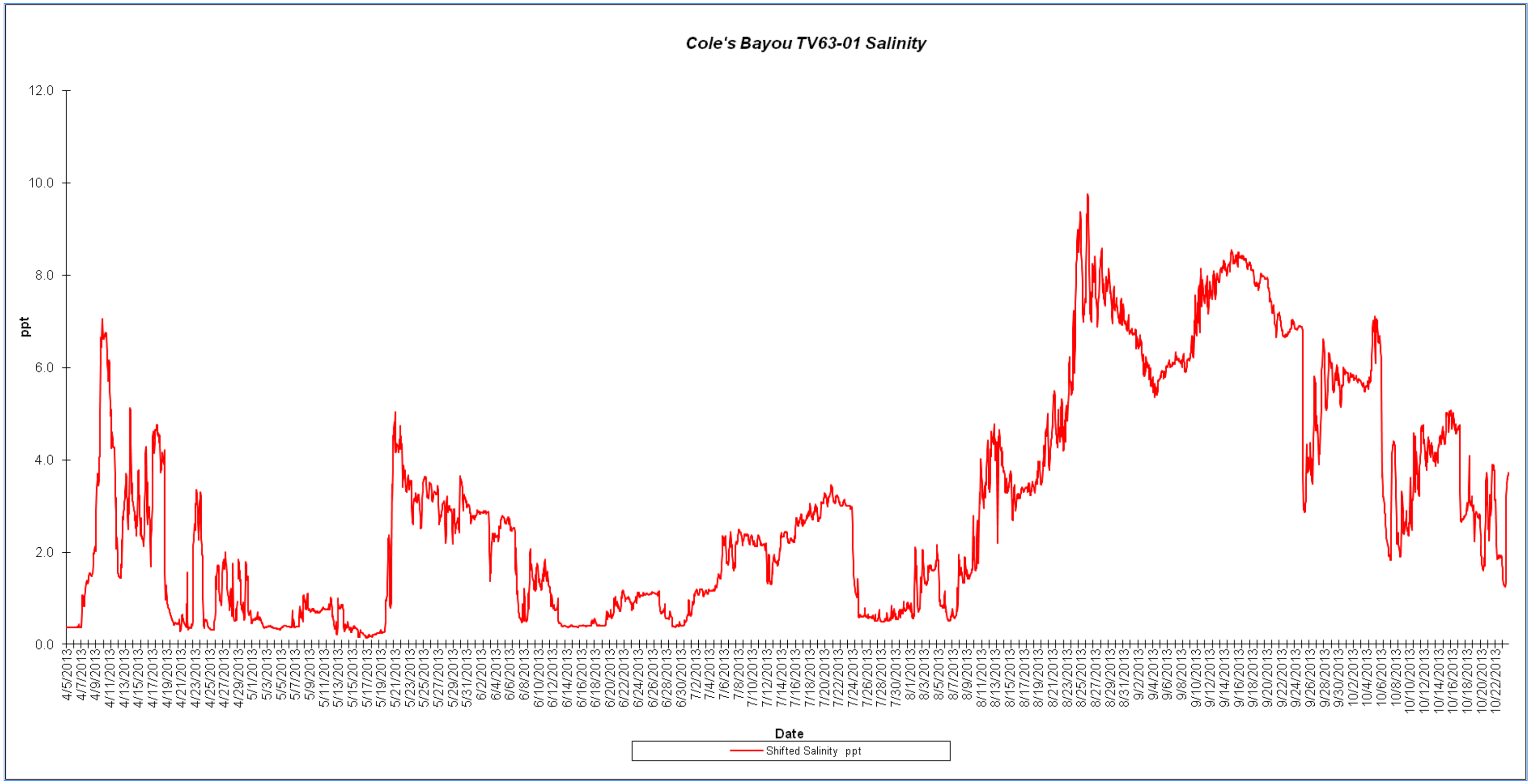

Figure 12 – Salinity data for station TV63-01

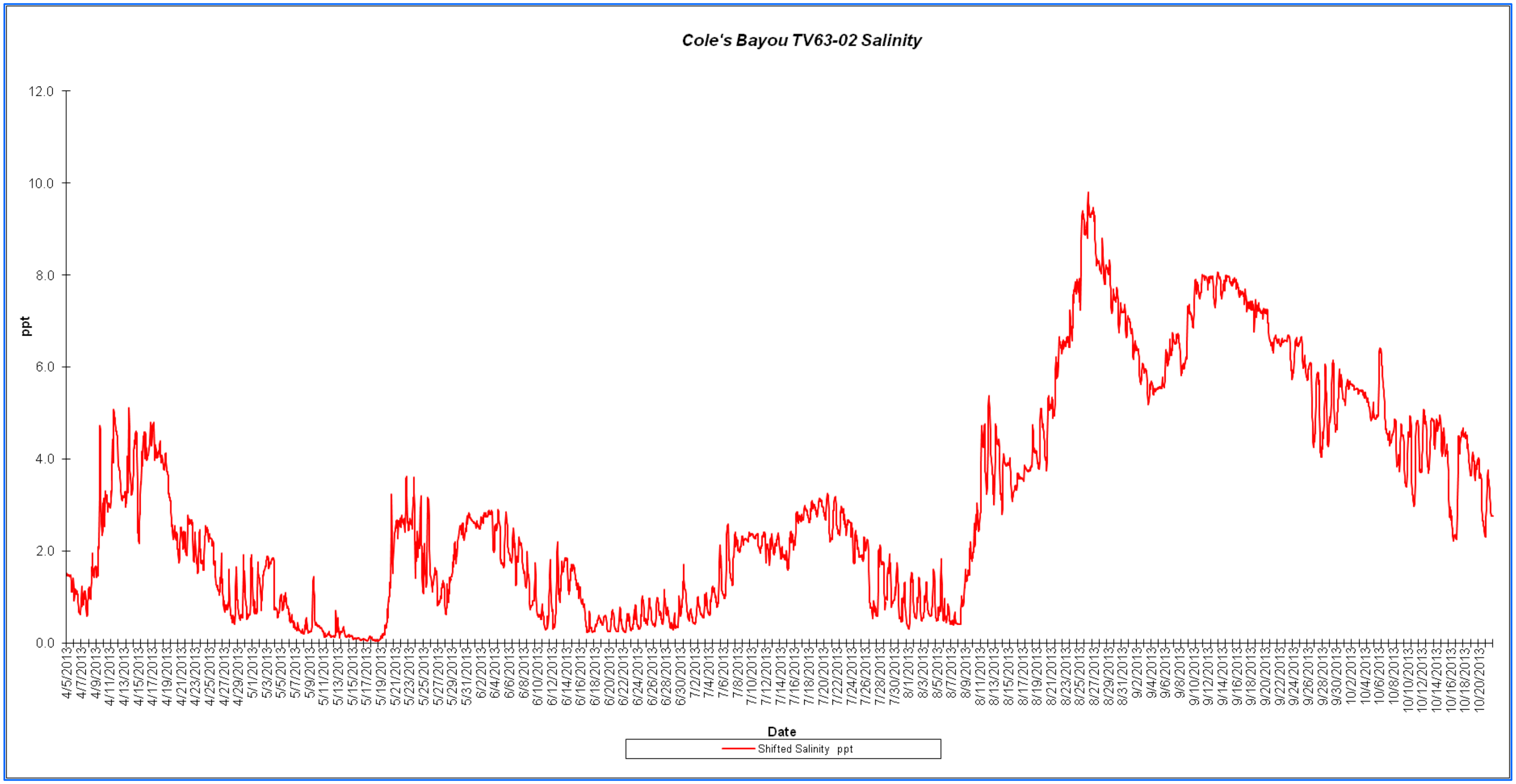

Figure 13 – Salinity data for station TV63-02

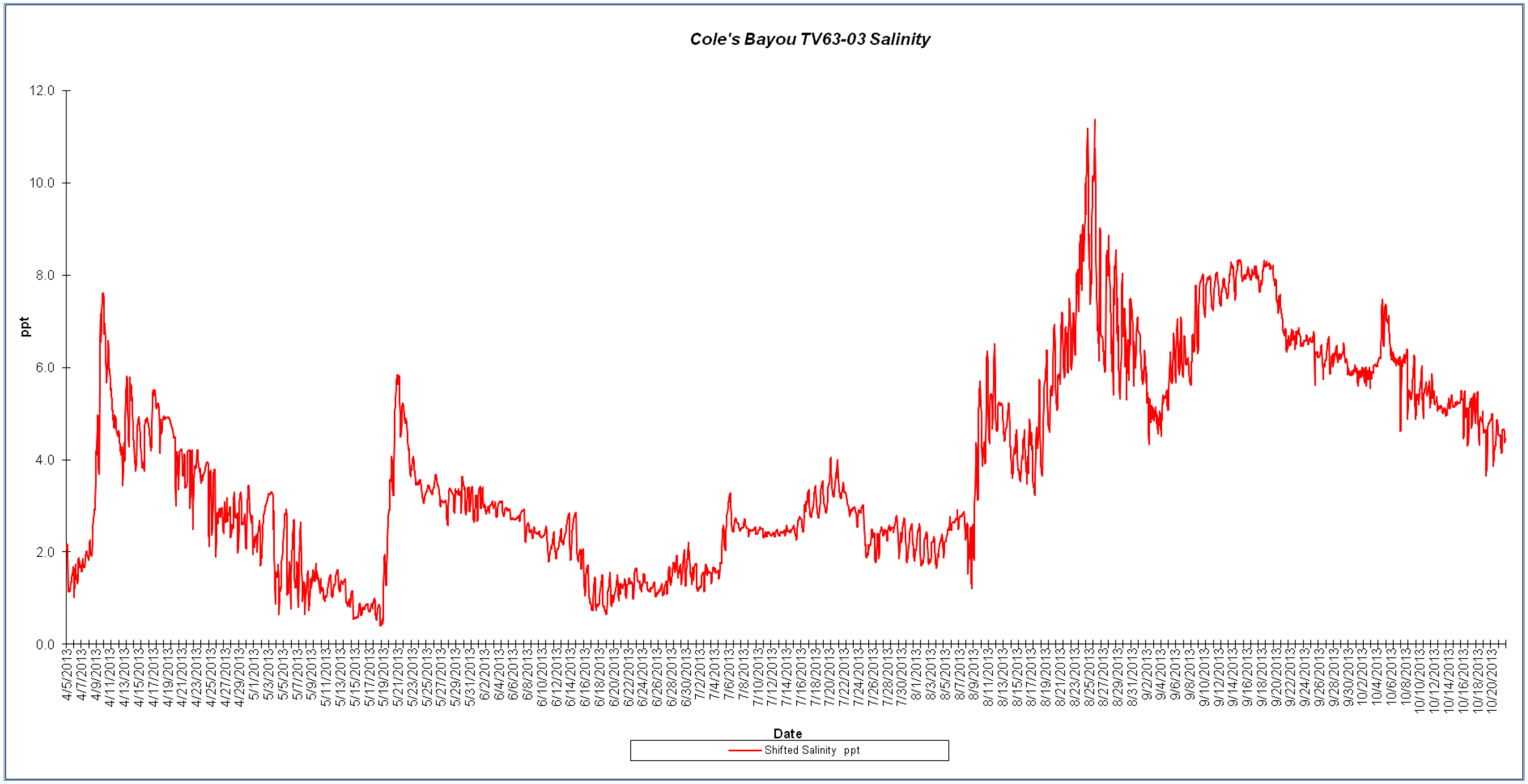

Figure 14 – Salinity data for station TV63-03

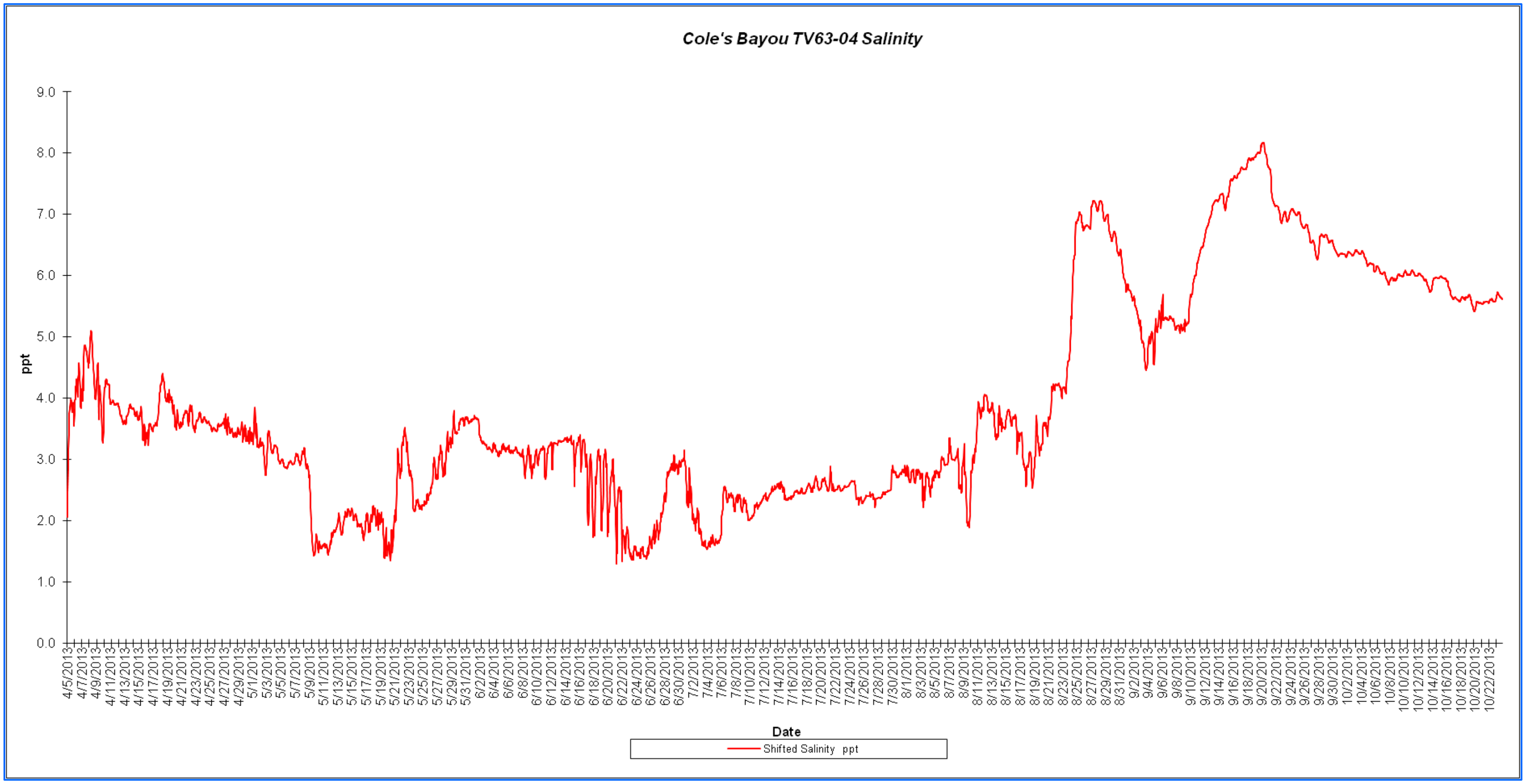

Figure 15 – Salinity data for station TV63-04

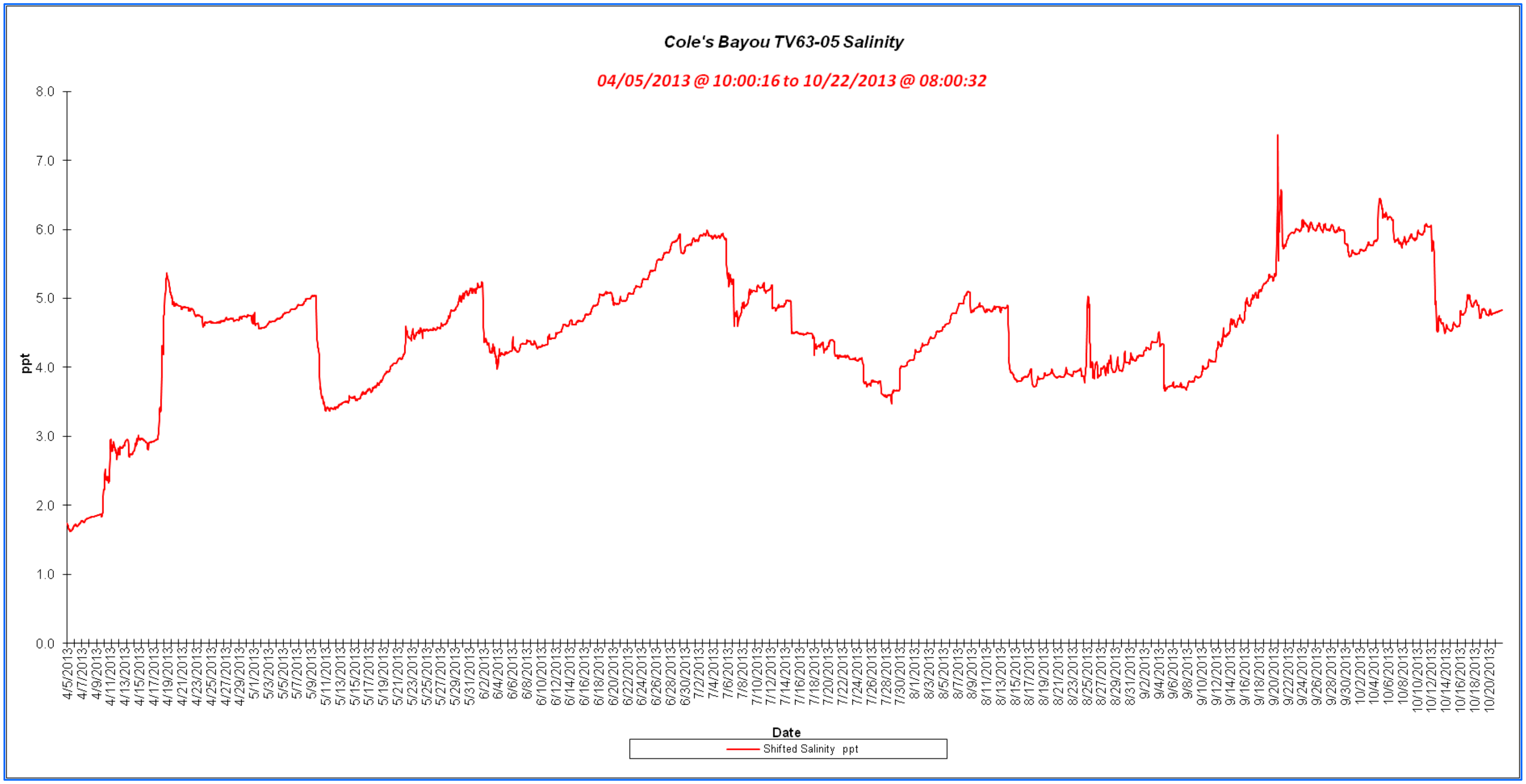

Figure 16 – Salinity data for station TV63-05

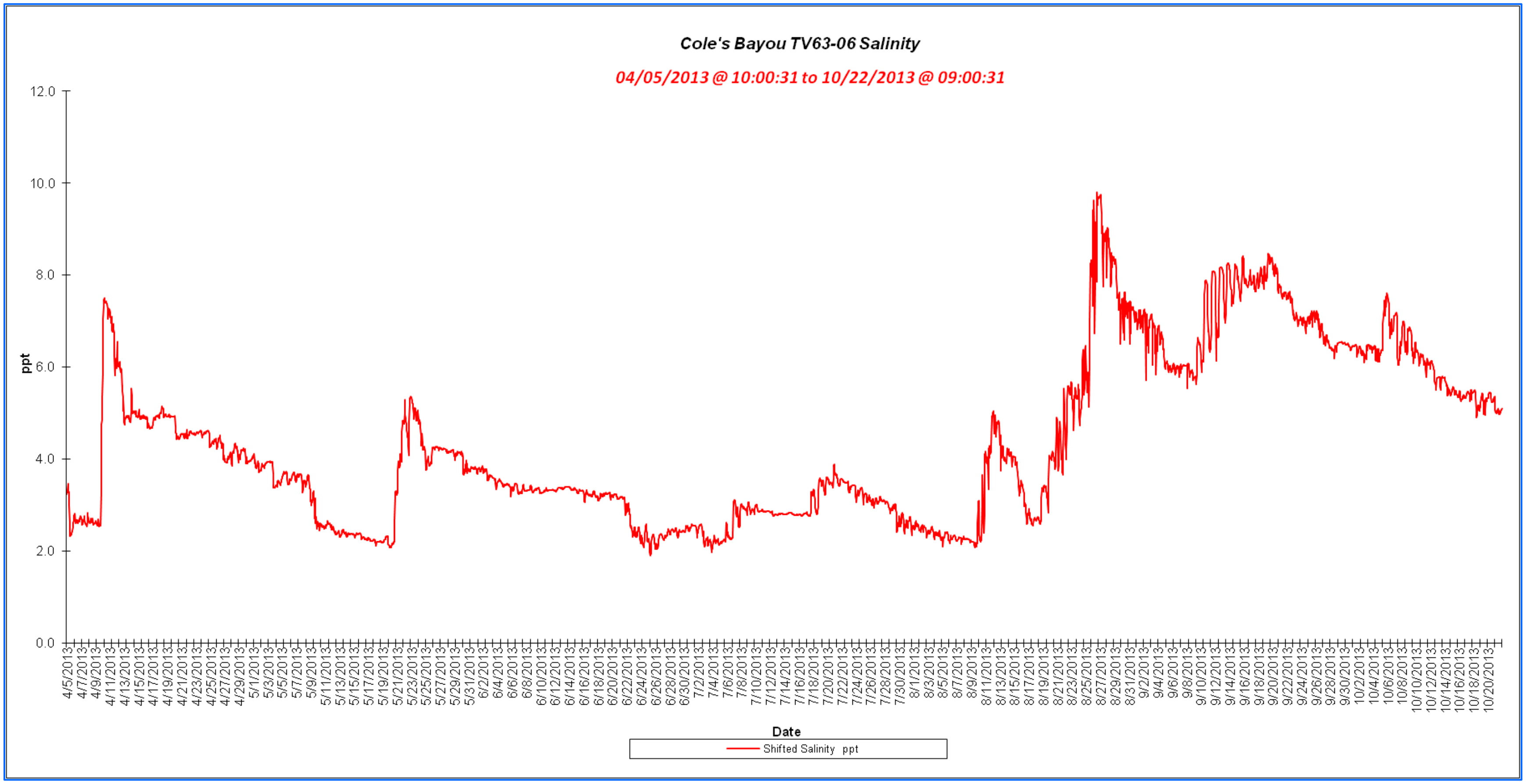

Figure 17 – Salinity data for station TV63-06

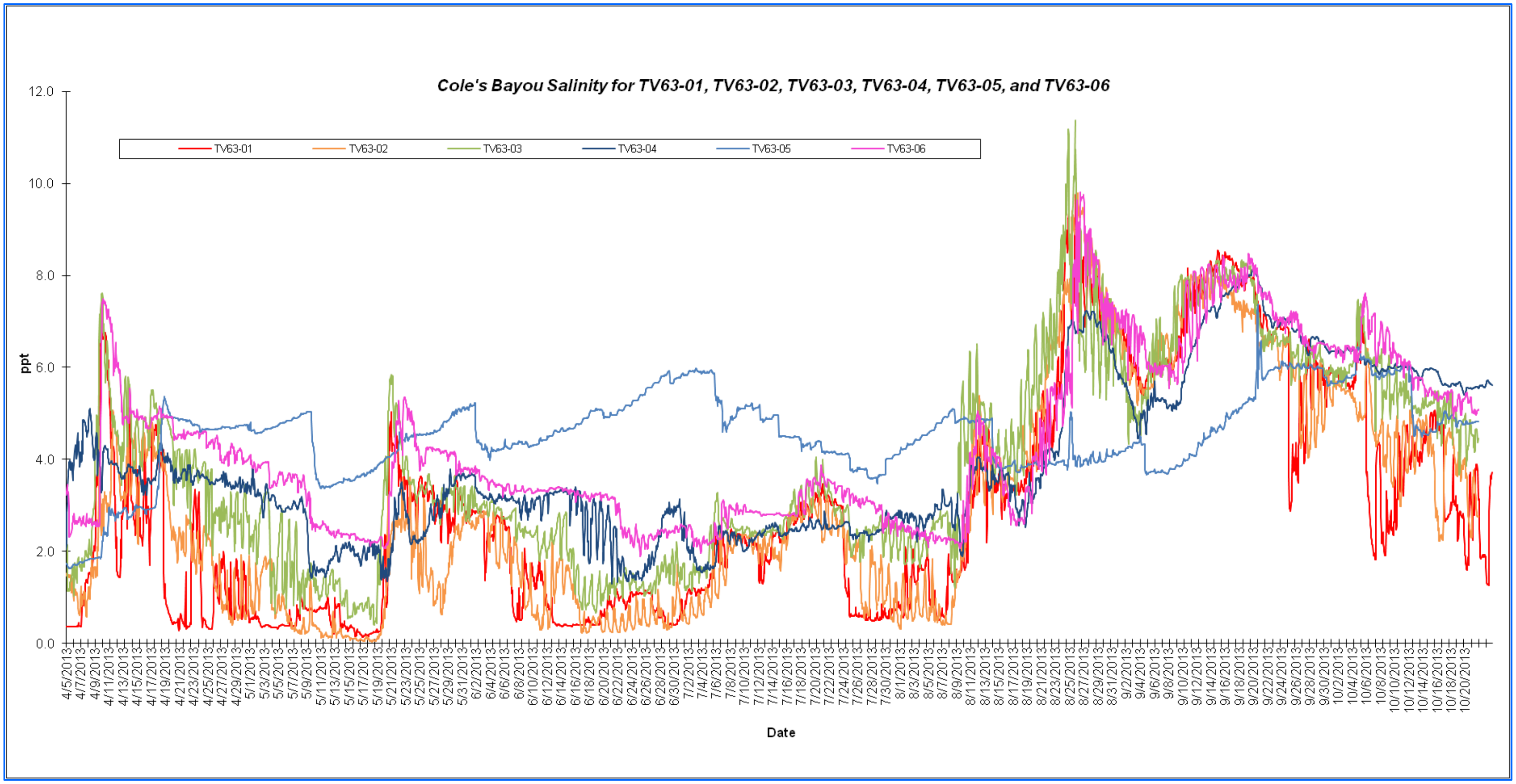

Figure 18 – Salinity data for all stations.
Stations in the marsh (TV63-04 and TV63-05 are colored in blue tones)

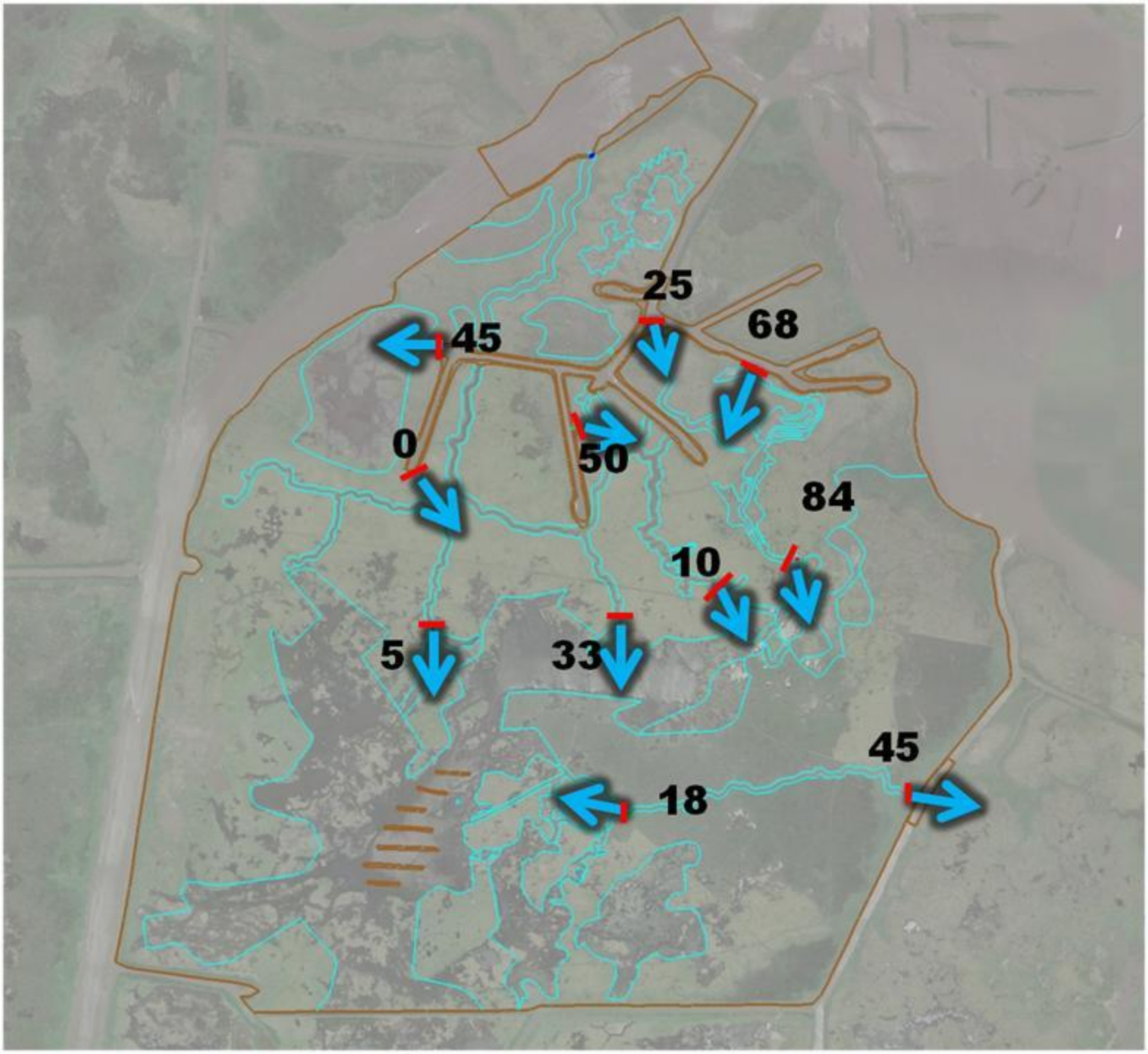

Figure 19 – Five levee breaches in the Oil Field Canals.
Location (red line), direction (arrow), and magnitude (cfs) of measured flow in the marsh channels at discrete times, recorded 12/5 – 12/6/13

2.1.4 Nutrients

Each month (except for September), water samples were collected at six stations in the marsh shown on Figure 20. Samples were analyzed to determine concentrations of Total Nitrogen and Total Phosphorus. These data are listed in **Table 1** and **Table 2**.

Table 1 – Values for Total Nitrogen (mg/L) samples

Date	TV63-07	TV63-08	TV63-09	TV63-10	TV63-11	TV63-12
4/29/2013	0.74	0.73	0.60	0.76	0.65	0.76
5/30/2013	0.94	0.66	0.52	0.81	0.62	0.68
6/26/2013	0.43	0.33	0.50	0.62	0.69	0.59
7/30/2013	0.99	1.04	0.80	1.88	1.42	0.89
8/27/2013	0.58	0.56	0.55	0.61	0.58	0.68
10/24/2013	1.33	0.76	0.76	0.75	0.71	0.77

Table 2 – Values for Total Phosphorus (mg/L) samples

Date	TV63-07	TV63-08	TV63-09	TV63-10	TV63-11	TV63-12
4/29/2013	< 0.05	0.05	< 0.05	0.61	0.15	0.48
5/30/2013	< 0.05	< 0.05	< 0.05	0.36	0.07	0.07
6/26/2013	0.46	0.23	0.30	0.26	0.26	0.19
7/30/2013	0.10	0.10	0.35	3.35	1.01	0.51
8/27/2013	< 0.05	< 0.05	0.06	0.05	0.06	0.22
10/24/2013	0.09	0.08	0.15	0.07	0.11	0.28

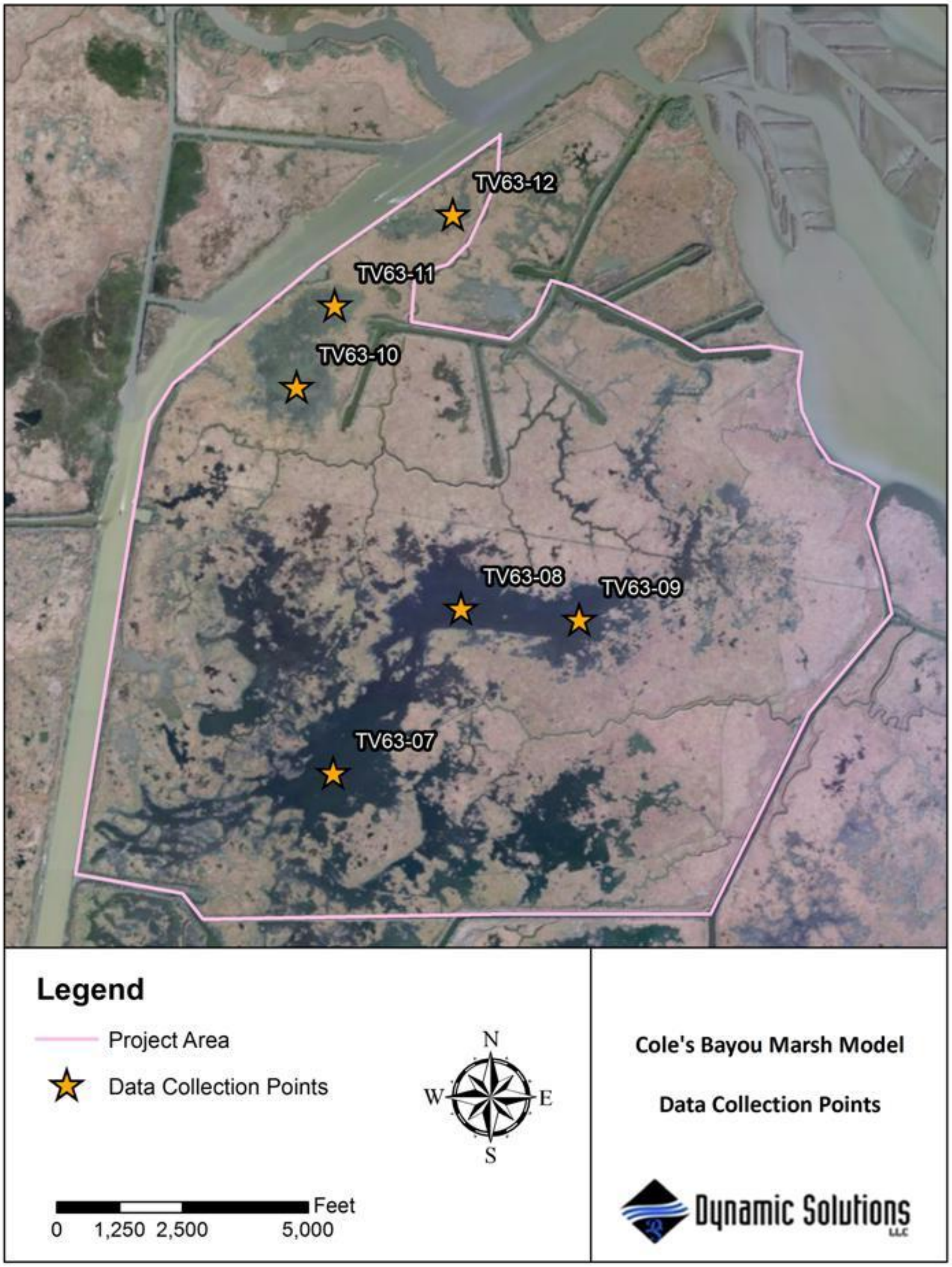

Figure 20 – Nutrient and bulk density sampling stations located within the project area

2.1.5 Total Suspended Solids

In order to better understand sediment dynamics in Cole's Bayou, Total Suspended Solids (TSS) data was taken for a 24-hour period during three types of conditions: (1) ambient summer conditions, (2) a frontal passage resulting in high water levels in Vermilion Bay, and (3) a wind event where significant suspension of sediments occurs. These samples will allow for the development of a relationship between turbidity and suspended sediment concentration that can be analyzed for tidal and storm event effects and provide important information for, in the future, computing restoration benefits using the Boustany or SAND modeling tools.

Suspended sediment samples were collected hourly in the middle of the water column using a pump sampling apparatus. The pump sampler is prone to fouling while collecting samples so there is a considerable amount of missing data. The processing of the samples to determine grain size distributions was recommended, but the samples resulted in such a small amount of sediment being collected that normal procedures for conducting a grain size distribution could not be used.

DSLLC and ENCOS employees monitored meteorological conditions over the project area and were able to capture TSS data for all three types of conditions. TSS samples were collected for the frontal passage event on April 25 - 26, 2014 and the data is shown in **Table 3**. The field report is contained in **Appendix D**. Samples were collected July 23 – 24, 2013 during normal summer conditions where winds were light and tides moderate. Results are show on Table 4, and the field report is contained in **Appendix E**. Tropical Storm Karen's remnants impacted the coast of Louisiana with winds of over 30 mph and samplers were deployed on October 6, 2013 to capture TSS samples for the characteristic wind event. Data are shown in Table 5 and the field report is contained in **Appendix F**.

Table 3 – TSS data (mg/L) collected for the April 24 frontal passage event

Date	TV63-01	TV63-02	TV63-03	TV63-04	TV63-05	TV63-06
4/24/13 15:00	50	228	192	134	56	48
4/24/13 16:00	93	124	98	196	54	48
4/24/13 17:00	57	200	84	96	58	52
4/24/13 18:00	51	232	78	102	56	48
4/24/13 19:00	48	274	80	68	54	42
4/24/13 20:00	122	330	120	60	50	60
4/24/13 21:00	179	310	142	44	54	46
4/24/13 22:00	128	320	148	44	54	46
4/24/13 23:00	104	184	76	60	56	48
4/25/13 0:00	132	404	220	36	52	50
4/25/13 1:00	144	276	164	66	52	42
4/25/13 2:00	166	210	532	62	52	50
4/25/13 3:00	160	248	184	64	56	56
4/25/13 4:00	198	236	174	58	54	52
4/25/13 5:00	252	386	146	76	52	50
4/25/13 6:00	194	360	116	70	48	50
4/25/13 7:00	112	420		58	54	50
4/25/13 8:00	328				50	
4/25/13 9:00	116				52	
4/25/13 10:00	132				48	
4/25/13 11:00	186				54	
4/25/13 12:00	356				50	
4/25/13 13:00	160				44	
4/25/13 14:00	200				64	

Table 4 – TSS data (mg/L) collected for the July 13 ambient conditions event

Date	TV63-01	TV63-02	TV63-03	TV63-04	TV63-05	TV63-06
7/24/13 0:00	20	178		33	47	27
7/24/13 6:00	11	76	45	23	14	33
7/24/13 7:00	16	56	36	27	12	21
7/24/13 8:00	19	104	47	24	14	22
7/24/13 9:00	18	38	41	20	14	22
7/24/13 10:00	14	60	37	26	18	22
7/24/13 11:00	23	52	33		24	22
7/24/13 12:00		72	57	42	19	25
7/24/13 13:00		169	52		23	23
7/24/13 14:00		54	45		27	20
7/24/13 15:00		47	46	57	23	18
7/24/13 16:00		63	42	61	22	21
7/24/13 17:00		59	40	50	27	23
7/24/13 18:00		60	38	40	23	19
7/24/13 19:00	27	84	40		21	17
7/24/13 20:00	24	36	35		24	
7/24/13 21:00	20	46	40		15	
7/24/13 22:00	20	39	43		18	27
7/24/13 23:00	17	41	37	30	17	18
7/25/13 1:00	18	58	51	33	33	24
7/25/13 2:00	16	130	58	28	34	26
7/25/13 3:00	18	94	66	27	18	26
7/25/13 4:00	17	90	74	28	18	23
7/25/13 5:00	18	86	54	21	20	23

Table 5 – TSS data (mg/L) collected for the October 5 wind event, Tropical Storm Karen

Date	TV63-01	TV63-02	TV63-03	TV63-04	TV63-05	TV63-06
10/6/13 0:00						22.5
10/6/13 8:00			61	16	13	
10/6/13 9:00			107	8	12	
10/6/13 10:00			113	7	12	
10/6/13 11:00			173	8	18	
10/6/13 12:00			167	10	10	
10/6/13 13:00			187	10	18	
10/6/13 14:00			185	15	12	
10/6/13 15:00			212	6	20	
10/6/13 16:00			202	11	26	
10/6/13 17:00			177	11	18	
10/6/13 18:00			164	11	13	
10/6/13 19:00			137	9	17	
10/6/13 20:00			80	9	16	
10/6/13 21:00			120	11	21	
10/6/13 22:00			118	8	16	
10/6/13 23:00			125	8	14	
10/7/13 0:00			94	12	14	
10/7/13 1:00			112	11	13	
10/7/13 2:00			108	14	16	
10/7/13 3:00			117	7	14	
10/7/13 4:00			113	7	17	
10/7/13 5:00			107		12	
10/7/13 6:00			110		11	
10/7/13 7:00	32	62	119		14	

2.2 System Characterization

Vermilion Bay experiences a diurnal tide with a typical range of less than 1.5 feet. It is shallow with an average depth of approximately 9 feet. It has a large opening to the east, exchanging water with West Cote Blanche Bay (WCB) and narrow but very deep (nearing 100 feet) channel connecting to the Gulf of Mexico (GOM) through Southwest Pass. Water level and salinity patterns are governed by conditions in the northern GOM and WCB. The freshwater inflows from the Mississippi River, which influences salinity and sediment dynamics in the GOM, and the Atchafalaya River, which contributes freshwater and sediment to WCB, have an impact on the larger region.

During the summer, high pressure dominates over Vermilion Bay and water levels have little subtidal variation and have normal exchanges of water from the northern GOM and WCB. Tropical storms may cause notable water level, salinity, and suspended sediment events between late summer and late fall, but are rare. Annually, between October and April, dozens of cold fronts move through region producing strong winds with a specific pattern that greatly affect circulation and sediment transport in Vermilion Bay (Walker and Hammack, 2010). Strong southerly winds precede the frontal passage and cause considerable setup and high water levels in the Bay. Approximately 6-9 hours before the passage of the front water levels begin to fall due to the Ekman pumping effect (Feng, 2009). Winds shift as the front passes, blowing from the north and northwest and driving much of the water out of the system to the southeast through the wide opening to WCB (Walker and Hammack, 2010). During these events as much as 34 – 42 percent of the waters in Atchafalaya and Vermilion Bays can be flushed in a 32-hour time period with the largest outflux occurring 8 – 11 hours after the frontal passage (Feng, 2009). Sediment resuspension and water column turbidity can increase up to five times when water levels are low and strong north winds persist. Upon rebound of the water levels after the frontal passage Southwest Pass is an important conduit for restoring water level to Vermilion Bay as evidenced by rapid increases in salinity of greater than 10 ppt (Walker and Hammack, 2010).

Little Vermilion Bay lies between Vermilion Bay and Freshwater Bayou. Freshwater Bayou receives some freshwater input from the north, locally from the Vermilion River, but in the locale is largely dominated by process in Little Vermilion Bay. These waters are what comprise the water contained in the Oil Field Canals on the north side of the Cole's Bayou Marsh. Consequently, water levels (especially) and salinity in the Oil Field Canals and ultimately in Cole's Bayou Marsh are driven primarily by the conditions in Vermilion Bay. This can be evidenced by examining observed water levels at Cypremort Point at the eastern boundary of Vermilion Bay, CRMS 0541 near Southwest Pass, and TV63-03 in the Oil Field Canals (**Figure 21**).

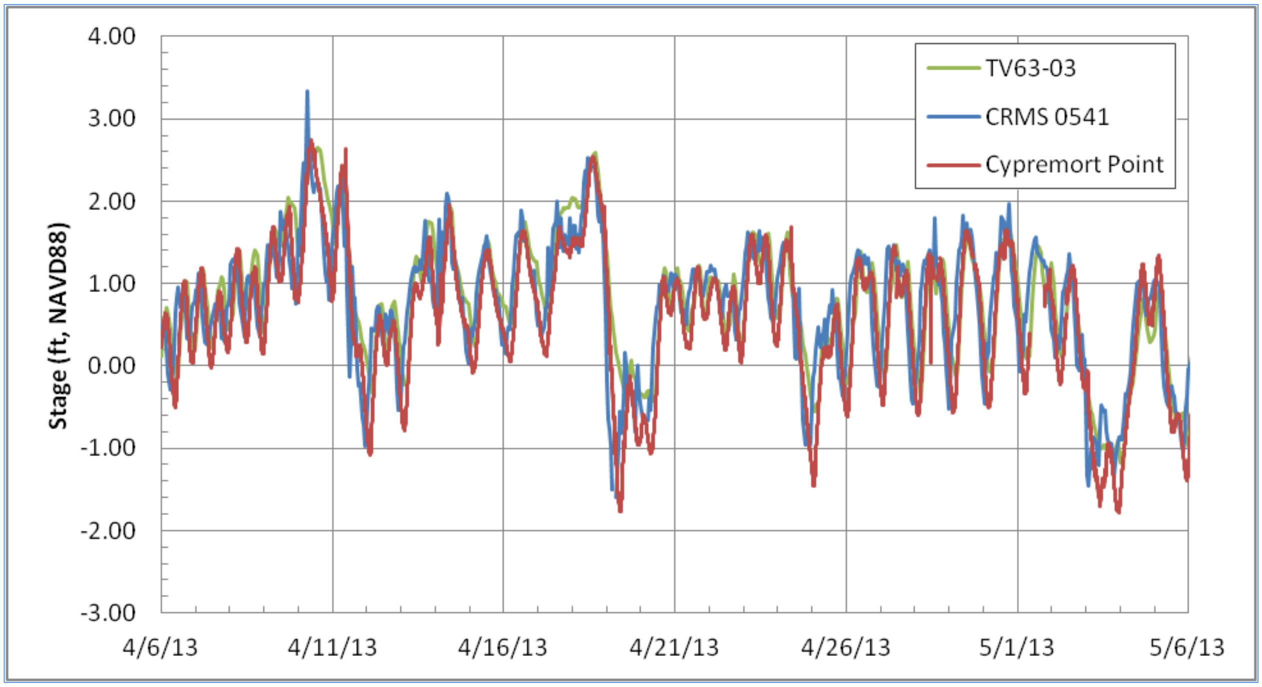

Figure 21 – Comparison of water levels, adjusted to the NAVD88 datum, at Cypremort Point, CRMS 0541, and TV63-03

Cole's Bayou Marsh is surrounded by a low levee which largely isolates its waters from those surrounding it at normal water levels. It is connected to the outlying waters via six primary gaps (breaches, an example of which is shown in **Figure 22**) in the levee in the Oil Field Canals and one primary opening to the McIlheny Canal (a typical view shown in **Figure 23**) in the southeast portion of the marsh. The connection to the McIlheny Canal consists of a collapsed culvert and a gap that has formed just southwest of the culvert. The majority of flow into and out of the marsh is through the breaches in the north. Many of these breaches directly connect to the network of distributary marsh channels (**Figure 24**) which exist in the marsh. These channels are between 20 and 75 feet wide, evident in aerial photographs, and carry much of the flow in the marsh at low water levels. Numerous smaller channels exist (**Figure 25**); some natural and some caused by pipelines or preferential airboat tracks. Four main channels connect the northern breaches to the central open water area, where TV63-04 exists. This station serves as the main indicator of conditions in the marsh as it is connected to the four main channels to the north and to the levee breach in the southeast by an approximately 75-foot wide channel running to the east. TV63-05 lies in an open water area in the southern part of the marsh that is somewhat hydraulically isolated during low waters, with only small connections to the central open water area.

The average elevation of the marsh is currently 0.95 feet (0.29 m), +/ 0.1 feet. This elevation does not vary greatly throughout the marsh with the exception of some high ground at the perimeter of the marsh, evidenced by woody species of vegetation. The median water level in the marsh is 0.85 feet at TV63-04.

Figure 27 shows a distribution of the water level at TV63-04 during the observation period. The marsh top sits about 0.1 feet above the average water level measured during the period of data collection. The marsh top is typically vegetated with *Spartina* grasses between two and five feet high (as in Figure 25) so it is difficult to see water on the marsh top. Small rivulets and potholes exist which also transport water through the marsh.

The channel connecting the eastern-most breach to the central open water area is the dominate path of flow into and out of the marsh. At the breach, the channel is 30 feet wide and 6 feet deep. The channel winds through several open water areas and pinches of marsh but persists, often at a much narrower width but with sufficient depth, to the central open water area. The snapshot of flow data taken during the December field visit supports this observation.

Figure 22 – View of gap (breach) in the levee surrounding Cole's Bayou Marsh

Figure 23 – Typical view of a canal surrounding the Cole's Bayou Marsh, in this case the McIlheny Canal

Figure 24 – Typical view of primary distributary channel in the marsh.

Figure 25 – Typical view of narrow, 8-foot wide, channel in the marsh

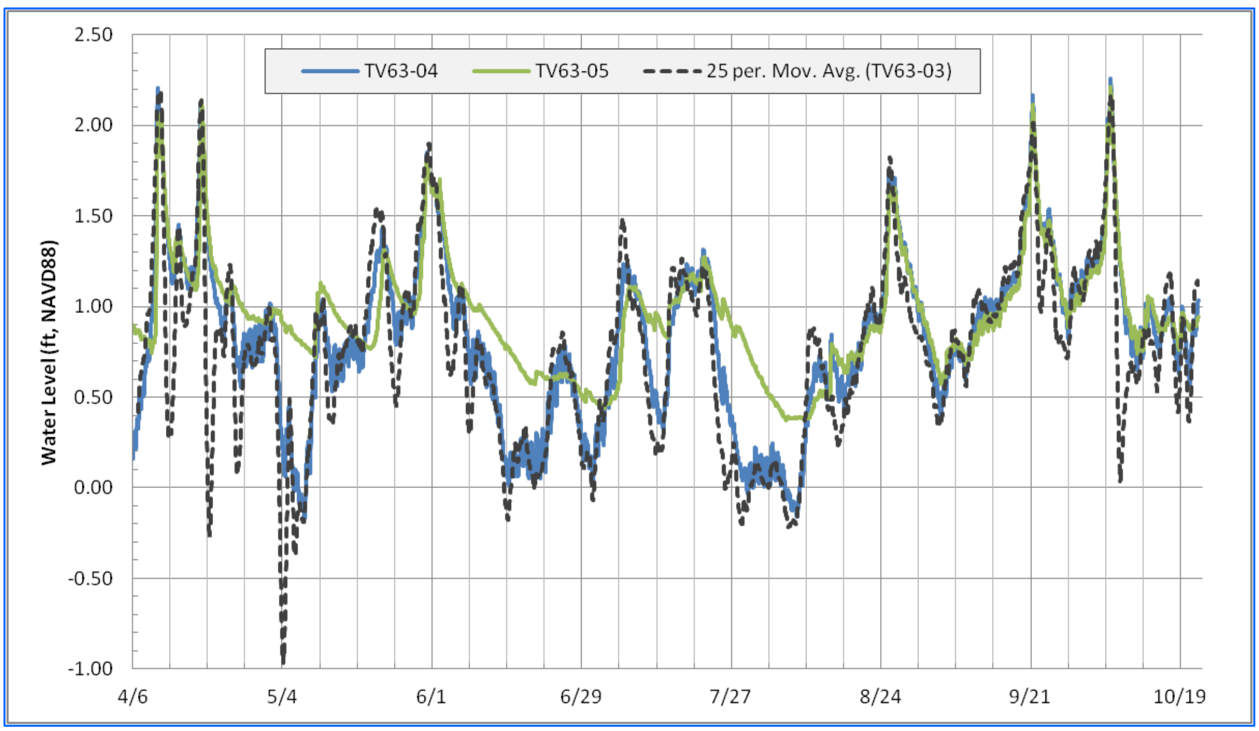

Figure 26 – Water levels, adjusted to the NAVD88 datum, in the Oil Field Canals (TV63-03) and in Cole's Bayou Marsh (TV63-04 and TV63-05)

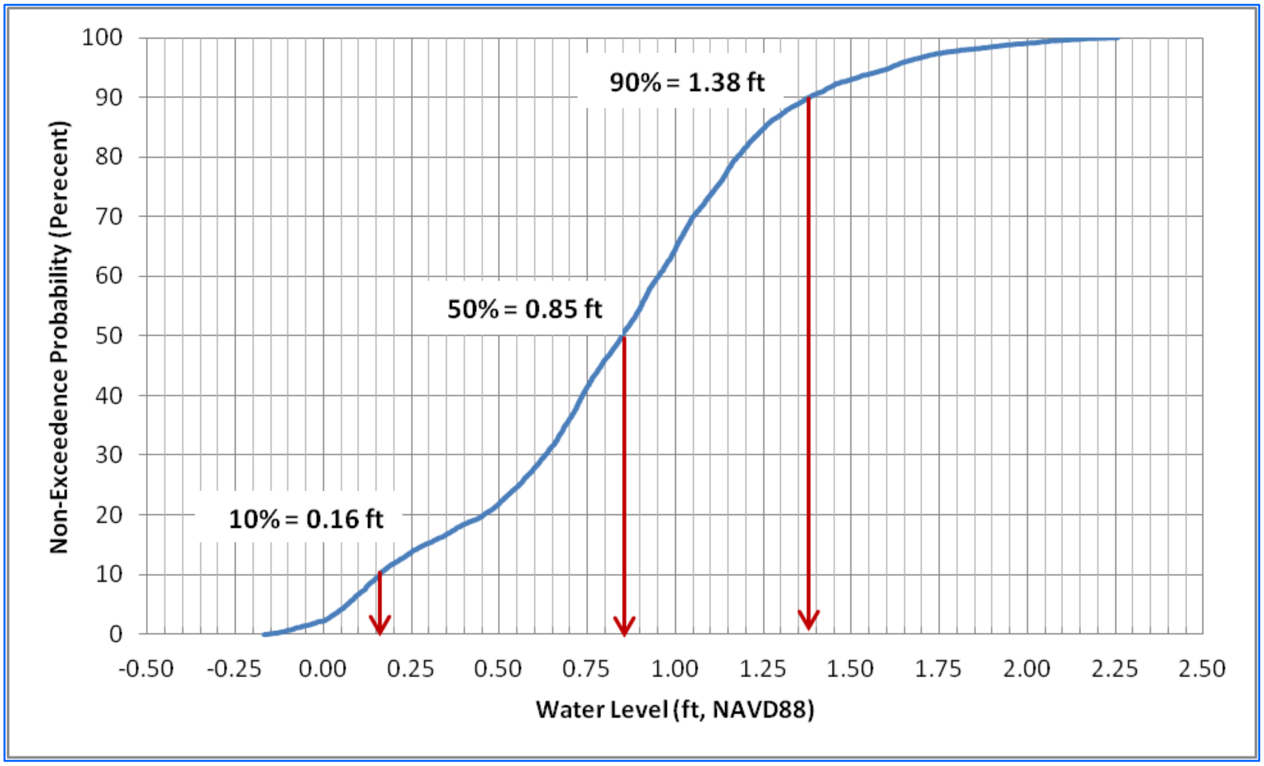

Figure 27 – Non-exceedence probability of water level at TV63-04, highlighting the 10 percentile, median, and 90 percentile water levels.

SECTION 3 MODEL SETUP

3.1 Model Description

The ADH model software was recommended as the hydrodynamic modeling software best suited for the Cole's Bayou Marsh Restoration project. It utilizes an unstructured mesh that allows the model to handle complex and intricate domains of varying scales. This is particularly important for this application, as the model must cover vast areas of open water as well as small channels within Cole's Bayou itself. ADH has been proven to efficiently handle wetting and drying and has the ability to simulate flow through hydraulic structures, such as culverts and flap gates, which are specified in the scope of work. The combination of these attributes and the fact that ADH is open-source make it a reliable model to accurately simulate the complex hydraulic conditions at the site.

ADH is a conservative, implicit, finite element hydrodynamic and constituent transport model developed by the US Army Engineer Engineering Research and Development Center, Coastal and Hydraulics Laboratory. It is capable of simulating both saturated and unsaturated groundwater, overland flow, and two- or three-dimensional shallow water problems, with the current study utilizing the two-dimensional shallow water module. The 2D shallow-water equations used for this application are a result of the vertical integration of the equations of mass and momentum conservation for incompressible flow under the hydrostatic pressure assumption. Written in conservative form, the 2-D shallow water equations are:

$$\frac{\partial \mathbf{U}}{\partial t} + \frac{\partial \mathbf{F}}{\partial x} + \frac{\partial \mathbf{G}}{\partial y} + \mathbf{H} = 0$$

where:

$$\mathbf{U} = \begin{Bmatrix} h \\ uh \\ vh \end{Bmatrix}$$

$$\mathbf{F} = \begin{Bmatrix} uh \\ u^2 h + \tfrac{1}{2} g h^2 - h\dfrac{\sigma_{xx}}{\rho} \\ uvh - h\dfrac{\sigma_{yx}}{\rho} \end{Bmatrix}$$

$$\mathbf{G} = \left\{ \begin{array}{c} vh \\ uvh - h\dfrac{\sigma_{xy}}{\rho} \\ v^2h + \tfrac{1}{2}gh^2 - h\dfrac{\sigma_{yy}}{\rho} \end{array} \right\}$$

and

$$\mathbf{H} = \left\{ \begin{array}{c} 0 \\ gh\dfrac{\partial z_b}{\partial x} + n^2 gh\dfrac{u\sqrt{u^2+v^2}}{C_o h^{1/3}} \\ gh\dfrac{\partial z_b}{\partial y} + n^2 gh\dfrac{v\sqrt{u^2+v^2}}{C_o h^{1/3}} \end{array} \right\}$$

where:

ρ = fluid density
g = gravitational acceleration
z_b = riverbed elevation
n = Manning's roughness coefficient
h = flow depth
u = x-component of velocity
v = y-component of velocity
C_o = dimensional conversion coefficient (1 for SI units, 1.486 for U.S. customary units)
σ's = the Reynolds stresses due to turbulence, where the first subscript indicates the direction, and the second indicates the face on which the stress acts.

The Reynolds stresses are determined using the Boussinesq approach to the gradient in the mean currents:

$$\sigma_{xx} = 2\rho v_t \frac{\partial u}{\partial x}$$

$$\sigma_{yy} = 2\rho v_t \frac{\partial v}{\partial y}$$

and

$$\sigma_{xy} = \sigma_{yx} = 2\rho v_t \left(\frac{\partial u}{\partial y} + \frac{\partial v}{\partial x} \right)$$

where v_t = kinematic eddy viscosity (which varies spatially).

The ADH shallow-water equations are placed in conservative form so that mass balance and the balance of momentum and pressure are identical across an interface. This is important in order to match the speed and height of a surge or hydraulic jump.

The equations are solved in a finite element approach. The quality of the numerical solution depends on the choice of the basis/trial function and the test function. The trial function determines how the variables are represented and the test function determines the manner in which the differential equation is enforced. In the Galerkin approach the test functions are chosen to be identical with the trial functions. When the flow is advection-dominated, the Galerkin approach produces oscillatory behavior. The Galerkin form of the test function cannot detect the presence of a node-to-node oscillation and so allows this spurious solution. The approach used in ADH is to enrich the standard Galerkin test function with an additional term that can detect and control this spurious solution (Savant et al., 2010).

One of the major benefits of ADH is its ability to automatically adapt the mesh in areas where additional resolution is needed to properly resolve the hydrodynamics. This process is done by normalizing the results so that an error quantity is determined for each element. If this error exceeds the tolerance set by the user, then the element is refined. ADH is also able to unrefine previously refined areas when the added resolution is no longer needed. ADH contains other essential features such as wetting and drying, completely coupled sediment and salt transport, and wind effects. A series of modularized libraries make it possible for ADH to include vessel movement, friction descriptions, as well as a host of other crucial features. ADH can run in parallel or on a single processor and runs on both Windows systems and UNIX based systems.

Please refer to Berger et al. (2010) and Savant et al. (2010) for a more in-depth description of the ADH surface water model.

3.2 Model Domain

The primary area of interest is the Cole's Bayou Marsh proper, as shown in Figure 1. The overall hydrodynamic model extents were determined to include Vermilion Bay, extending as far as Cypremort Point and Southwest Pass, Little Vermilion Bay, and Freshwater Bayou from west of Intracoastal City to its terminus at the Freshwater Canal Locks (Figure 2). This model captures the processes occurring in Vermilion Bay, Little Vermilion Bay, Freshwater Bayou, and those bounding the Cole's Bayou Marsh.

The significantly larger extents of the model domain were chosen because: (1) a model must extend a significant distance from the area of interest so any changes made within the area of interest do not propagate back to the boundary, rendering the model inadequate, (2) future scenarios must be considered when designing a model domain, so that the domain extends far enough to handle a wide range of possible future configurations, and (3) it allows the model to be connected to long-term tidal stations at Cypremort Point and Southwest Pass which allows it to be run for time periods when supplemental data was not collected.

To maximize efficiency, the development and calibration of the Cole's Bayou Marsh model was completed using a smaller domain encompassing a small section of Freshwater Bayou near the entrance of the Cole's Bayou channel, in the northern Oil Field Canals terminating at station TV63-03, and in the southern McIlheny Canal terminating before reaching Little Vermilion Bay. This nested approach allows the flexibility and added understanding from the larger domain but significantly lowered the computational burden when running simulations focused on the Cole's Bayou Marsh proper. When necessary, boundary condition data for the smaller Marsh model could be extracted from the larger scale model. From here forward, the large-scale model will be referred to as the Vermilion Bay model and the small-scale model focused on the Cole's Bayou Marsh project area will be referred to as the Cole's Bayou Marsh model.

3.3 Calibration Period

The calibration period encompassed the period of data collection, from April 6, 2014 to October 21, 2014. During this period, the maximum and minimum water levels within the marsh were 2.21 and -0.17 feet, respectively. Typical summer conditions of moderate water levels and high pressure characterized much of this period, but it did contain two significant frontal passage events, on April 10 and 18, and the passage of the remnants of Tropical Storm Karen on October 6, 2013. Significant periods of low water levels occurred in late May and early August.

3.4 Vermilion Bay Model

3.4.1 Input Data and Model Mesh

The Vermilion Bay model was developed to provide forcing information to the smaller, higher-resolution Marsh model. This mesh includes Little Vermilion Bay, Vermilion Bay, and portions of West Cote Blanche Bay and the Gulf of Mexico south of Southwest Pass (Figure 2)

During the data collection phase bathymetric data for Vermilion and Little Vermilion Bays was collected and analyzed. The bathymetric data for portions of these areas dates back to the 1800's. This is not uncommon in many coastal areas and there have been many studies performed in this region using these data. Some of these models performed poorly in the vicinity of Vermilion Bay. The ADCIRC hurricane storm surge modeling done by USACE and FEMA under-predicted high water marks from Hurricane Rita by around three feet in the areas surrounding Vermilion Bay (Dietrich et al., 2011). This was attributed to the high viscosity of those waters at the bed interface but may also be a function of outdated bathymetry. A significant amount of sediment has been introduced to coastal waters in the region over the last few decades so the morphology of the coastal waters may have changed. Based on these issues, new hydrographic surveys were conducted of the areas seen in Figure 3.

A combination of the most recent bathymetric data obtained from NOAA National Geophysical Data Center (http://www.ngdc.noaa.gov/mgg/bathymetry/hydro.html) and the HydroTerra surveys were used to create a comprehensive scatter set of bathymetric data in the region. This data was then interpolated as part of the development of the model mesh, yielding a bathymetric representation of the model domain.

The mesh for the Vermilion Bay model was created to capture the general hydrodynamics in Vermilion Bay, Little Vermilion Bay, and the waters leading to the Oil Field Canals north of Cole's Bayou Marsh. The mesh contains 16,657 nodes and 29,634 elements, and is shown in its entirety in **Figure 28.** The elements in Vermilion Bay were typically 1000 feet (300 meters) across, 250 feet (76 meters) in Little Vermilion Bay, and 150 feet (46 meters) across in Freshwater Bayou and the constricted and very deep channel in Southwest Pass.

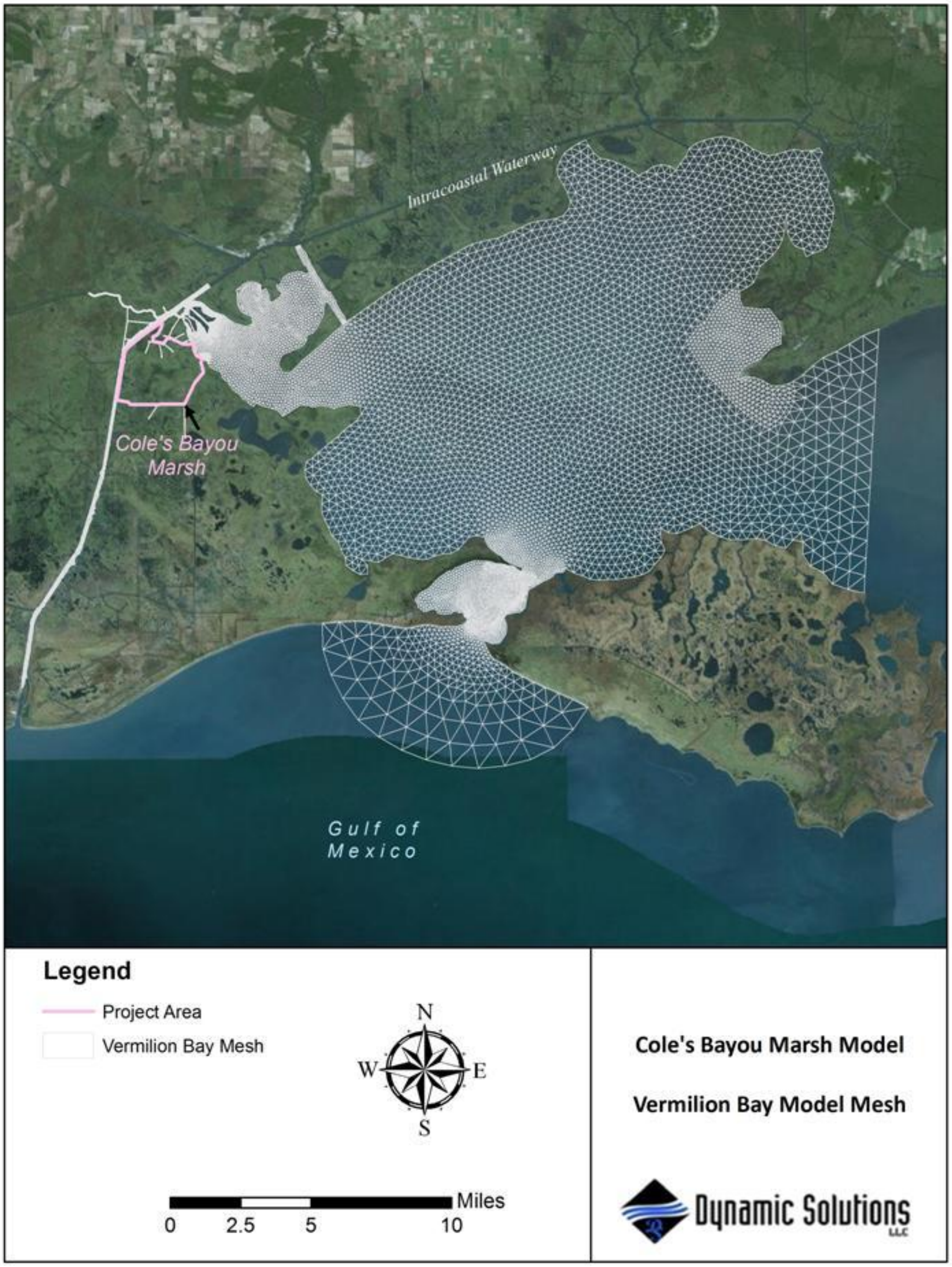
Intracoastal Waterway
Cole's Bayou Marsh
Gulf of Mexico
Legend
Project Area
Vermilion Bay Mesh
N
W
E
S
Miles
0
2.5
5
10
Cole's Bayou Marsh Model
Vermilion Bay Model Mesh
Dynamic Solutions LLC

Figure 28 – Vermilion Bay model mesh

3.4.2 Boundary Conditions

The boundaries for the Vermilion Bay model were chosen to represent forcings from West Cote Blanche Bay on the eastern boundary, the Gulf of Mexico outside of Southwest Pass to the south, and waters from Freshwater Bayou and the Vermilion River nearer to the project area. Boundary conditions in the east and south were positioned to utilize existing, ongoing data collection stations at Cypremort Point, CRMS0541, CRMS0527, and WAVCIS 03 (*http://www.wavcis.lsu.edu*). The gage locations and model boundary can be seen in, and the gage information is shown in **Table 6**. The southern boundary was placed outside Southwest Pass far enough so flux through the Pass could be realized but not as far as the WAVCIS station as this would have resulted in modeling a much larger portion of the Gulf, increasing complexity due to the need to simulate currents for that area (Rouse et al., 2005). The eastern boundary was placed just east of the Cypremort Point gage so the gage could be used to help tune the boundary condition. The boundary condition data for this model required adjustment from the observed data due to the uncertainty of gage datums in this region and the sensitivity of currents in Vermilion Bay to even small changes in relative water level between the eastern and southern boundaries. Adjustments to the boundary condition time series were made during model development and calibration so modeled water level and salinity data matched the observed data at the calibration stations.

Table 6 – Data station information for those used in the Vermilion Bay model

Site No.	Site Name	Location	Datum	Agency	Data Type
CSI-03	WAVCIS 03	Offshore in Gulf/ Southwest Pass	NAVD88	LSU	Water Level
07387050	USGS Bayou Fearman	Vermilion Bay/ Fearman Lake	Unknown	USGS	Water Level, Salinity
073807040	USGS Cypremort Point	Vermilion Bay/ Cypremort Point	NAVD88	USGS	Water Level, Salinity
0541	CRMS0541	Southwest Pass/ Shell Reefs	NAVD88	CRMS	Water Level, Salinity
0527	CRMS0527	West Cote Blanche Bay/ Cypremort Point	NAVD88	CRMS	Water Level, Salinity
TV63	Cole's Bayou	Near Cole's Bayou Marsh	NAVD88	CPRA	Water Level, Salinity

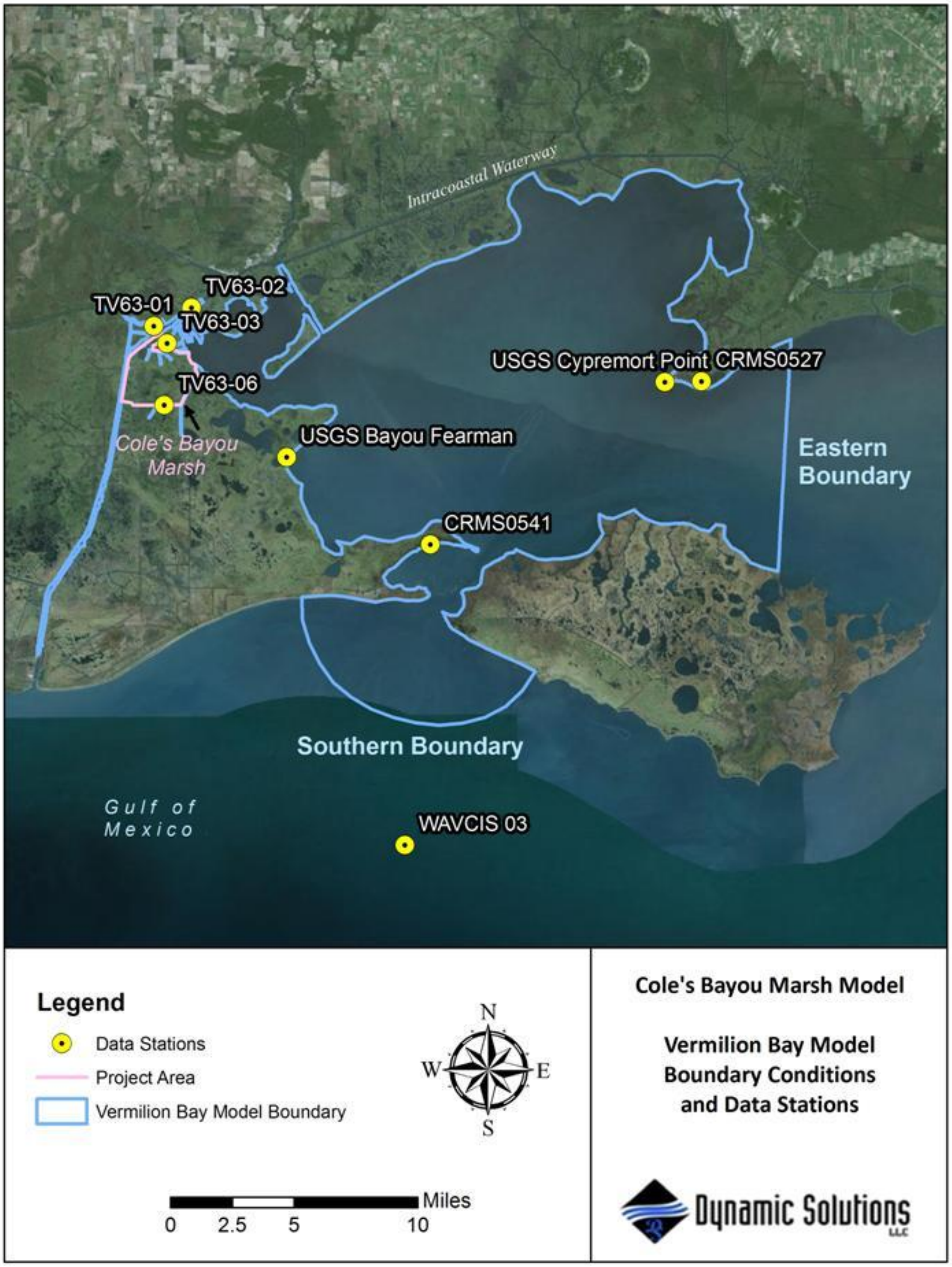

Figure 29 – Data stations and boundary conditions for the Vermilion Bay model

Additional information for constructing the southern boundary came from the Northern Gulf of Mexico Operational Forecast System (NGOFS; *http://tidesandcurrents.noaa.gov/ofs/ngofs/ngofs.html*) model. The NGOFS is a regional-scale numerical model of the Northern Gulf of Mexico used to provide predicted water levels and salinity based on astronomical tides, major inflows, and regional meteorological conditions.

To construct the southern boundary condition water level time series, WAVCIS #3 data was adjusted by 1.49 feet (0.457 m) to match the average water level of NGOFS model at the location of the southern boundary. The predicted water levels from NGOFS are less affected by local variance than the WAVCIS station and also provide water level at the proper location (nearer to Southwest Pass). The tidal amplitude was increased by 20% and the time lagged by six hours to account for the difference between the model boundary and the gage location, matching the tidal signal at CRMS0541. For salinity at the boundary, the CMRS0541 salinity data was used. The values for salinity were adjusted by increasing them 20% and lagging them by -24 hours.

Initial water level and salinity data for the Eastern boundary was taken from the USGS Cypremort Point gage. The gage datum was resurveyed by the USGS in 2013 and the adjustment to NAVD88 is -1.48 feet (-0.45 m). Data from CRMS0527 was used to fill any missing water level and salinity data in the Cypremort Point data. The datum adjustment to NAVD88 for CRMS0527 water level data is 0.85 feet (0.259 m). To construct the eastern boundary condition salinity and water level time series the USGS Cypremort Point data was lagged 3 hours and CRMS0527 data was lagged 2 hours to account for the difference in location between the model boundary and each gage. This magnitude of water levels was increased by 25% and salinity values were unchanged.

For the Western boundary locations, observed data at TV63-02 and TV63-01 were used with no modifications for water level or salinity.

During calibration, it became clear that the overall flux of water in Vermilion Bay, as evidenced by salinity values, was dependent on gradient between water levels between the eastern boundary and the southern boundary. Additionally, the flux was found to be sensitive to small (on the order of .03 feet, or 1 cm) changes in gradient. Ultimately, the water level at the southern boundary was raised by 0.033 feet (0.010 m) and the eastern boundary raised by 0.098 feet (0.030 m) to correctly simulate water level and salinity throughout Vermilion Bay.

The ADH model is capable of simulating the hydrodynamic effects of wind. Sensitivity testing was performed using data from the surrounding NOAA meteorological stations to ascertain the impact of adding wind forces to the model. The result was that salinity values at the calibration stations changed by less than 1 ppt with nearly identical trends, with run times increasing by 22%. This indicates that the primary wind forcings on Vermilion Bay were captured in the boundary condition data, so wind within the domain was not applied in the model.

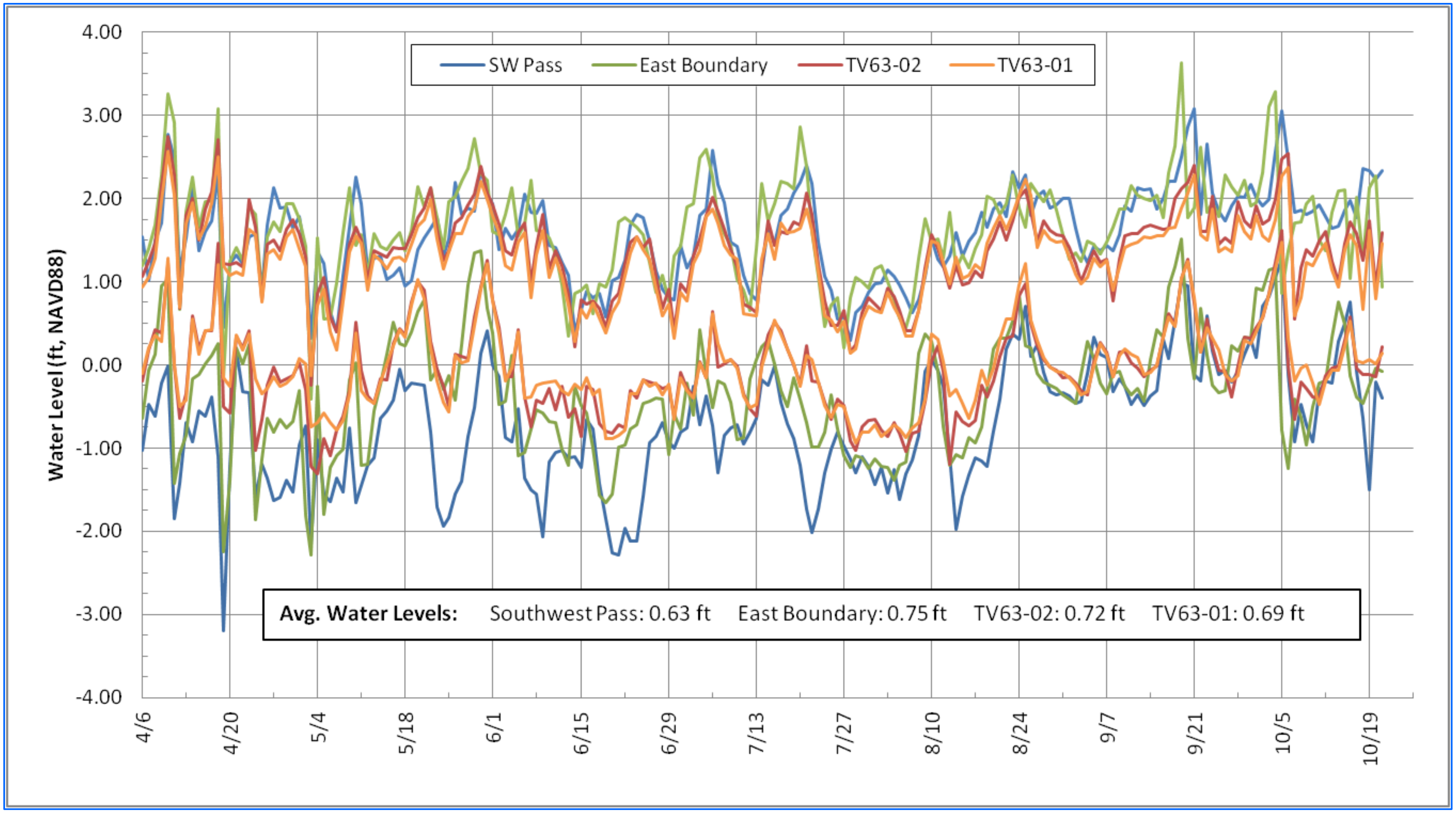

Figure 30 – Daily maximum and minimum water level of boundary condition time series for the Vermilion Bay model

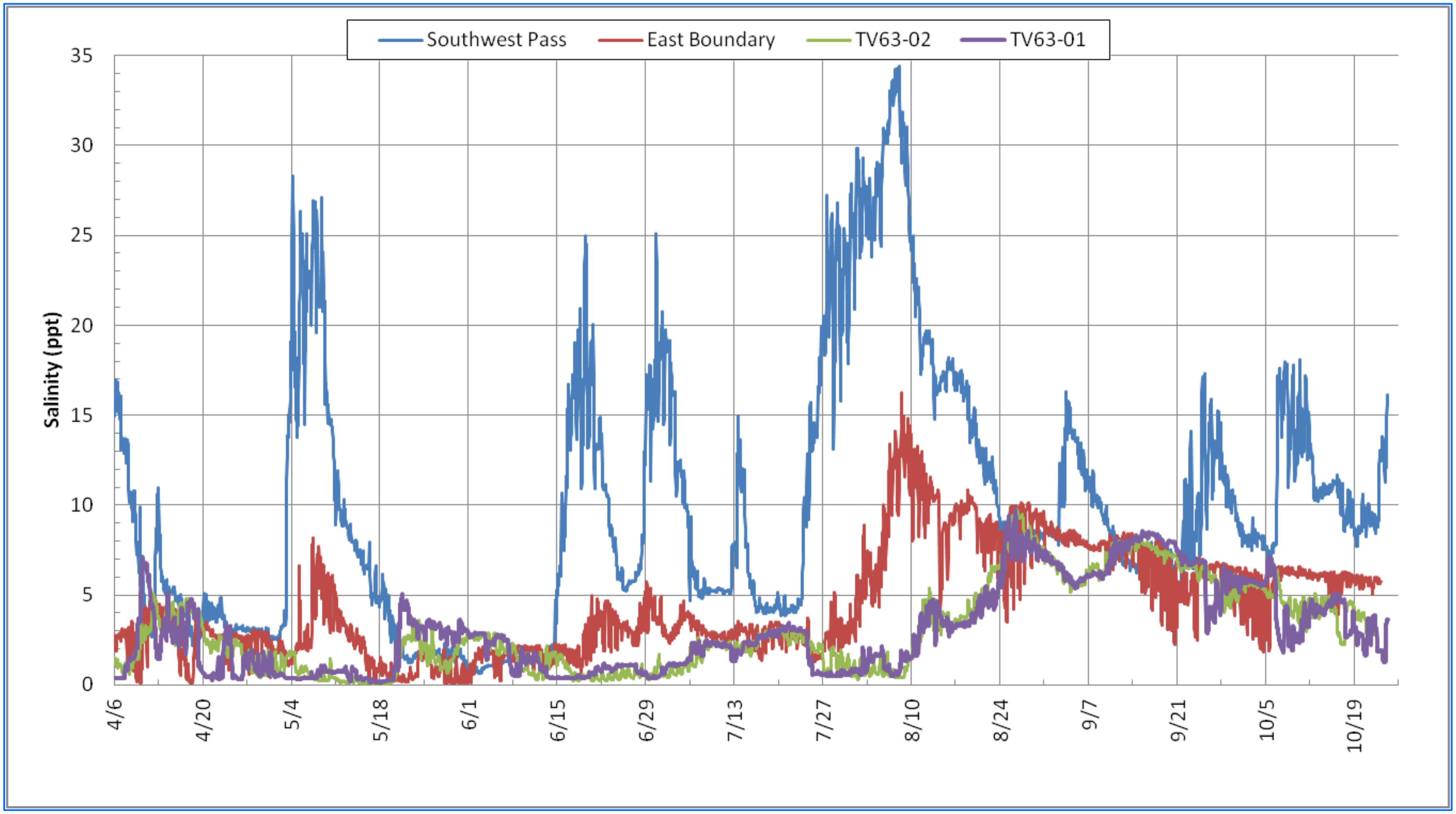

Figure 31 – Salinity boundary conditions for the Vermilion Bay model

3.4.3 Model Setup

The model was divided into two material types to be able to partition roughness, eddy viscosity, molecular diffusion, and mesh adaption parameters. A Manning roughness value of 0.025 was used throughout the domain. The molecular diffusion factor was set to 25. During calibration diffusion was adjusted to correctly model salinity patterns in Vermilion Bay. The diffusion parameter is higher than normal to account for the increased mixing due to winds over the shallow areas.

Eddy viscosity represents turbulence that occurs at scales smaller than that of the mesh resolution. ADH has two formulations for parameterizing eddy viscosity, a specified eddy viscosity, EVS, and an estimated eddy viscosity, EEV. EVS uses a measure of the kinematic eddy viscosity and has units of length^2/time. It is recommended for typical flows that this value be set to 1/40th of the product of a characteristic length and velocity in meters per second (Berger et al., 2010). For areas with higher turbulence, it should be increased as required to represent the physical mixing process. EEV for anisotropic (directionally dependent) flows allows the user to specify a coefficient to be used within the Rodi (1984) formulation. EEV requires an extra computation within ADH so utilizing this formulation typically causes the model to run slower. For the Vermilion Bay model EVS values of 0.01 were used throughout the domain. The wetting and drying tolerance for the model (expressed in ADH as a DTL card) was set to 0.2 m.

ADH utilizes a semi-implicit scheme with adaptive time stepping. The maximum time step allowed for this model was 450 seconds, but ADH will automatically cut the time step if the hydrodynamic solution does not converge numerically.

3.4.4 Calibration Data

The Vermilion Bay model was calibrated at 5 stations – Cypremort Point, CRMS 0541, Bayou Fearman, TV63-03, and TV63-06 - shown in Figure 29. The spatial variation of these stations allows for a broad evaluation of the model performance throughout the domain. The primary stations of interest are those near the project area so those were given greater weight when evaluating calibration results, especially for salinity.

3.5 Cole's Bayou Marsh Model

3.5.1 Input Data and Model Mesh

Setting the physical context for the model is the elevation[1] data. The survey data collected provided sufficient detail to effectively characterize the open water areas in the northwest part of the project area, the central part of the open water area in the center of the marsh, and the dominant marsh channels. The low-lying areas in the southern portion of the marsh had sparse coverage. The higher elevation marsh areas, vegetated areas which are typically above the median water level, had sparse coverage because of the difficulty to efficiently gather data by airboat. Based on field observations, these areas are largely flat – the average top of marsh elevation varying less than 0.25 feet over hundreds of feet, pocked with occasional rivulets and potholes. Efforts were made to record representative top of marsh elevations in critical areas.

A LiDAR survey performed at low water would be the best way to collect topographic information over the higher-elevation (not wetted) areas of the marsh. The budget did not allow for a targeted LiDAR study. LiDAR data covering the project area from 2004 was acquired from the LSU Atlas database (LSU). Between 2004 and the 2013 two major hurricanes, Katrina and Rita in 2005, have caused significant pond enlargement as evidenced from aerial imagery (**Figure 32**) as is typical for tropical storm impacts on wetlands over a half-century in Southern Louisiana (Morton and Barras, 2011). However, this is the best source of elevation data for areas of the marsh not covered by the surveys. Field surveys performed in December 2013 by DSLLC staff indicated that a representative, median top of marsh elevation was 0.95 feet (0.29 meters), NAVD88. A corresponding collection of LiDAR points was selected, the median top of marsh elevation computed, and lowered by 1.64 feet (0.50 meters) to match the surveyed median. The entire collection of marsh LiDAR data was then lowered by 1.64 feet.

[1] Elevation data is the combination of bathymetry, which typically refers to below-water elevation data, and topography which refers to above-water elevation data. Since the much of the Cole's Bayou marsh landscape is intermittently wet, the use of either of these terms may be confusing, so we will use the term "elevation data" moving forward.

(a)

(b)

Figure 32 – DOQQ images of the project area in (a) 2005 and (b) 2008

Stepping back, the purpose of the model is to accurately simulate the major hydrodynamic processes occurring in the Cole's Bayou Marsh and surrounding area. During periods of low stage (low tide), the predominant pathway for flow in the marsh is through the network of marsh channels and open water areas. As water begins flowing over the top of the marsh, sheet flow over the top of the marsh will dominate flow within the marsh, with the total flow entering governed by the geometry of the breaches in the levee allowing conveyance. When looking at the processes on the whole, across the entire marsh, once flow gets on the marsh surface it begins to act like a storage volume which is governed by a stage-volume relationship. Decades ago, when computing power was considerably less, 2-dimensional models of marshes had very large grid cells but were still serviceable tools used to understand hydrodynamics. The critical point was to get elevation-volume curve correct. While each individual node may not have observed data, the modeler may adjust the data to achieve a good representation of this curve. This idea has been used to effectively model marshes in South Louisiana (Letter, 1993). A sensitivity analysis was performed to test whether top of marsh elevation data, and the related stage-volume relationship, were acceptable and the results are discussed in detail Section 4.2.2. The analysis showed the procedures used to define elevation data in the marsh were acceptable.

The procedure used to define elevation data in the model began with the known elevations of the recent survey. A scatter set of the survey data was imported into SMS (Aquaveo, 2010). In areas where survey data did not exist, scatter data from the LSU Atlas LiDAR data was utilized. Breaklines were implemented to define continuous and defined features such as channels or terraces. This data was then triangulated to create a simulated elevation surface.

The mesh for the Cole's Bayou Marsh model was created to capture the major marsh channels and their connections to areas of open water so conveyance of water through the system was reasonably accurate. The mesh contains 35,897 nodes and 69,861 elements, and is shown in its entirety in **Figure 33**. The Elements in the marsh (higher elevation areas) and open water areas were typically 100 feet across (**Figure 34**). Each major channel had a minimum of four elements across its width, resulting in a trapezoidal cross-section in the model. Elements along narrow sections of the channel connecting the eastern most breach to the open water area were as small as 5 feet wide, as shown in **Figure 35**. Elements at the connections between the Oil Field Canals and the marsh channels, areas where the marsh's perimeter levee had breached, were typically on the order of 3 – 6 feet wide so an accurate cross-section could be defined. This was of critical importance since these serve as the hydraulic control for waters flowing into and out of the marsh from the surrounding waters.

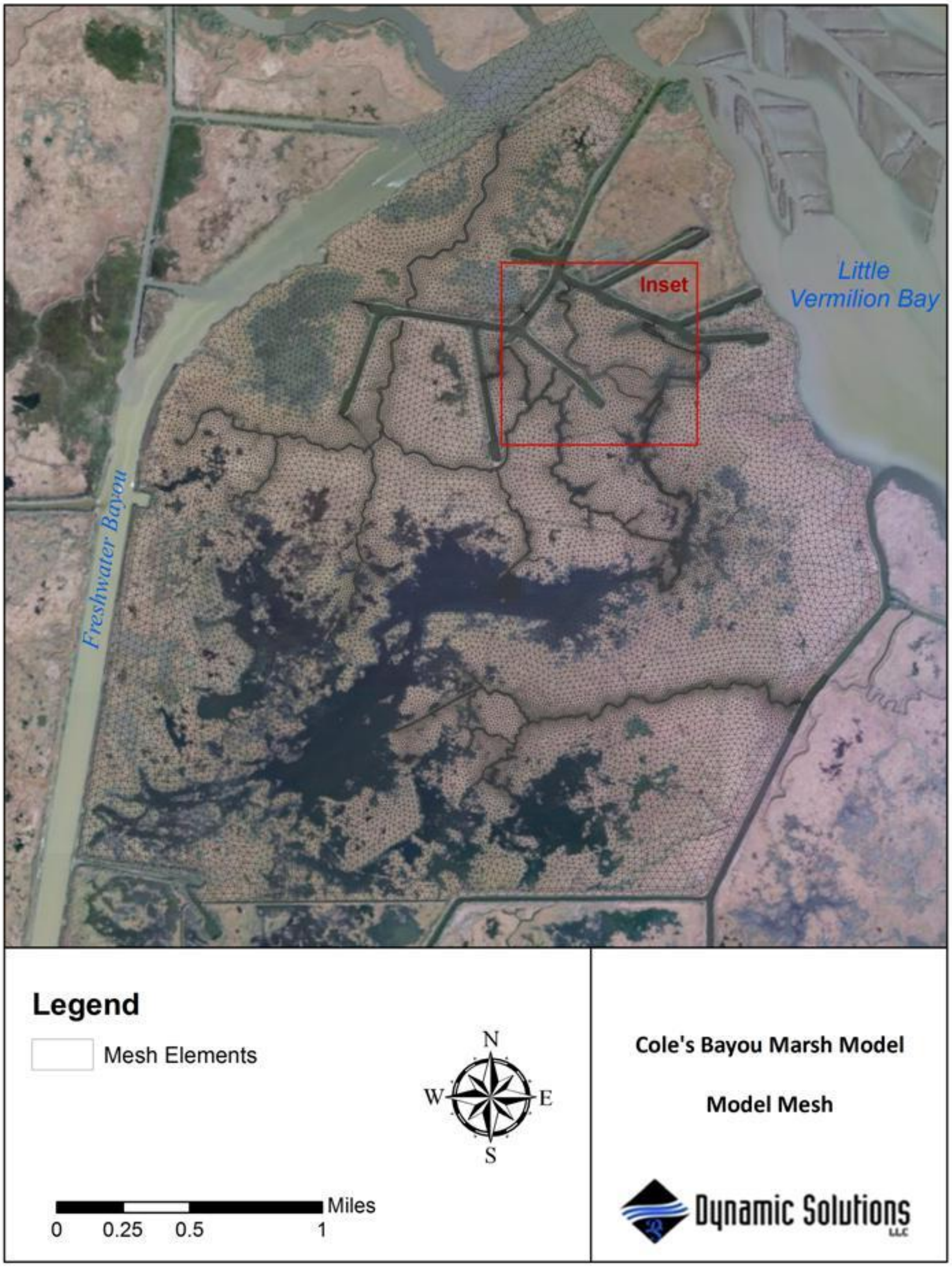

Figure 33 – Cole's Bayou Marsh model mesh, showing location of Figure 34 in the inset

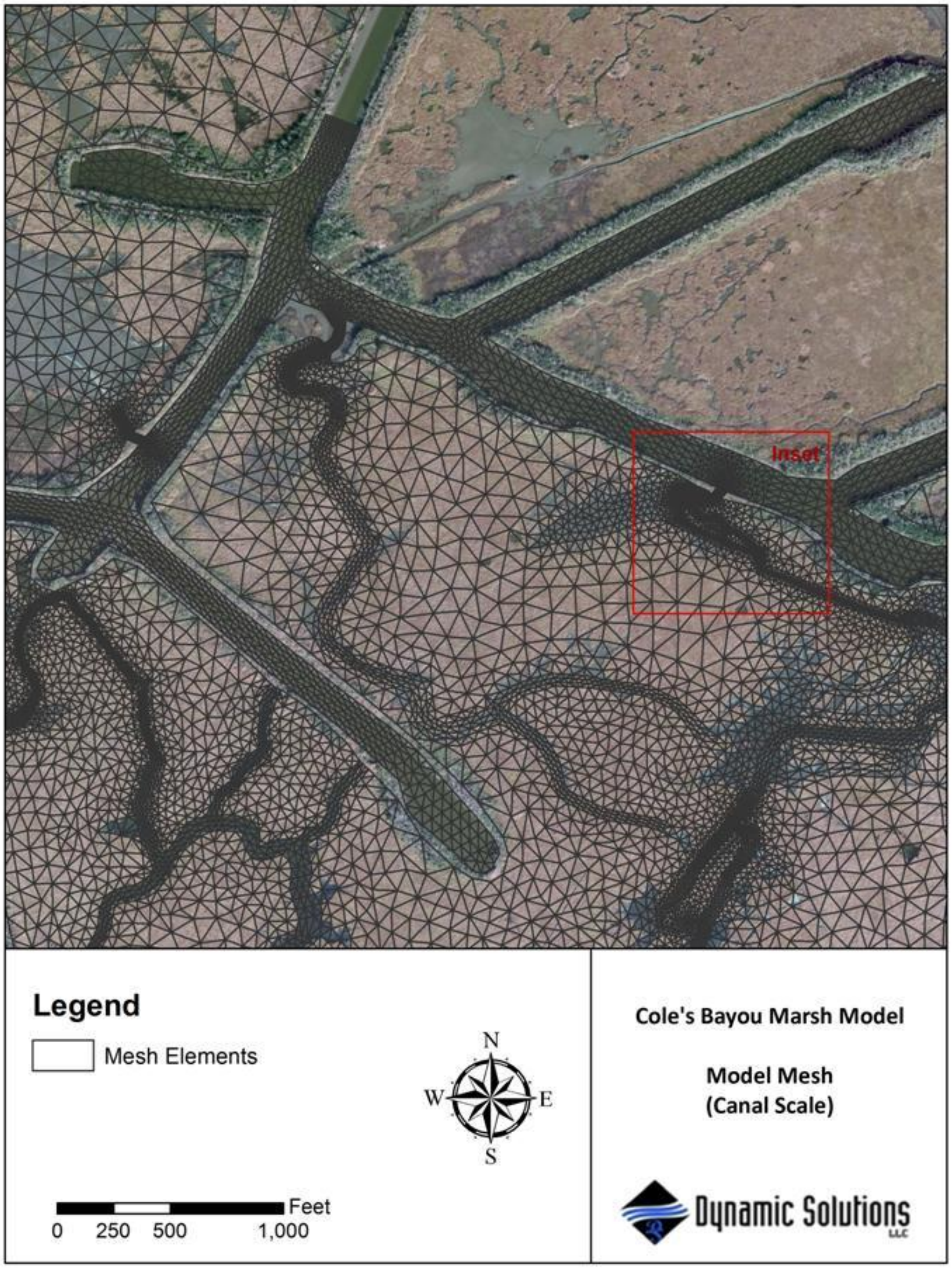

Figure 34 – Smaller scale view of the model mesh, highlighting elements in the Canals and marsh. The inset shows the location of Figure 35

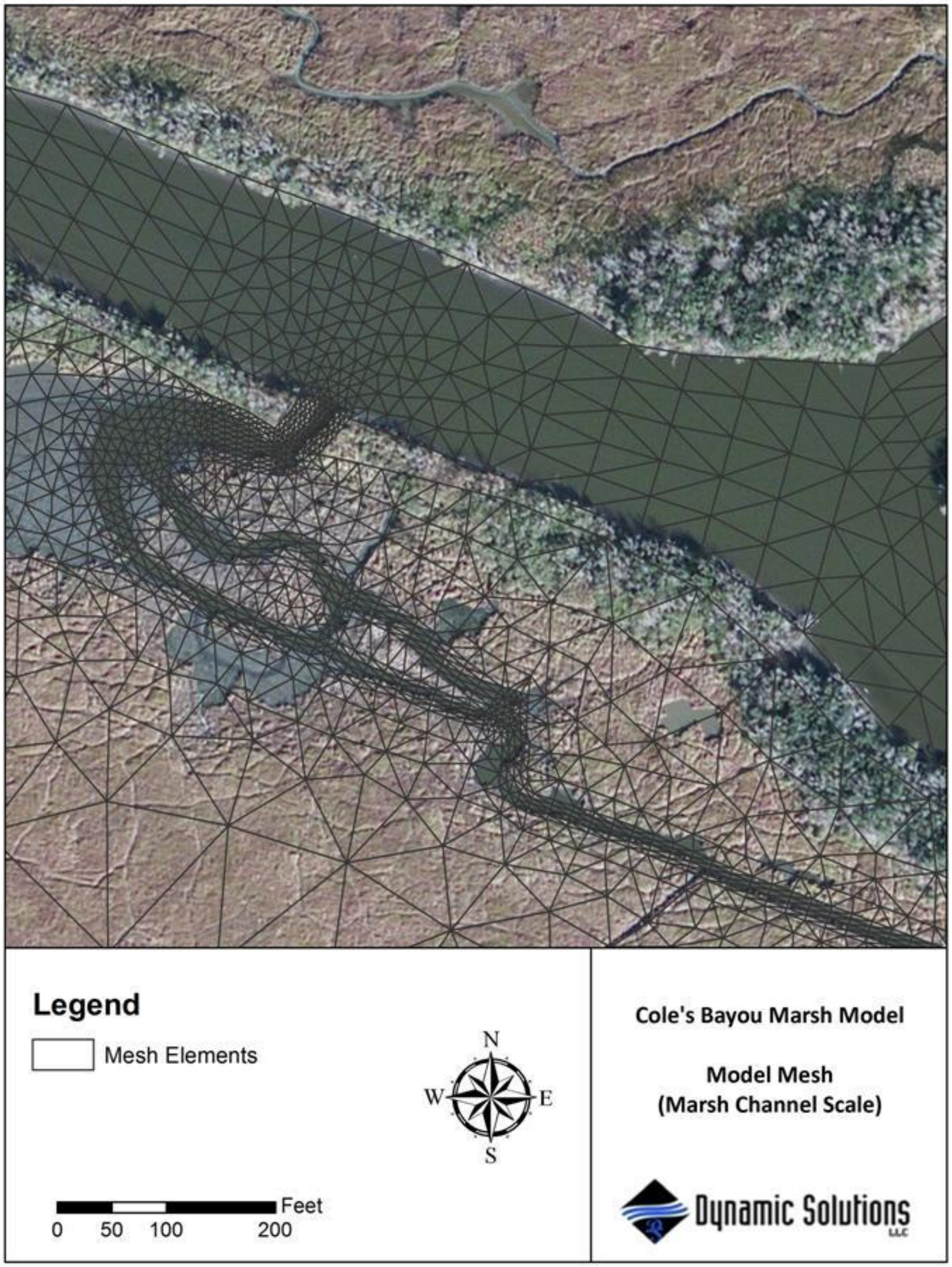

Figure 35 – Detail of Marsh model mesh showing greater resolution in the marsh channel connecting the eastern most breach and the central open water area

There are a number of very small channels, on the order of 5 – 10 feet wide, which convey water through the system yet were not explicitly accounted for in the model mesh. The model is intended to represent major processes and conveyance in the system, which is tested and proven in the calibration process. Not all of these minor channels can be included as the model would result in excessive run times and be inefficient when carrying out the modeling study. All channels that were associated with possible culvert locations identified in the Scope of Work (SOW) were detailed, as well as those which were observed to be conveying the most discharge in the system during field studies. One very small gap in the perimeter levee on the southeast side of the marsh, adjacent to the McIlheny Canal, was not explicitly modeled as it was on the order of 5 feet wide, no survey data was available for the connecting channels, and it was not identified as a structure location in the SOW. It is possible that due to long length of perimeter levee and dense vegetation that other gaps of this size may exist which were not surveyed. However, it will be shown in the model calibration that the major conveyance processes in the system are captured.

The elevation data was then applied to the mesh. The mesh was then reviewed in great detail and adjustments were made to ensure channels were continuous and connected to open water areas as accurately as known. Aerial photography was used to make further adjustments as they give the modeler a way to distinguish between higher-elevation vegetated areas and lower-elevation open water areas. In areas not covered by the survey, places shown by the photography to be lower-elevation which had been assigned marsh-level elevations were adjusted to an elevation representative of other open-water areas in the vicinity. The result was a mesh that represented the hydrodynamic processes of the Cole's Bayou Marsh subject to the constraints of available elevation data and mesh resolution.

3.5.2 Boundary Conditions

Boundary conditions provide the driving forces for the model. **Figure 36** shows the location of boundary conditions used for the Cole's Bayou Marsh model. Stage data were used at each of the boundaries: TV63-02 data for the boundary in Freshwater Bayou, TV63-03 for the Oil Field Canals and TV63-06 for the southern boundary in the McIlheny Canal. Flow at the model boundary is computed by the model based on water level gradients near the boundary. Water level is the primary hydrodynamic driver in the Oil Field Canals, McIlheny Canal, and Freshwater Bayou. Flow into and out of the marsh itself is governed by the hydraulic control of the cross-sections where the gaps in the levee exist. **Figure 37** shows the daily maximum and minimum water levels for each of the Marsh model boundary conditions.

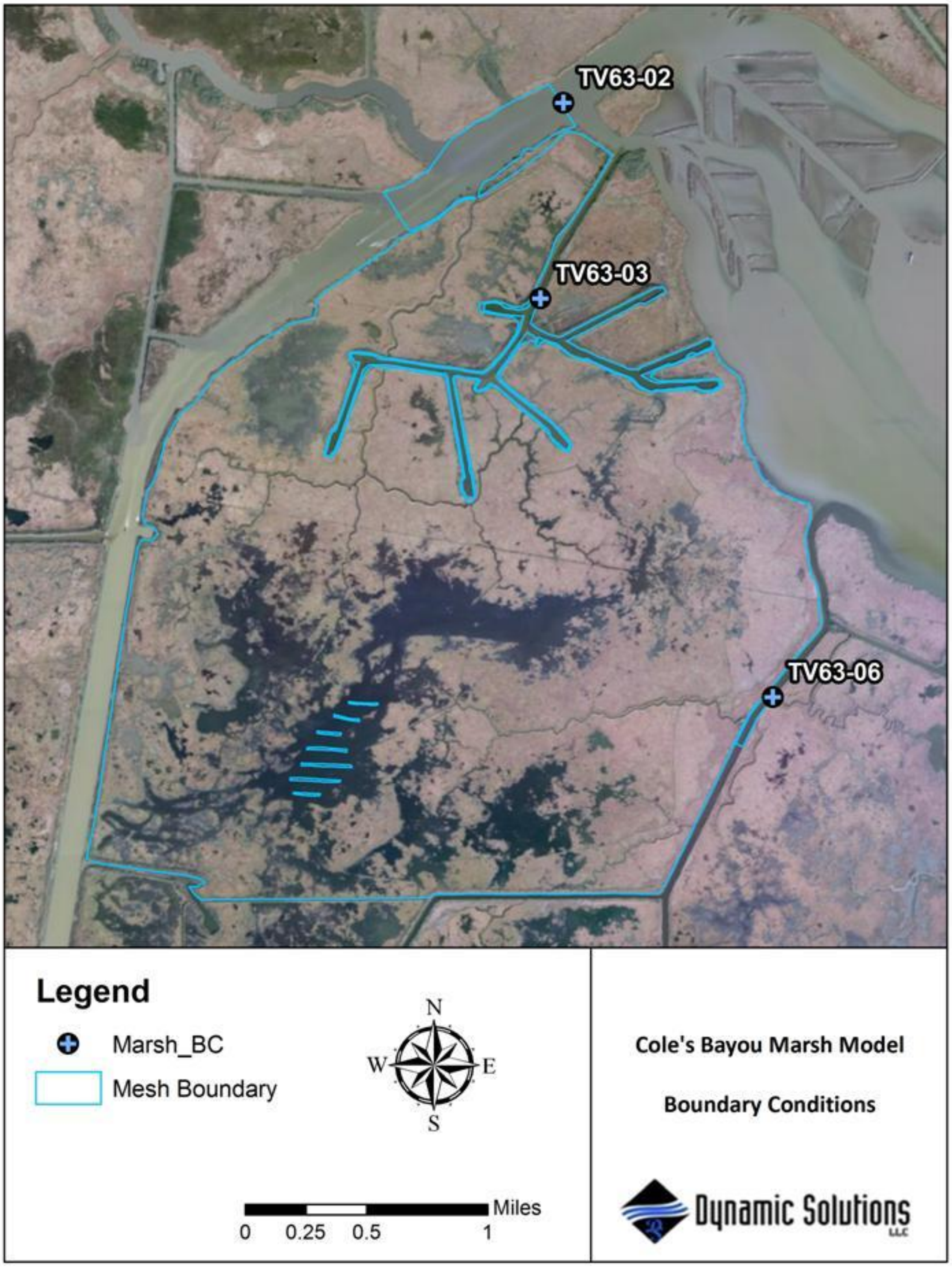

Figure 36 – Location and data series used for boundary conditions of the Cole's Bayou Marsh model

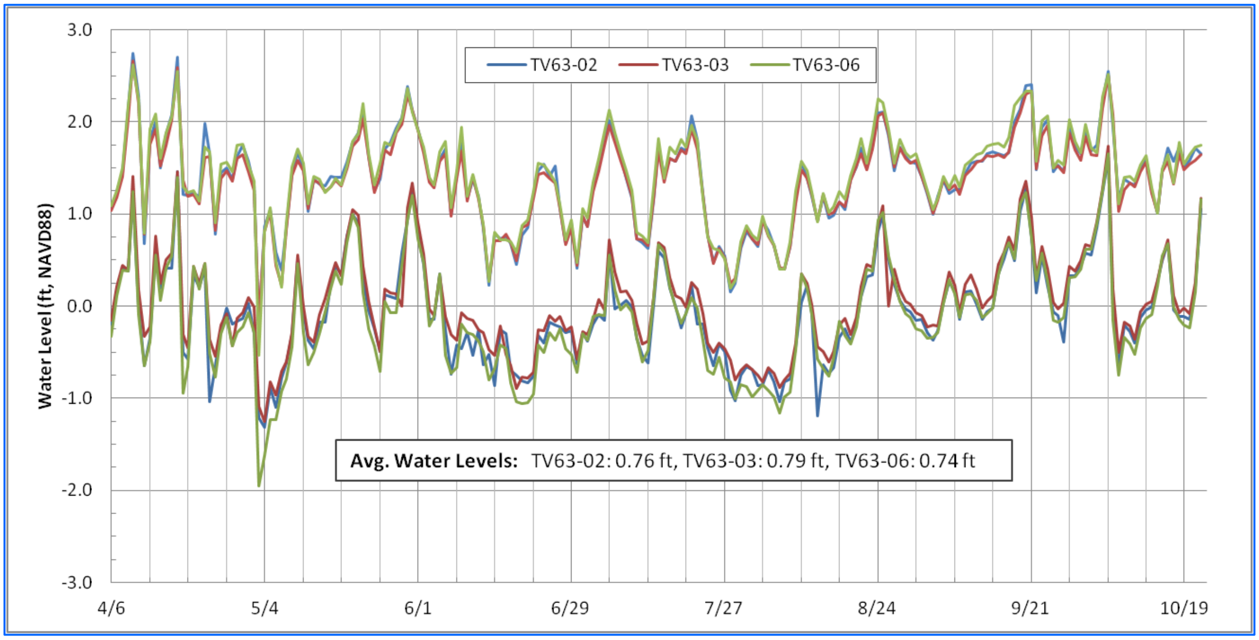

Figure 37 – Daily minimum and maximum water levels for the Cole's Bayou Marsh model boundary conditions, with average water level shown.

3.5.3 Model Setup

In order to properly partition roughness, eddy viscosity, and mesh adaption parameters five material types (categories of elements) were defined in the model: (1) northern marsh, (2) open water areas within the marsh, (3) the distributary marsh channels, (4) southern marsh, and (5) the Oil Field and McIlheny Canals, and Freshwater Bayou were one type representative of larger channels. The material types are shown in **Figure 38.**

Table 7 shows the model parameters for each material type. Roughness is parameterized two different ways in the model. The Manning's roughness coefficient (Manning's n) are used for channels and open water areas. The value of 0.02 is somewhat lower than what would be expected for the meandering, grass lined marsh channels for a 1-dimensional calculation in the literature (e.g. Chow et al., 1988). Internally, ADH converts the Manning's n provided to a roughness height which is then used to calculate a drag on the fluid. This roughness height implementation is depth-dependent, meaning large flow depths will result in a relatively lower drag force. Thus, the Manning's n values cannot be compared to those utilized by 1-dimensional models that use Manning's n to reflect losses due to boundary roughness and form losses. Two-dimensional models have turbulent form losses built in to the eddy viscosity formulation, so Manning's n is only a reflection of boundary roughness.

Table 7 – Model parameters for each material type

Material	Description	Roughness Scheme	Roughenss Value(s)	EEV	EVS
1	Northern marsh	URV[1]	0.1, 0.003, 500[2]	--	1
2	Open water in marsh	Manning	0.02	0.5	--
3	Marsh Channels	Manning	0.02	0.5	--
4	Southern Marsh	URV[1]	0.1, 0.003, 1500[2]	--	1
5	Surrounding canals, waters	Manning	0.02	0.5	--

[1] URV - Unsubmerged rigid vegetation

[2] Surface roughness (m), stem diameter (m), stem density (stems/sq. m)

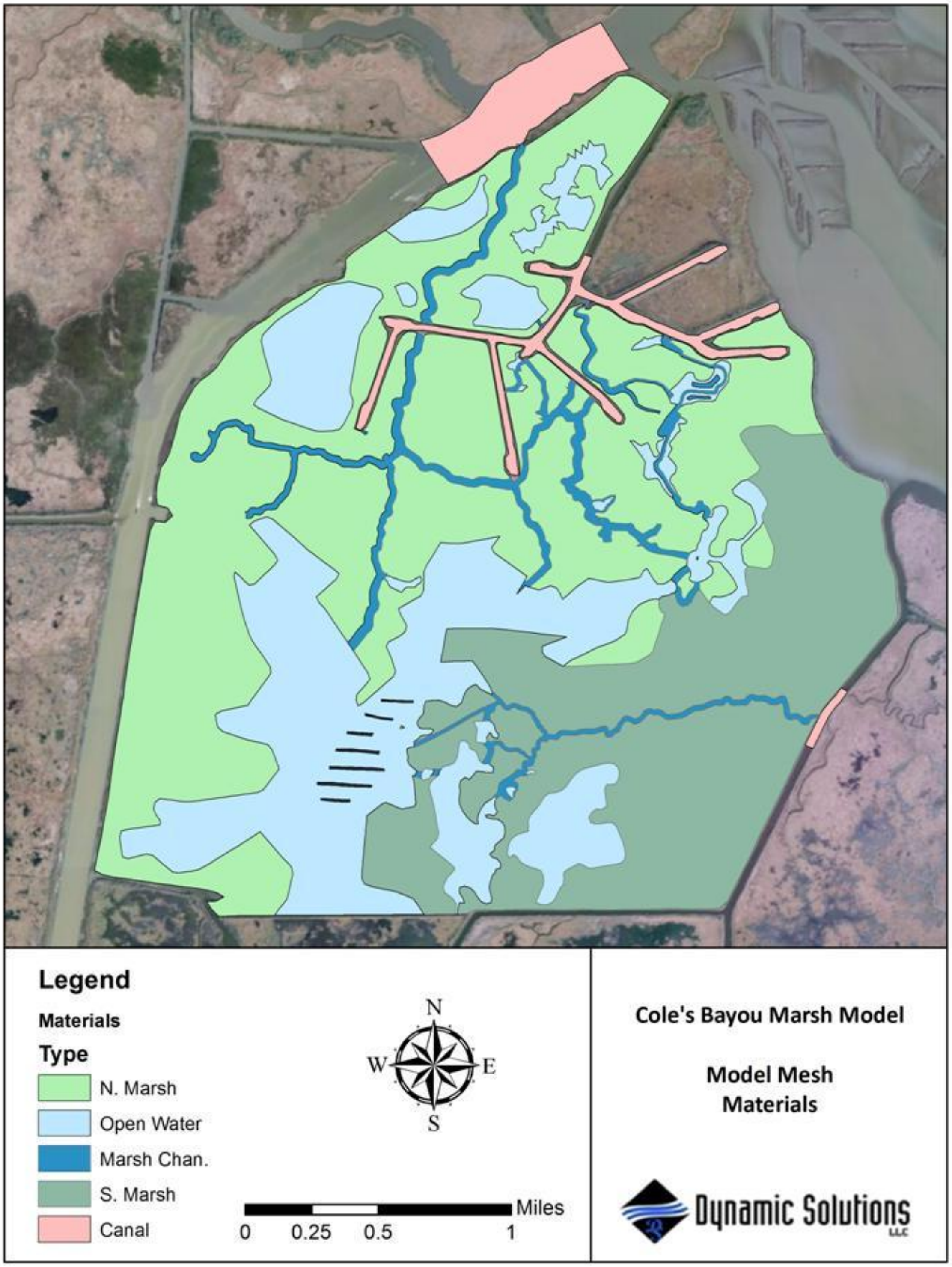

Figure 38 – Material types defined for the marsh model

Roughness for areas in the model that are high marsh and vegetated with *Spartina* grasses used the unsubmerged rigid vegetation (URV) friction option in ADH. The URV friction method uses the parameters entered - roughness height, stem diameter and stem density - to compute a shear stress coefficient to use in computing shear stress resulting from current through rigid vegetation. This accounts for the drag flow through the obstructions and the skin drag (Berger et al., 2010). Beginning with values utilized from past marsh models, the roughness parameters were adjusted during model calibration so that high flow timing and magnitude, where water levels are dependent on flows over the top of the marsh, reasonably matched observed data. The values used for marsh roughness were: a roughness height of 0.1m, stem diameter of 0.003m, and densities of 500 stem/m^2 for areas in the north (material 1) and 1500 stems/m^2 for the southern marsh (material 4).

For eddy viscosity in these simulations, EEV was used in the channels and EVS for marsh areas based on successful past experience by the modeling team.

The wetting and drying tolerance for the model (expressed in ADH as a DTL card) was set to 0.2 m. While this value has units of length, it is not simply a threshold for which a cell is considered dry; it controls the way ADH captures the hydrodynamic shock of a cell becoming wet or dry. Lower values simulate wetting and drying more exactly. The value of 0.2 was chosen based on prior experience with marsh models dependent on accurate, efficient wetting and drying computations. It was also subjected to a sensitivity analysis discussed in Section 4.2.2.

ADH utilizes a semi-implicit scheme with adaptive time stepping. The maximum time step allowed for this model was 400 seconds, but ADH will automatically cut the time step if the hydrodynamic solution does not converge numerically.

3.5.4 Calibration Data

The Cole's Bayou Marsh model was calibrated to stage two stations within the marsh; TV63-04 in the central open water area, and TV63-05 in an open water area in the southern part of the marsh (**Figure 39**). The discharge data collected during the December 2013 field visit was not synoptic however, field observations of the magnitude and direction of flows and connectivity of open water area provided the modeling team great insight into flow processes in the marsh.

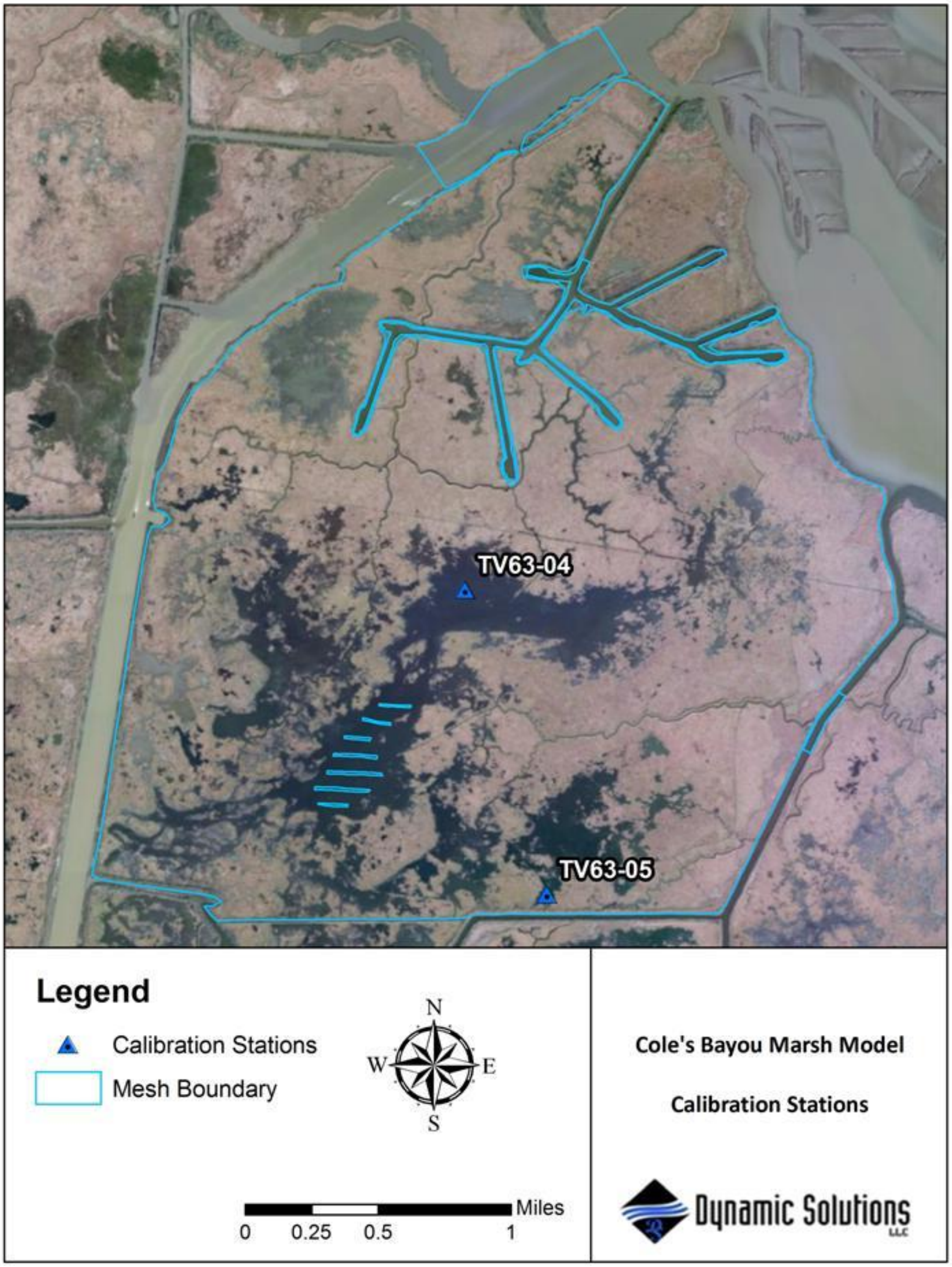

Figure 39 – Cole's Bayou Marsh model calibration stations

SECTION 4 MODEL CALIBRATION AND RESULTS

Calibration is a multi-step process by which the model is skillfully adjusted so it satisfactorily reproduces the critical system processes and the results match observed data. Root mean squared (RMS) error is used as the model-data comparison statistic for stage calibration. It is computed using the following equation

$$RMS = \sqrt{\frac{\sum_{i=1}^{N}(O_i - X_i)^2}{N}}$$

where *O* is the observed value, *X* is the corresponding model value in space and time, and *N* is the number of valid model-data pairs. Relative RMS (rRMS) is simply the RMS value divided by the range of the observed data. This provides a normalized value of RMS error. In some cases where the range of data is very small, rRMS can be very large even though the absolute errors are minor. Both RMS and rRMS should be examined to understand the accuracy of the model. Typical targets for water level RMSE are less than 0.3 feet, with an rRMSE of less than 15%. Targets for salinity are an RMS error of less than 3 ppt, or 25%.

4.1 Vermilion Bay

During calibration, it became apparent that modifications to the boundary condition time series were needed to accurately replicate the behavior of the system. The modifications to these series are noted in the "Boundary Conditions" section. Additionally, adjustment of the diffusion parameter was important to achieving calibration to observed salinity data. Calibration results for both water level and salinity at the Cypremort Point, CRMS0541, Bayou Fearman, TV36-03, and TV36-06 are summarized in **Table 8** and discussed herein.

Table 8 – Summary of Vermilion Bay Model calibration results

	Water Level		Salinity	
Station	**RMS (ft)**	**rRMS**	**RMS (ppt)**	**rRMS**
Cypremort Point	0.28	6%	1.6	10%
Bayou Fearman	0.31	7%	3.0	26%
CRMS0541	0.21	4%	4.0	14%
TV63-03	0.09	2%	2.7	24%
TV63-06	0.16	4%	2.9	37%

Overall the calibration can be considered good. Typical targets for water level calibration is for RMS error less than 0.3 feet and relative RMS errors less than 15%. All stations meet the targets for water level RMS and rRMS with the exception of the RMS error at Bayou Fearman, which is very close. The water level errors near the marsh, at stations TV63-03 and TV63-06, are excellent. Target RMS errors for salinity are 3 ppt and relative RMS error of 25%. The target for one of these is met at each station. At

CRMS0541 the RMS error is 4.0, but because of the large range of salinity the relative RMS is only 14%, which is acceptable. At TV63-06 the RMS error meets the target but due to the smaller range of salinity values the relative RMS is higher than the target (37%). On the whole, the model can be considered to represent the dominant processes in the Vermilion Bay system.

The RMS error for stage calibration at Cypremort (**Figure 40**) is 0.28 feet with a relative RMS error (rRMSE) of 0.06. The model slightly over-predicts low tide. The trend is excellent, and the model simulates large changes in water level very well in magnitude, timing, and the rate of rise and fall. The RMS error is less the target. Overall, the calibration can be considered excellent.

The RMS error for stage calibration at Bayou Fearman (**Figure 41**) is 0.31 feet with an rRMSE of 0.07. The model again slightly over-predicts low tide. The trend is very good, and the model simulates large changes in water level very well in magnitude, timing, and the rate of rise and fall. The RMS error is slightly above the target. Overall the calibration can be considered adequate.

The RMS error for stage calibration at CRMS0541 (**Figure 42**) is 0.21 feet with an rRMSE of 0.04. The model is slightly low at high tide. The overall trend is very good, and the model simulates large changes in water level very well in magnitude, timing, and the rate of rise and fall. The RMS error is below the target. Overall, the calibration can be considered good.

The RMS error for stage calibration at TV63-03 (**Figure 43**) is 0.09 feet with an rRMSE of 0.02. The model very accurately predicts stage throughout the model time period. The overall trend is very good, and the model simulates large changes in water level very well in magnitude, timing, and the rate of rise and fall. This station is very important, as it is the closest to the study area. Overall, the calibration can be considered excellent.

The RMS error for stage calibration at TV63-06 (**Figure 44**) is 0.16 feet with an rRMSE of 0.04. The model accurately predicts stage, although results are slightly high at low tide. The overall trend is very good, and the model simulates large changes in water level very well in magnitude, timing, and the rate of rise and fall. This station is very important, as it is close to the study area. Overall, the calibration can be considered good.

The RMS error for salinity calibration at Cypremort Point (**Figure 45**) is 1.6 ppt with a relative RMS error (rRMSE) of 0.10. The model does not capture the full range of the salinity, which is likely due to the protected location of the gage compared to the open model or minor local freshwater inflows. The trend is good, and the model simulates large changes in salinity in magnitude, timing, and the rate of rise and fall. The RMS error is less the target. Overall, the calibration can be considered good.

The RMS error for salinity calibration at CRMS0541 (**Figure 46**) is 4.0 ppt with an rRMSE of 0.14. While the RMS error is large, the rRMSE is low, due to the large range of values at this location (less than 1 ppt to more than 28 ppt). The model captures the general trend and magnitude of salinity at this location. The continued high salinity after the spike on 8/10 is due to a smaller than actual outflux through Southwest Pass following this event. This causes elevated salinity values after 8/10 over much of the model domain due to the large volume of high-salinity of water that persists in Vermilion Bay and is advected throughout the model. The trend following the overreaction of the model is correct, but salinity values from this point forward are high. Overall, the calibration can be considered satisfactory.

The RMS error for salinity calibration at Bayou Fearman (**Figure 47**) is 3.0 ppt with an rRMSE of 0.26. The model is not as accurate at this location, although the overall trend is fairly good. Especially at this location, errors are likely due to flows through local marsh and small channels that are not represented in the model. The RMS error is slightly above the target. Overall the calibration can be considered adequate.

The RMS error for salinity calibration at TV63-03 (**Figure 48**) is 2.7 ppt with an rRMSE of 0.24. The model generally captures the trend of salinity, with some lingering higher salinities at the end of the calibration period. Overall, the calibration can be considered sufficient.

The RMS error for salinity calibration at TV63-06 (**Figure 49**) is 2.9 ppt with an rRMSE of 0.37. At this location, at the end of a dead end channel, the model does not capture the small variations in salinity seen in the field data. This is likely due to some flow through the channel, either subsurface or minor channels that are not represented in the model. The general trend is replicated in the model, and the calibration results are acceptable at this location.

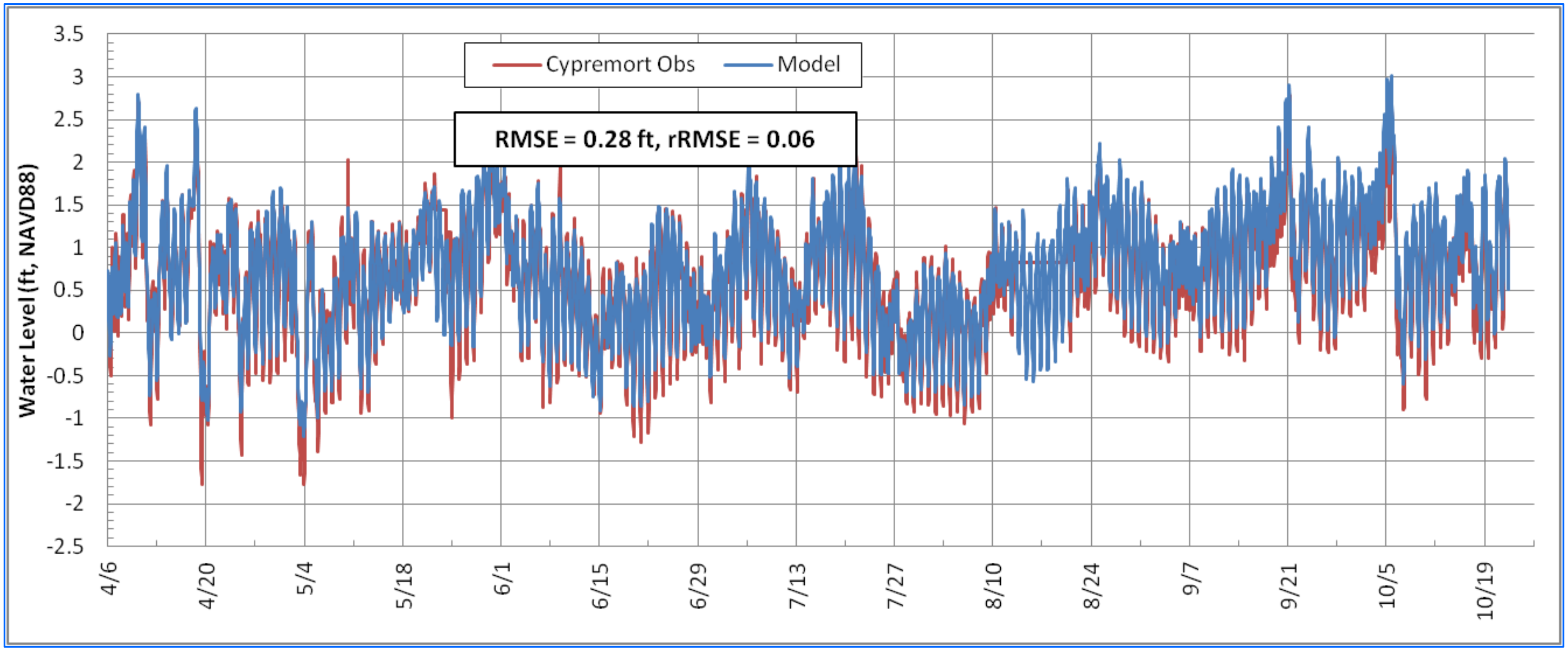

Figure 40 – Water Level calibration at Cypremort Point

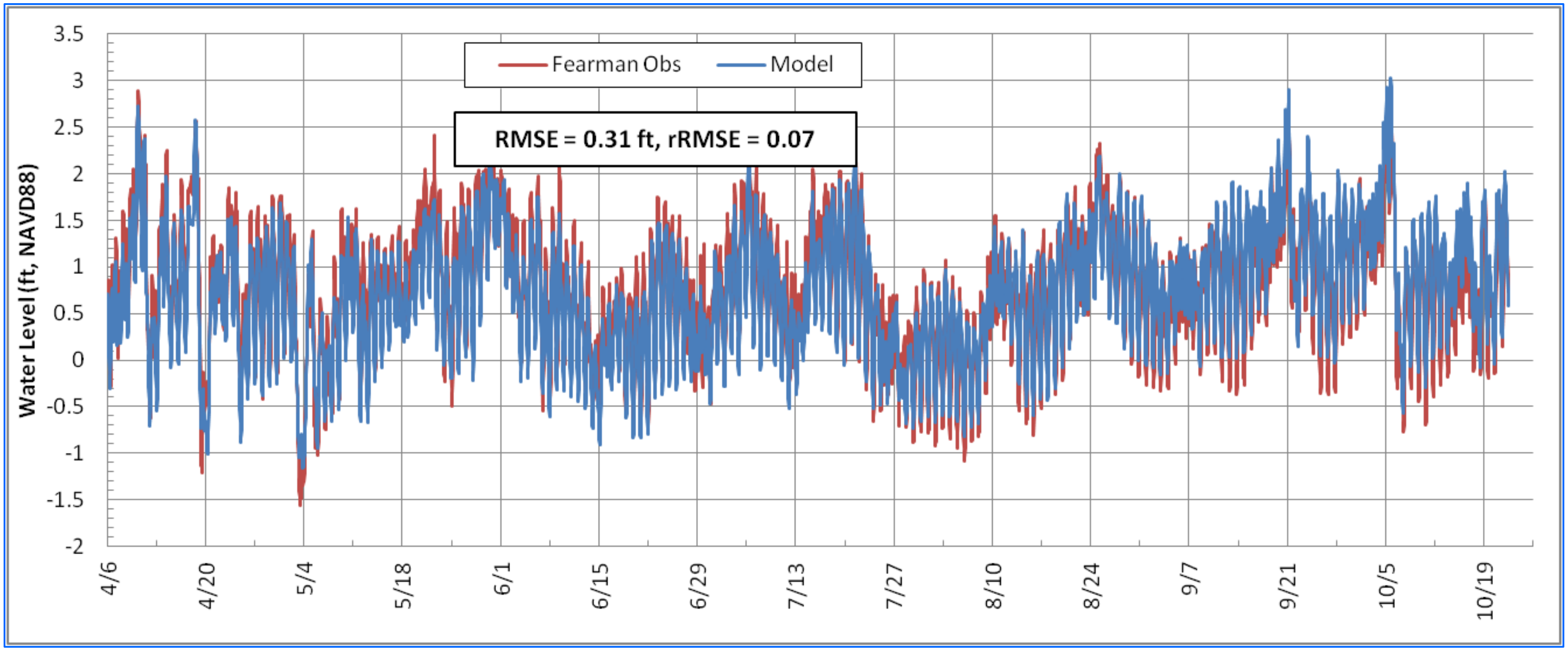

Figure 41 – Water Level calibration at Bayou Fearman

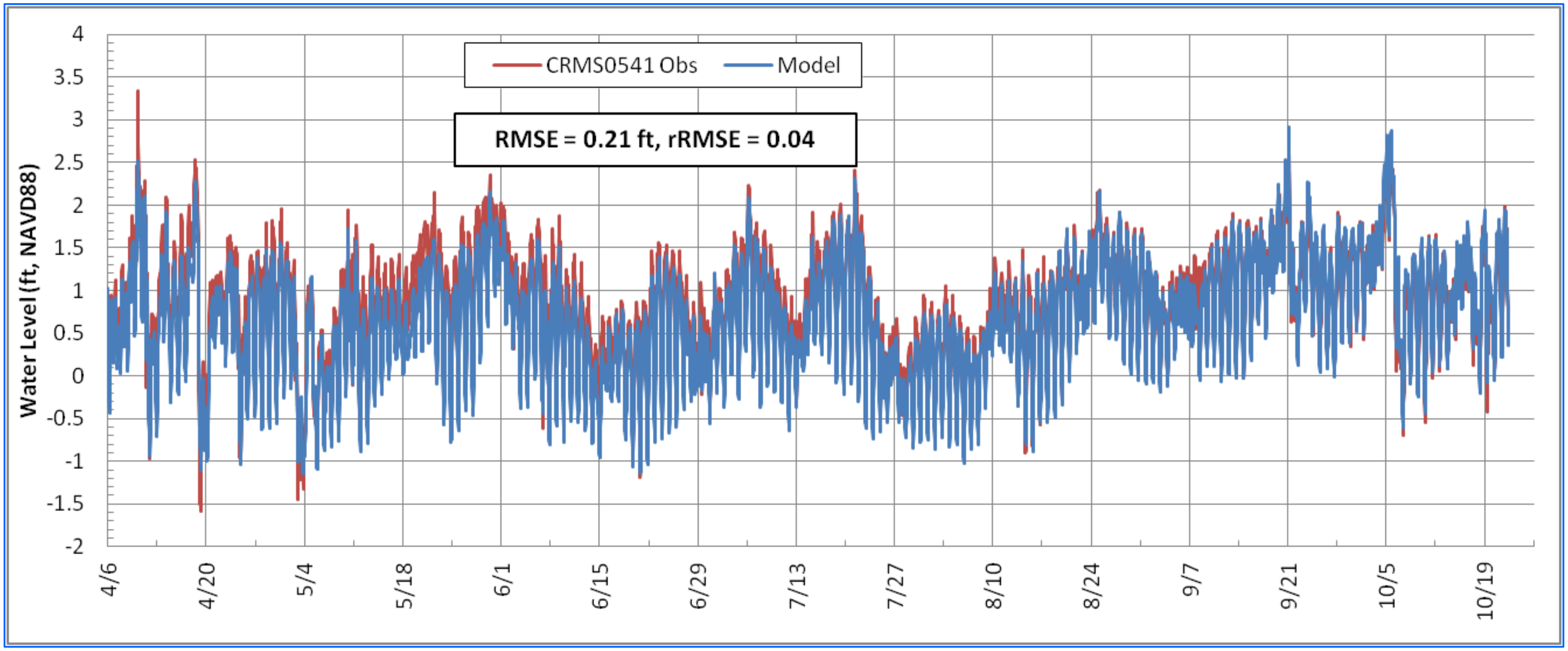

Figure 42 – Water Level calibration at CRMS0541

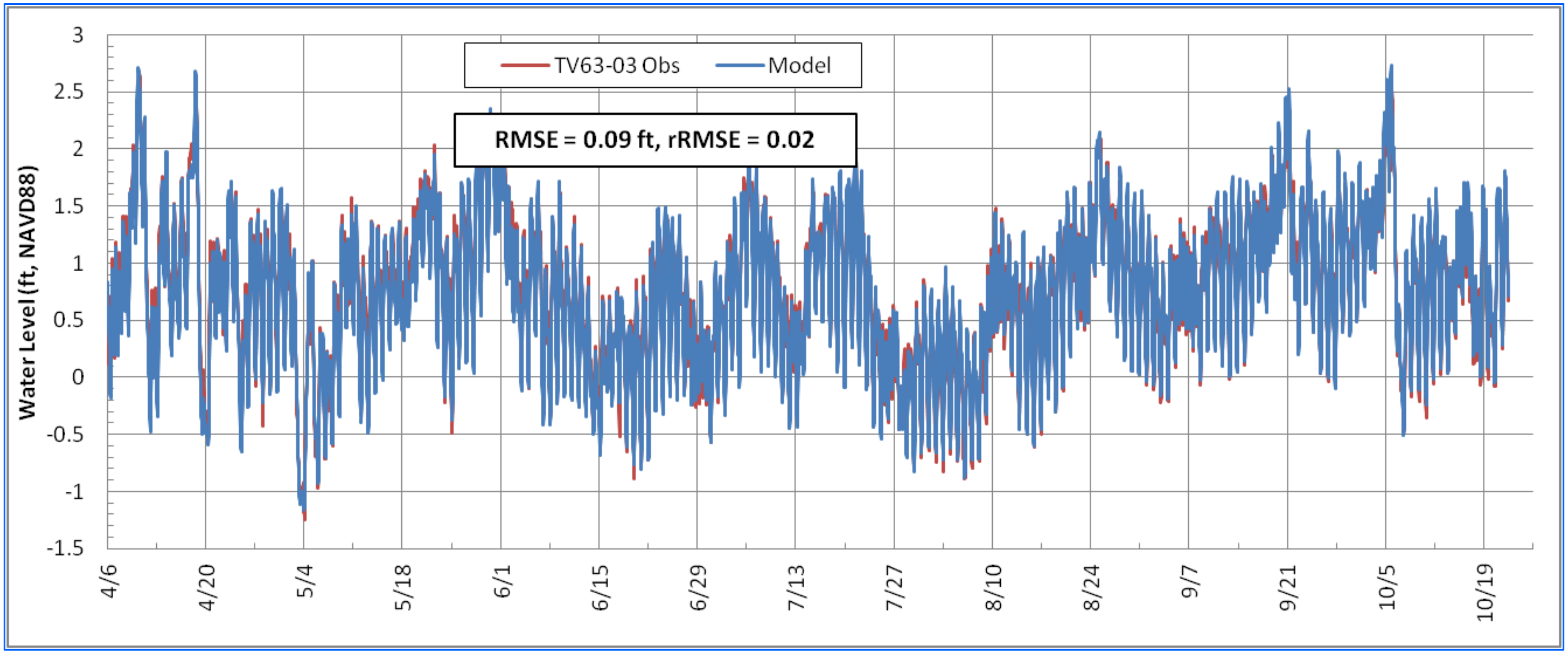

Figure 43 – Water Level calibration at TV63-03

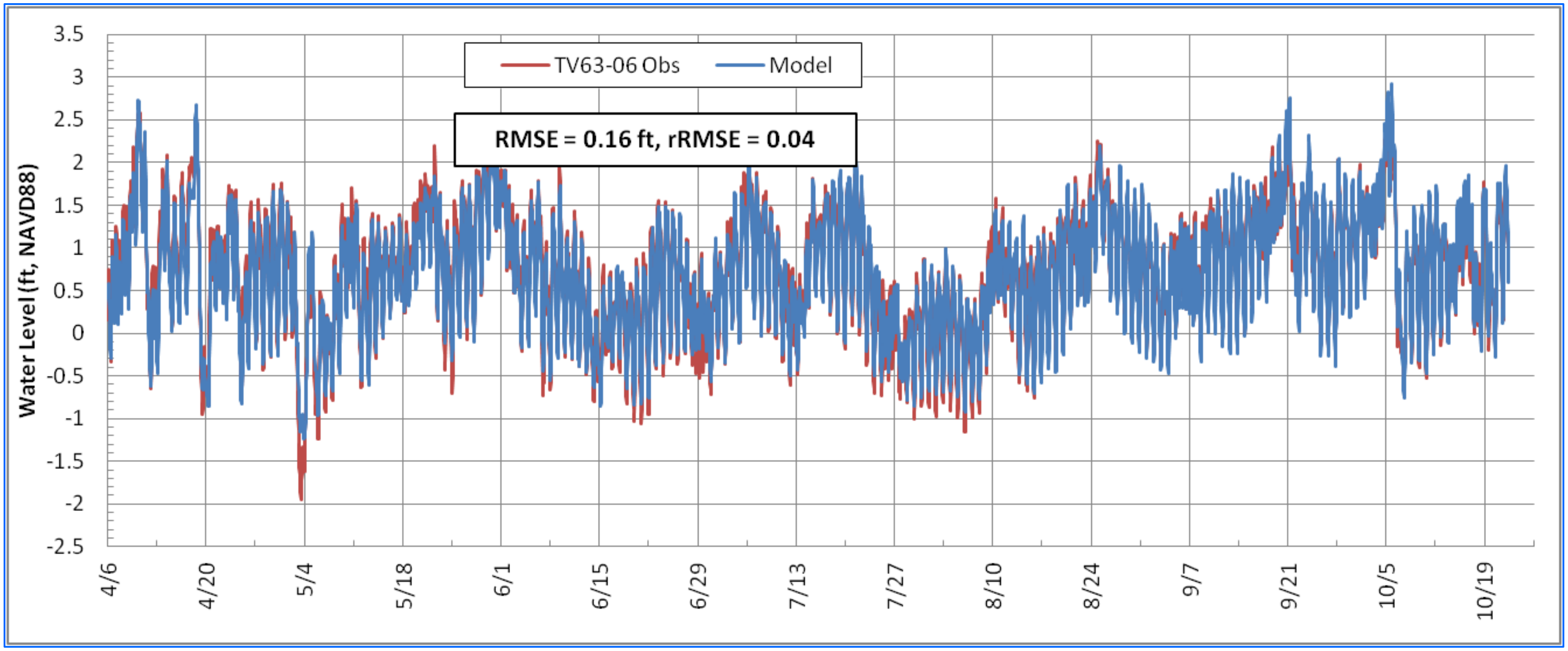

Figure 44 – Water Level calibration at TV63-06

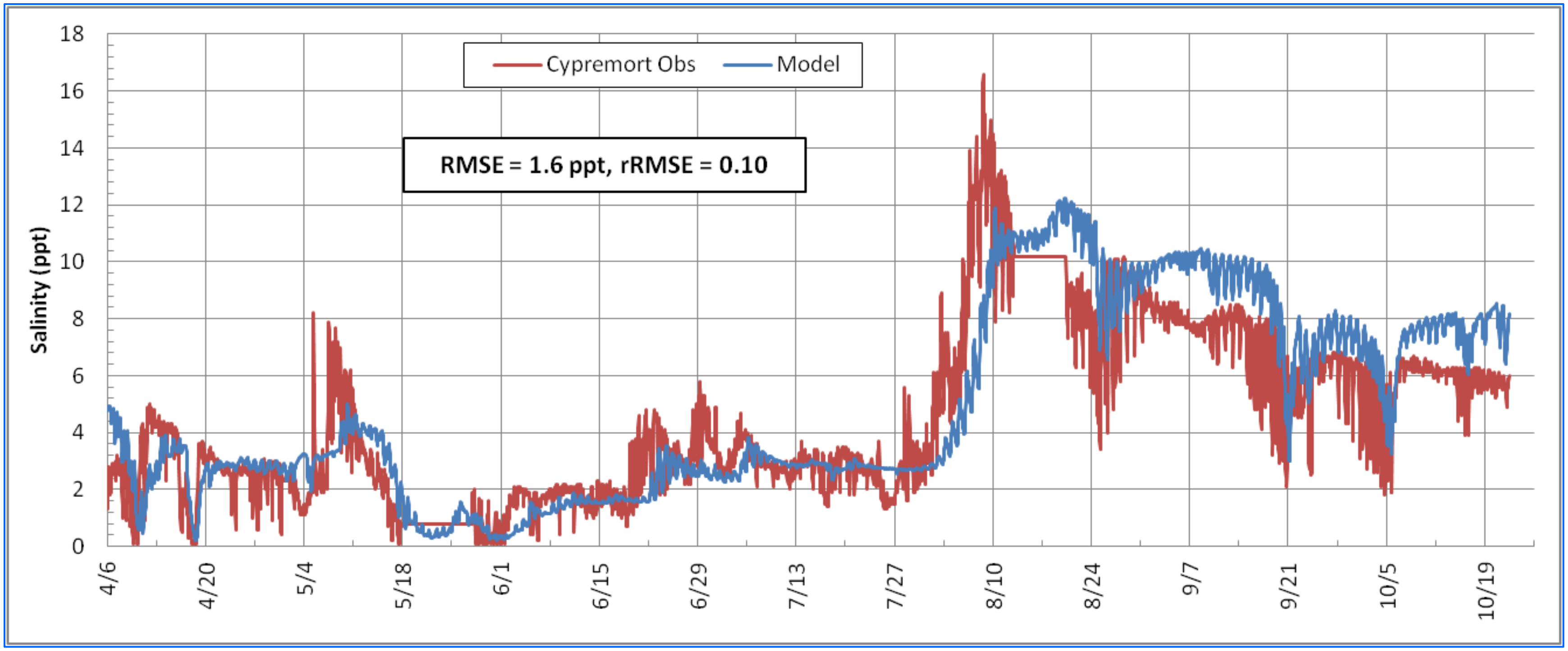

Figure 45 – Salinity calibration at Cypremort Point

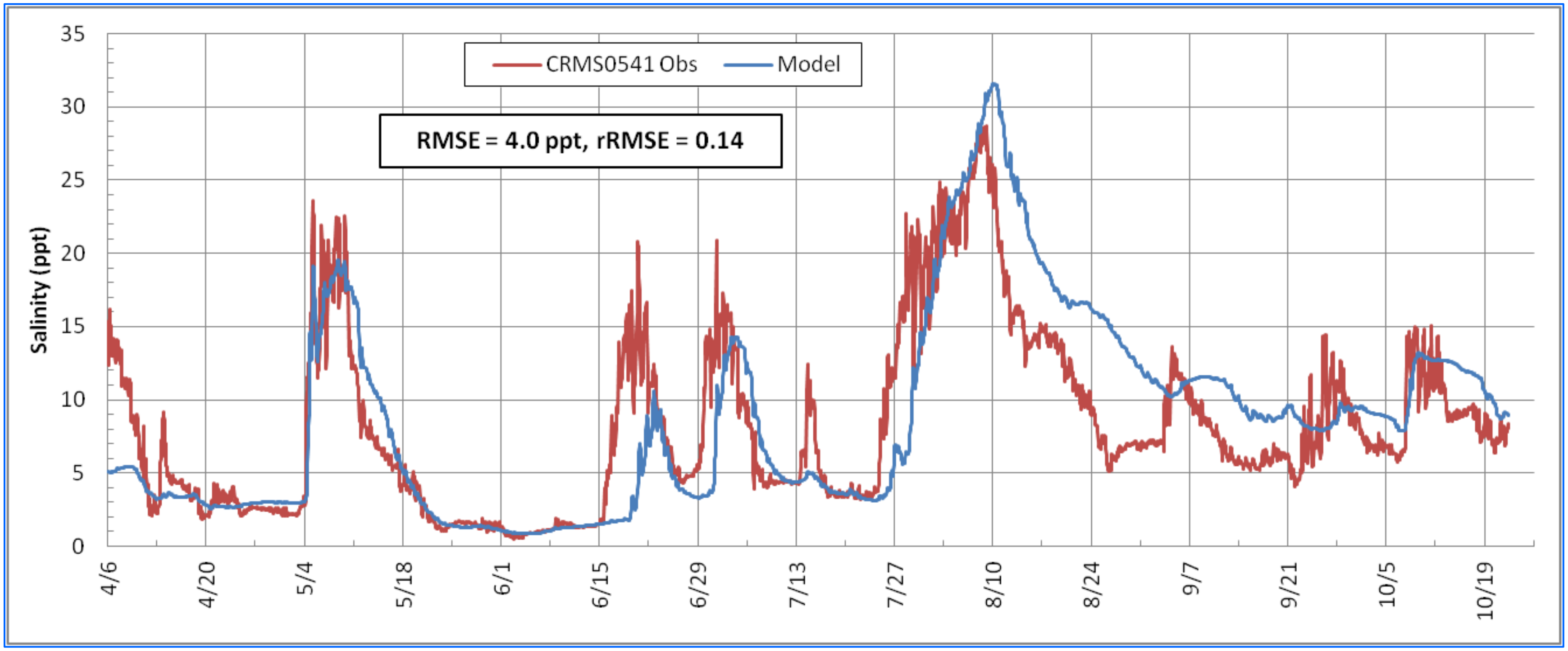

Figure 46 – Salinity calibration at CRMS0541

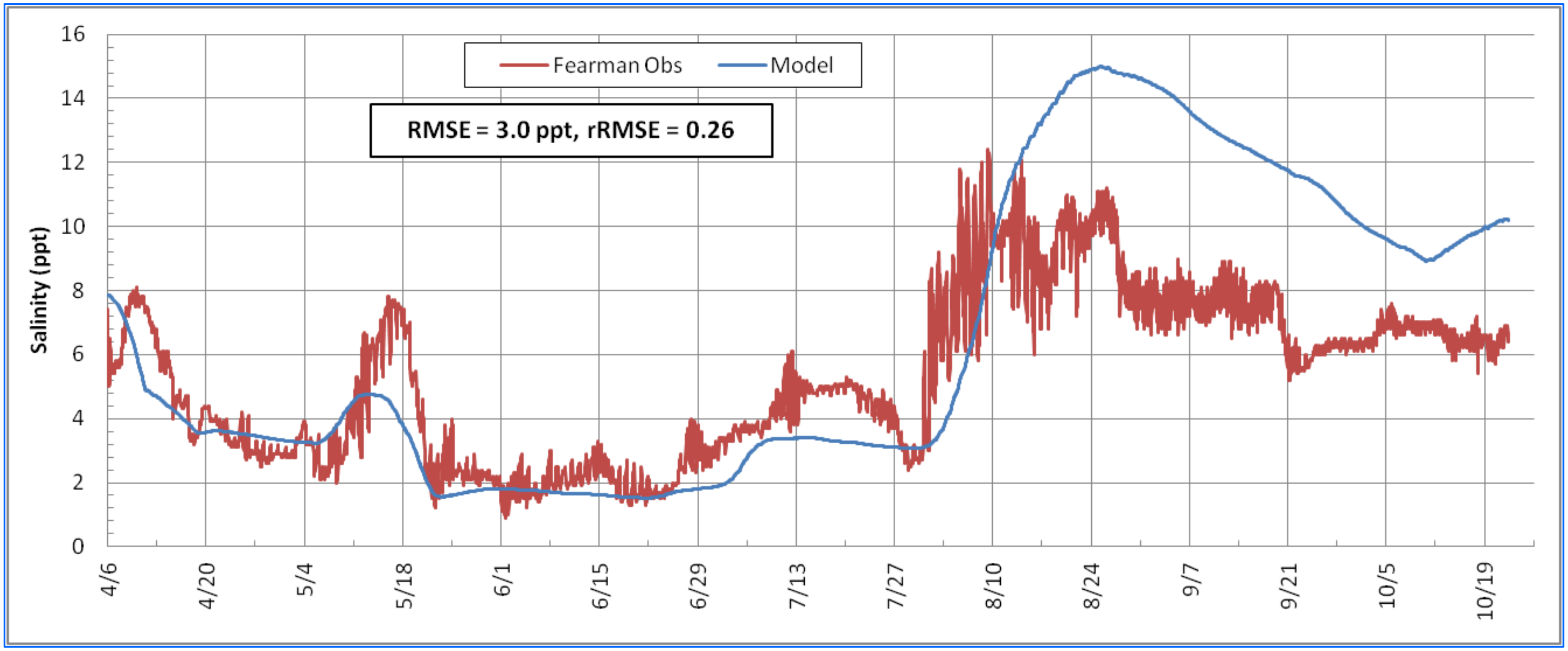

Figure 47 – Salinity calibration at Bayou Fearman

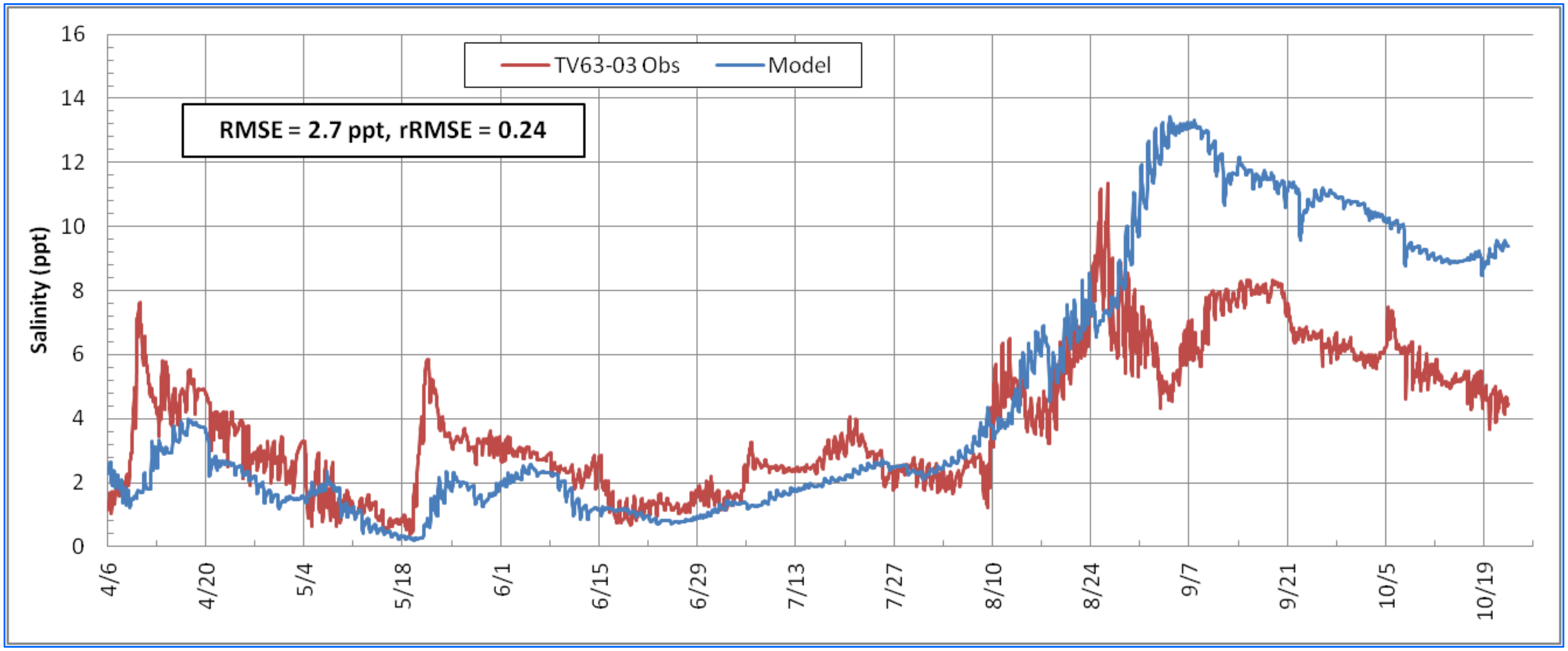

Figure 48 – Salinity calibration at TV63-03

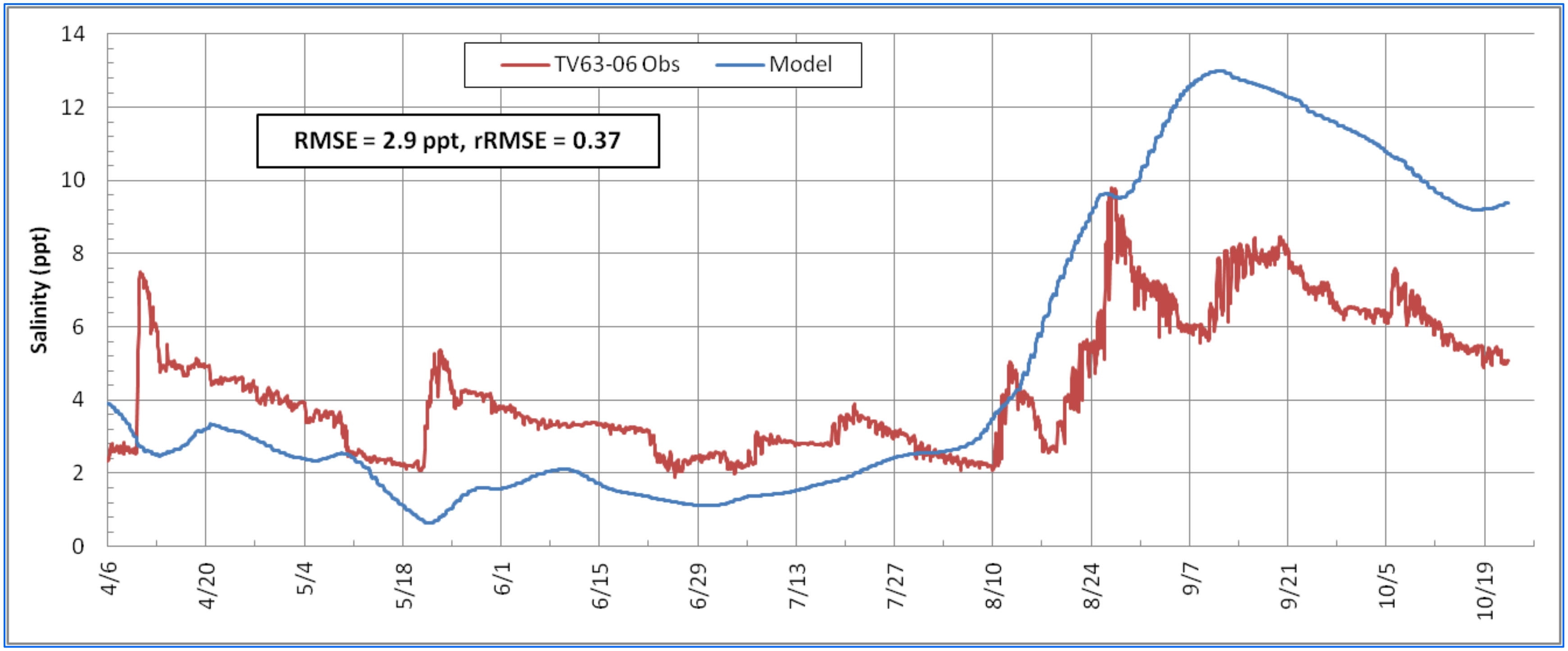

Figure 49 – Salinity calibration at TV63-06

4.2 Cole's Bayou Marsh

4.2.1 Calibration

The multi-step calibration process included adjusting, and by default performing sensitivity analyses on, model roughness, wetting/drying parameter, and top of marsh elevation. The model parameters used for the calibrated model are shown in Table 7. Stage (water level) calibration plots for TV63-04 and TV63-05 are shown in **Figure 50** and **Figure 51.** Salinity calibration plots for TV TV63-04 and TV63-05 are shown in **Figure 52** and **Figure 53**. A summary of the calibration results for the Cole's Bayou Marsh model is presented in **Table 9.**

Table 9 – Summary of Cole's Bayou Marsh model calibration results

	Water Level		Salinity	
Station	**RMS (ft)**	**rRMS**	**RMS (ppt)**	**rRMS**
TV63-04	0.14	6%	0.5	7%
TV63-05	0.19	11%	0.6	11%

The calibration to these two stations can be considered excellent. Typical targets for water level calibration is for RMS error less than 0.3 feet and relative RMS errors less than 15% and both stations are well below those targets. The range of salinity in the marsh is small, with a maximum observed value of about 8 ppt at TV63-04. Target RMS errors for salinity are less than 3 ppt which are easily met. Here the relative RMS is a more representative statistic; the target is typically 25%, which is met at both stations. The model can be considered to represent the dominant processes in the system.

The RMS error for stage calibration at TV63-04 is 0.14 feet with a relative RMS error (rRMSE) of 0.06. The model slightly over-predicts moderate and high stages. Tidal variation at stable, moderate stages is low but better for low stages. The trend is excellent and the model simulates large changes in water level very well in magnitude, timing, and the rate of rise and fall. The RMS error is considerably less the target. The calibration can be considered excellent.

The RMS error for stage calibration at TV63-05 is 0.19 feet with a relative RMS error (rRMSE) of 0.11. The model matches the trend of the observed data very well. The model exhibits more variation on the daily time scale and rises and falls at a higher rate than the observed data. This indicates that in this open water area the model has greater hydraulic connection to the outside forcings than exists. Ultimately the calibration is considered very good because the trend indicates the model is captures the major processes occurring in this region corresponding to an RMS error significantly less than the target.

The RMS error for salinity calibration at TV63-04 is 0.5 ppt with an rRMSE of 0.07. The modeled salinity exhibits the same trend as the observed data which indicates that the advection of salinity into the core of the marsh is good.

The RMS error for salinity at TV63-05 is 0.6 ppt with an rRMSE of 0.11. Modeled salinity values are on average lower than those observed an also exhibit less variation.

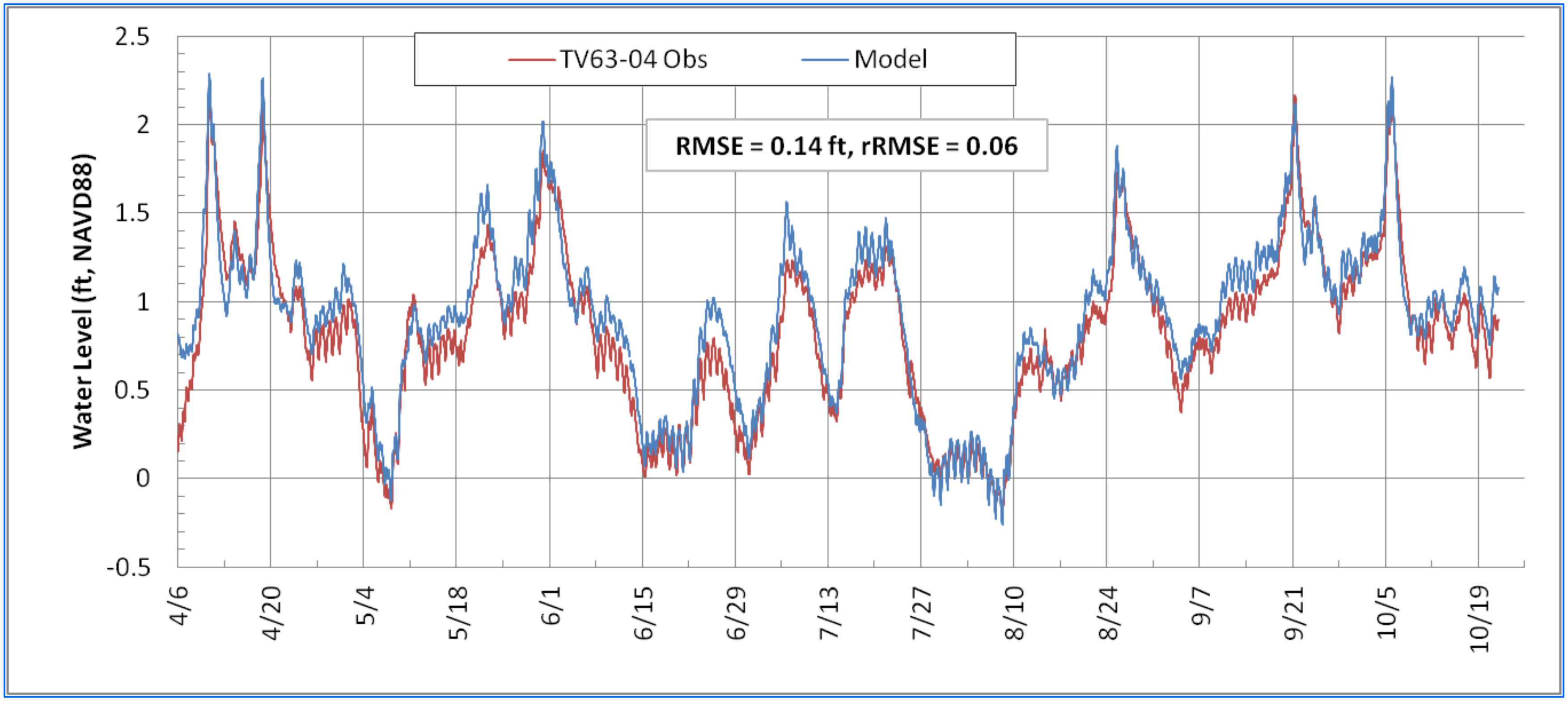

Figure 50 – Stage calibration for station TV63-04, central open water area

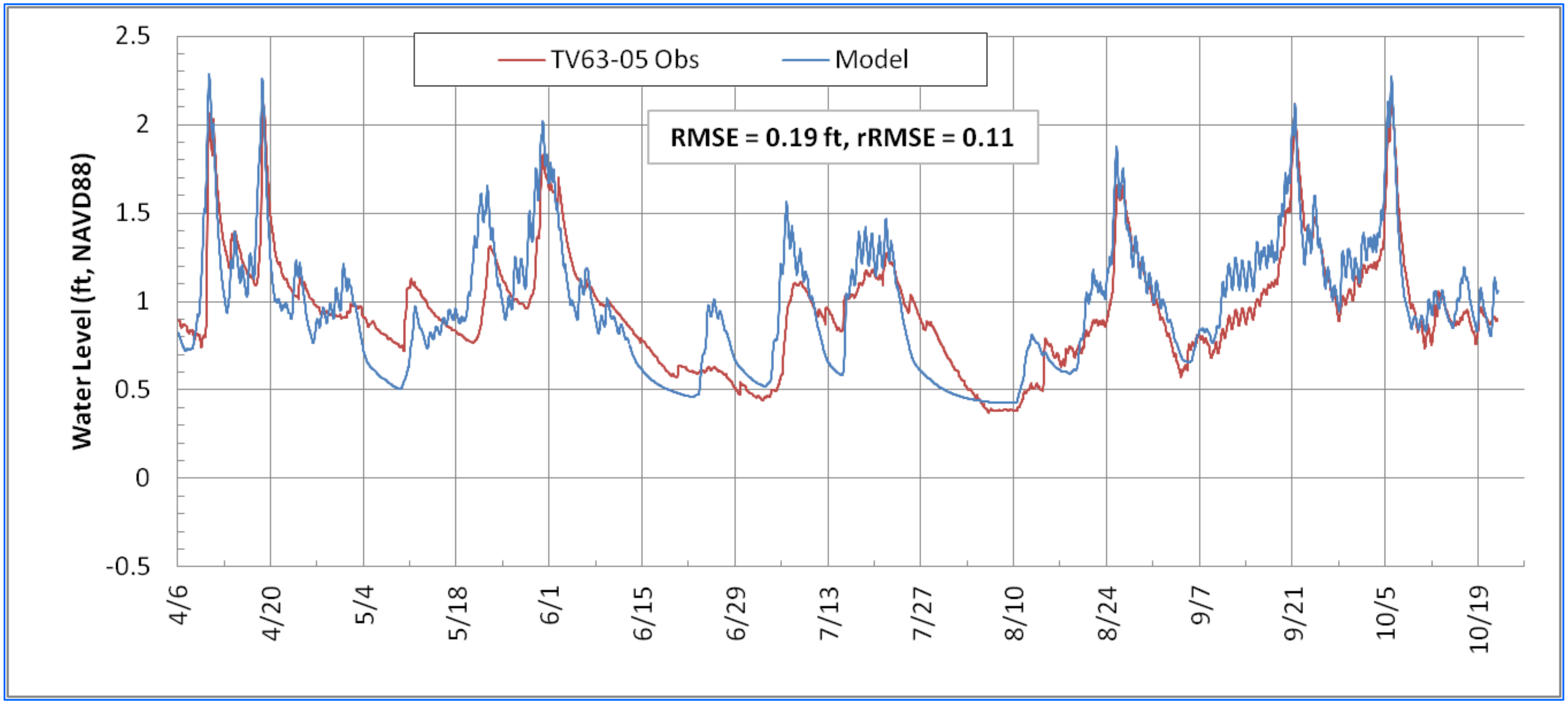

Figure 51 – Stage calibration for station TV63-05, southern open water area

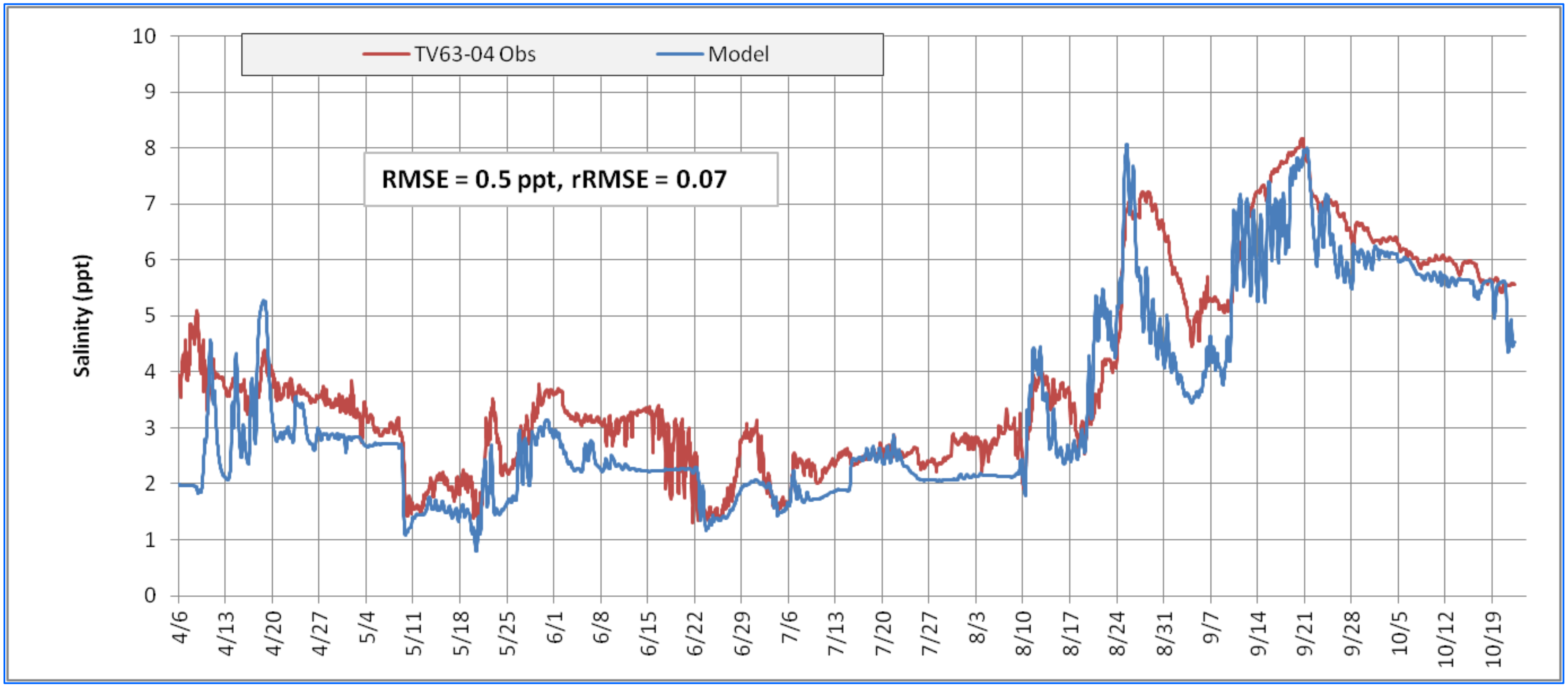

Figure 52 – Salinity calibration for station TV63-04, central open water area.

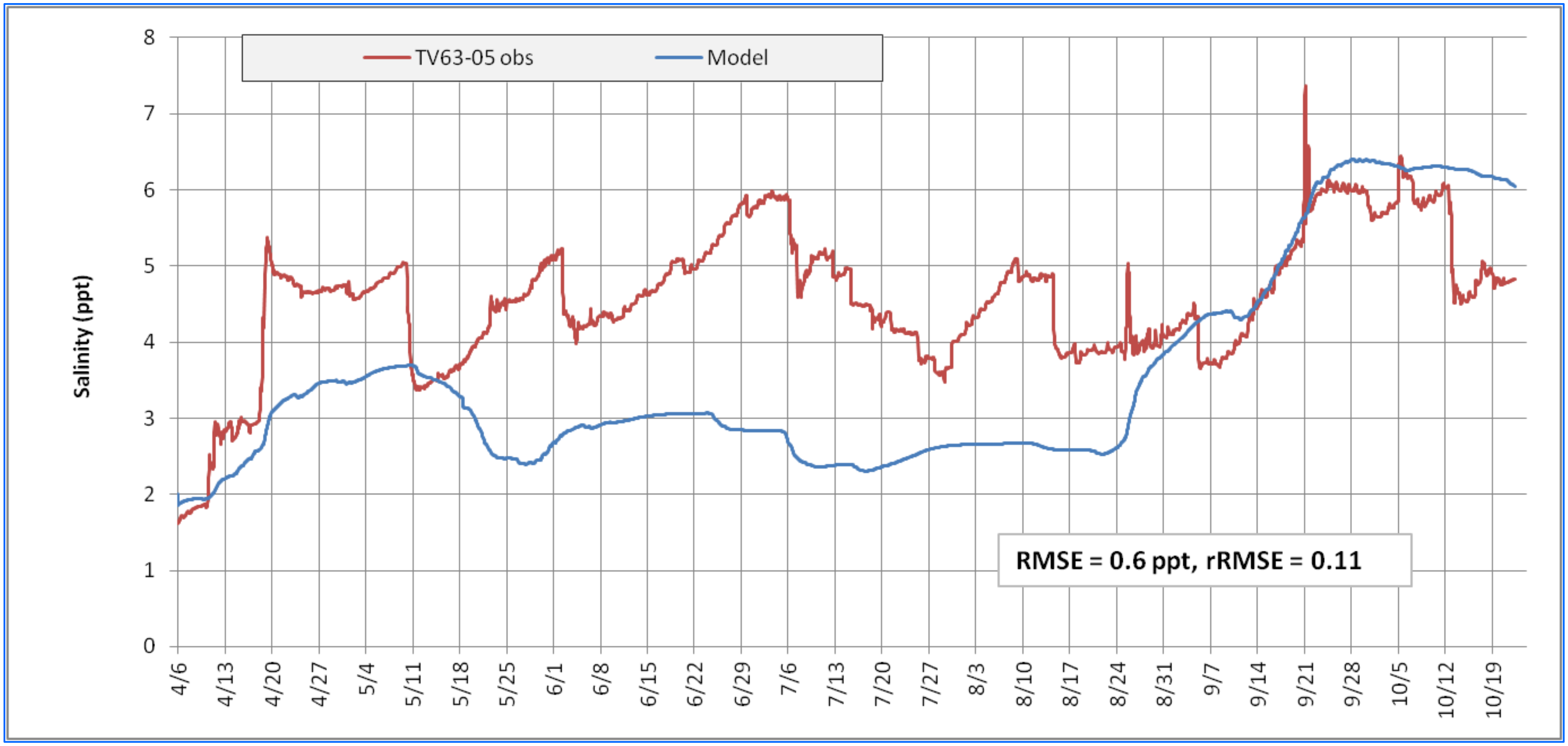

Figure 53 – Salinity calibration for station TV63-05, southern open water area.

4.2.2 Results

The percentage of time each point in the calibrated model is inundated is shown in **Figure 54.** The high marsh is inundated between 40 and 60% of the time for the time period modeled.

Flow information from the calibrated model was analyzed and is summarized on **Figure 55.** The average inflow was computed to be 19.8 cfs, the outflow 23.9 cfs, and consequently the net flow 4.1 cfs out of the marsh.

The breach with the largest flow magnitude is eastern-most breach in the Oil Field Canals (Arc 7, 125 cfs), followed by the breach at Arc 3 (79 cfs). Arcs 2 and 5 have nearly the same average flow magnitude (36 and 39 cfs). The largest magnitude of flow adjacent to the central open water area is at the channel connecting to the eastern breach (Arc 12, 120 cfs), followed by Arcs 10 and 11 (both 15 cfs). Arc 13 (9 cfs), adjacent to the open water where the channel connects to the southeast opening, conveys 60 percent the magnitude of Arcs 10 and 11. The southeastern breach (Arc 6, 65 cfs) conveys an average magnitude similar to the second largest breach in the north.

Comparing the modeled average flow magnitudes to the recorded flow data (see "Data Collection" section), the modeled flow magnitudes relative to one-another are consistent with that seen in the observed data. Given the limitations of observed data, which is non-synoptic and for only one snapshot in time, comparing relative flow magnitudes is the best way to use this data. Generally, the pattern in the model corresponds to the flows observed.

An exception is at Arc 2 where measured flow was zero. The survey shows there is a gap in the levee here, but a conveyance channel has not formed at this breach, rather it is backed by marsh terrain. The model computes the hydraulics based on the cross-sectional opening, which was matched to the survey data, and any backwater effects. It is possible that the backwater effects from the marsh combined with the high roughness losses significantly restrain flows through this breach and a large gradient is necessary to induce flow. It is also possible that the observation was an anomaly. This breach was modeled consistently with others in the model and produced an average flow magnitude of 36 cfs (Arc 2). Further investigation would be required to resolve this discrepancy.

The modeled flow magnitudes are higher than the observed data, but evaluating the calibration data presented above it seems that the model is adequately representing flows to the central marsh. The timing and rate of change of water levels in the model at TV63-04 is very good and the salinity trend, which can be seen as a surrogate for advection, is also good. This is evidence that, overall, flow magnitudes in the model are satisfactory.

Net flows were computed at each arc, with the positive assumed to be flow towards the center of the marsh. According to the model, the largest net flows into the marsh are through Arcs 5, 6, and 8 (8.3, 6.0, and 3.9 cfs) and the largest net outflows are through Arcs 7 and 3 (16.2 and 6.3 cfs).

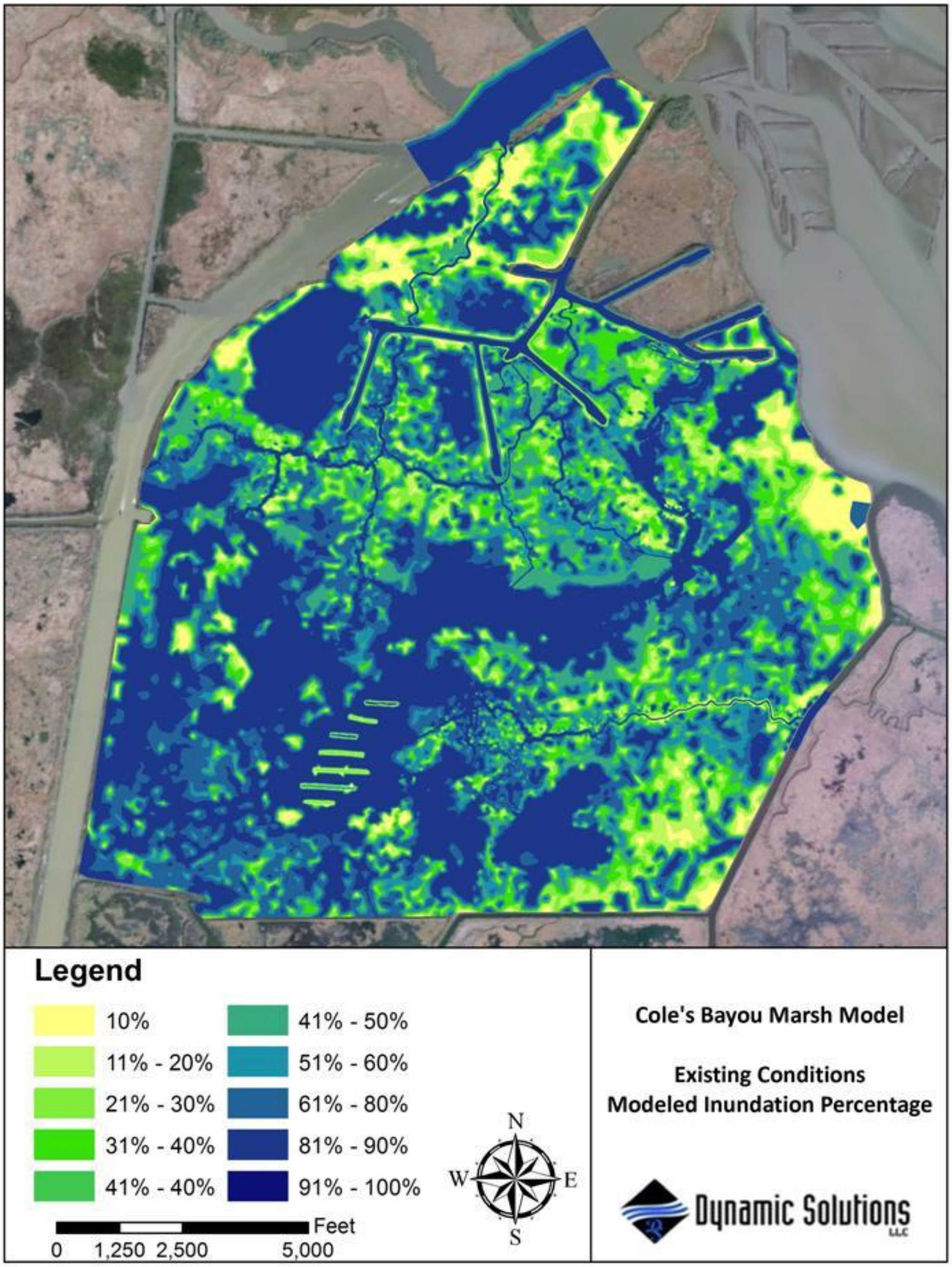

Figure 54 – Inundation percentages for the calibrated existing conditions model

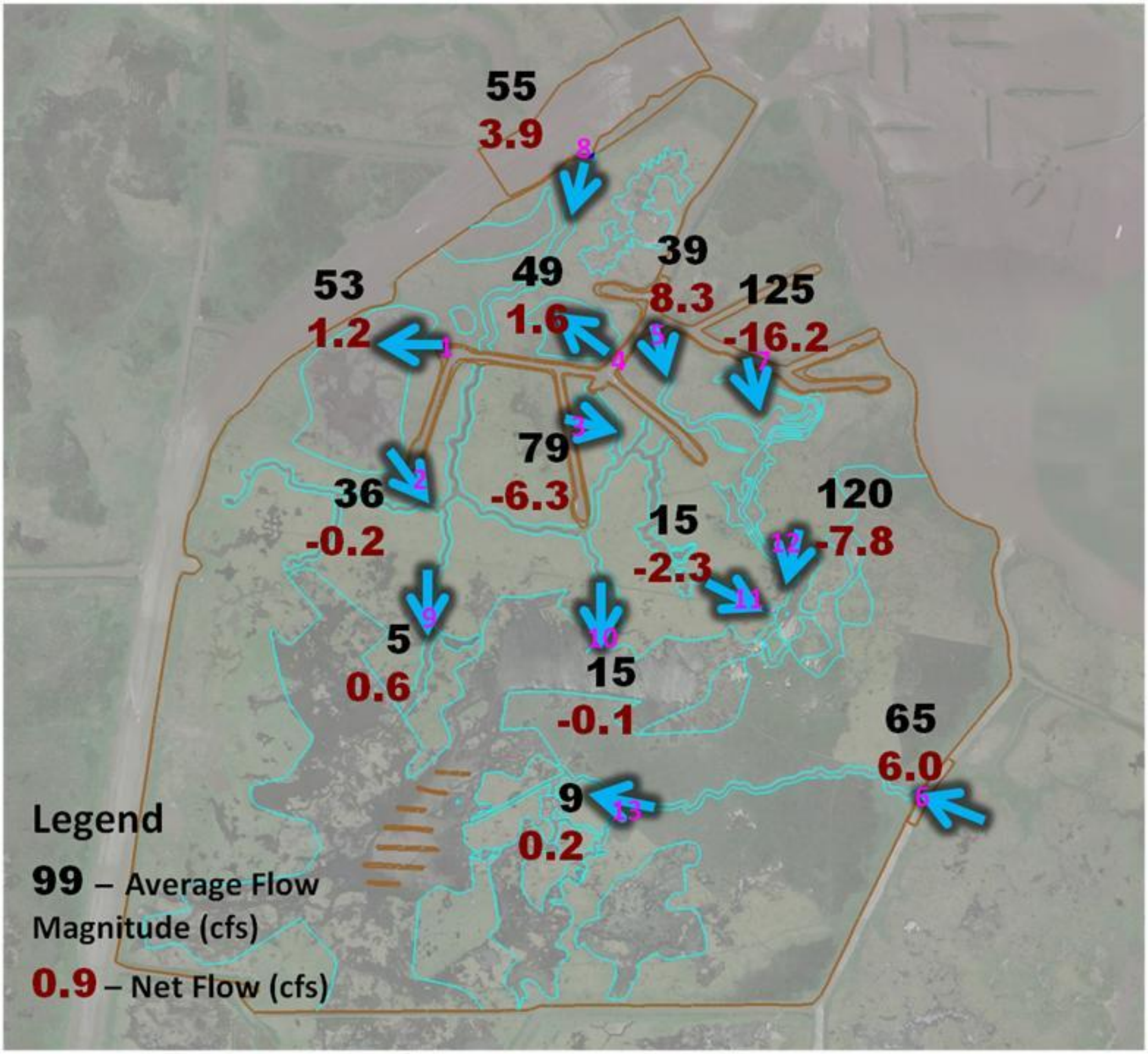

Figure 55 – Average flow magnitude at each flow observation point. Each arc is directed towards the center of the marsh; negative numbers indicate net flow in the opposite direction.

Model Testing

Model sensitivity tests are important to ensure the model is robust responding reasonably to changes in input data and parameters. During the calibration process tests were run evaluate the response of the model to changes in bathymetry and roughness. For the bathymetry test, the entire mesh was raised and lowered by 0.54 ft, which corresponds to one standard deviation of the high marsh elevations. The results of this test are shown in **Figure 56**. When elevations are raised there is less influx, evidenced by lower peaks, and lower outflux evidenced by consistently high water levels. When all elevations are lowered, this increases flows in and out of the marsh, causing a more pronounced diurnal signal and more rapid changes in elevation. These results are sensible and indicate the model responds to a shift in bathymetry accordingly[2].

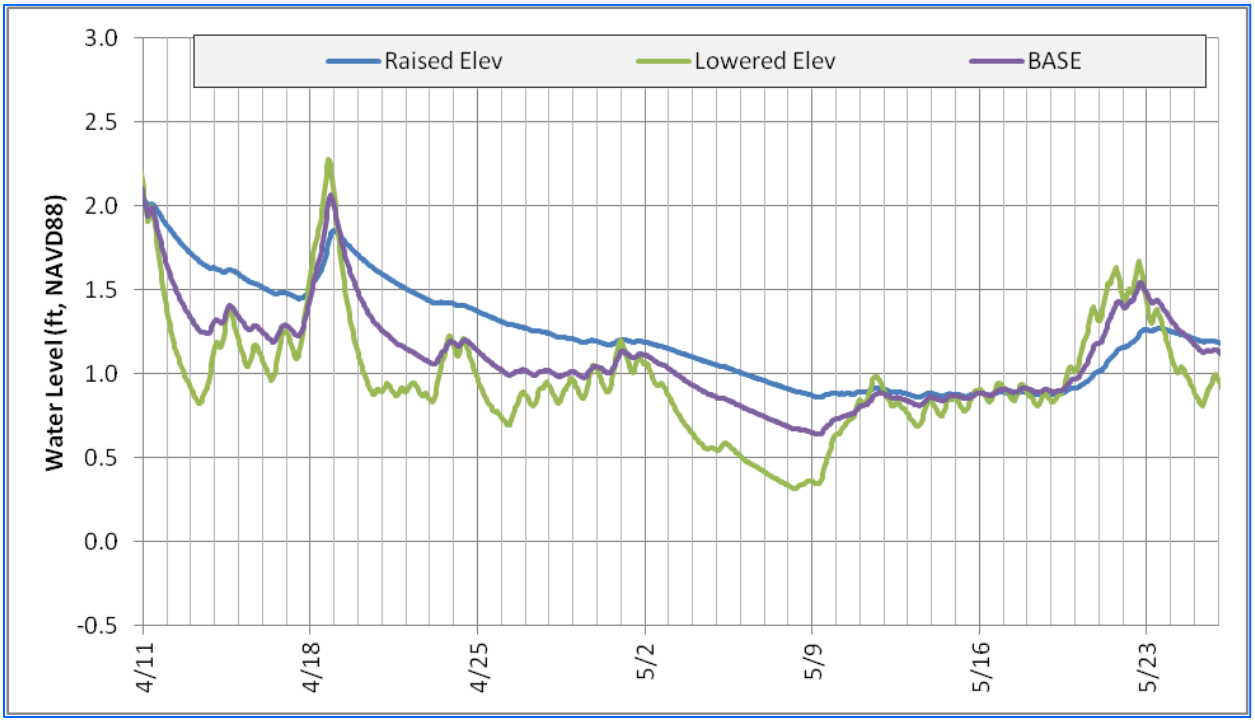

Figure 56 – Sensitivity test on model bathymetry where elevations were lowered and raised by 0.54 feet in the model mesh

Roughness was tested for the marsh and channel independently. **Figure 57** shows the difference between the marsh channel roughness for the calibrated model (n = 0.20 for channels and open water) and for a lower roughness (n = 0.012 for channels and 0.015 for open water). The difference is nearly negligible but the response is as expected; water levels exhibit greater change indicating increased flows through the channels with lower roughness. **Figure 58** compares marsh roughness[2] using a variety of parameters for the unsubmerged rigid vegetation scheme. The details of the parameters are shown in **Table 10**. The differences in roughness parameters lead stage results within a reasonable range. The greatest roughness is due to small stems with a great density (URV-2 and URV-3) and the least roughness caused by a larger stem with less density.

[2] The BASE run shown in this plot is not the calibration model rather an older model prior to finalization however, the comparison is still valid.

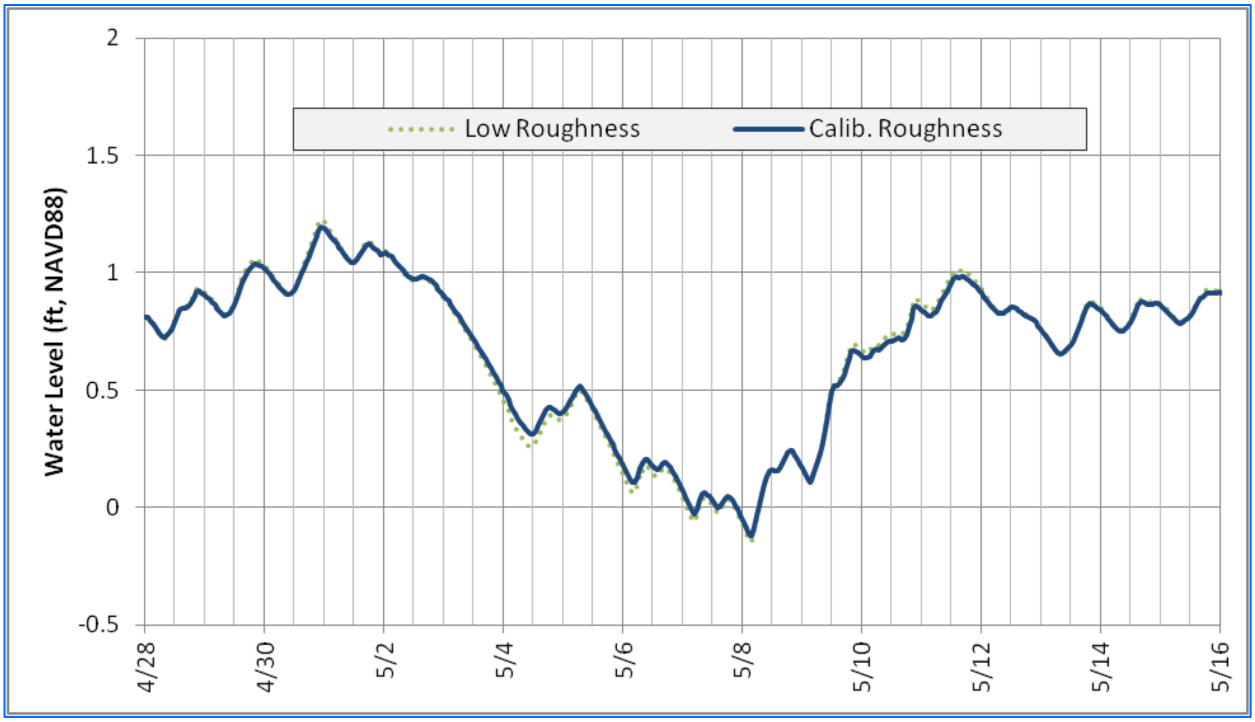

Figure 57 – Sensitivity analysis for channel roughness

Table 10 – URV parameters for marsh roughness sensitivity test

Run	Roughness Height (m)	Stem Diameter (m)	Density (stems/sq. m)	Density (% area blocked)
URV	0.1	0.01	5,625	75
URV-2	0.1	0.001	250,000	50
URV-3	0.01	0.001	250,000	50
URV-4	0.1	0.001	62,500	25
URV-5	0.1	0.003	6,945	25

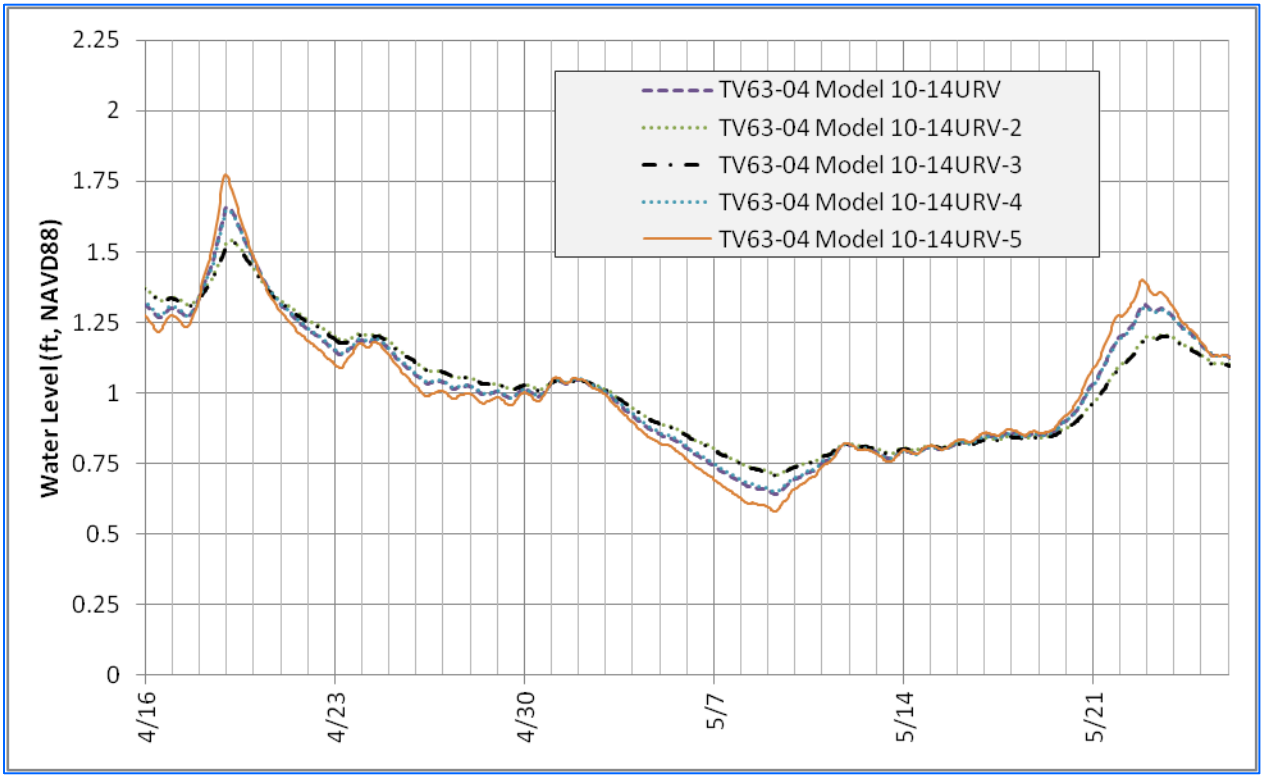

Figure 58 – Sensitivity analysis for marsh roughness

A mesh convergence test was performed to ensure the mesh has sufficient resolution. For the test, the model is run with a higher-resolution mesh and results analyzed to see if significant differences occur. Mesh adaption was used to refine the mesh in the channels. The mesh adaption tolerance was lowered by half in distributary channels and open water areas of the marsh and the resulting water levels at station TV63-04 are shown on **Figure 59**. The mesh convergence test had approximately 1,700 more nodes at the time of the greatest difference in water level (0.06 feet) on 5/6/13.

Boundary sensitivity tests were performed to ensure that changes induced by the scenarios did not cause errors at the boundary. Water surface elevations were evaluated at times of maximum influx and outflux (~ 1750 cfs) through the boundary at TV63-03 for the calibrated model and the scenarios. The differences in water surface elevations at the boundary were minimal. The trunk channel in the Oil Field Canals (where TV63-03 is located) connects directly to a huge volume of water in Little Vermilion Bay compared to the flow in the canals. The gradient between TV63-03 and Little Vermilion Bay at the largest flow modeled would be less than .01 feet (3 mm). Water levels in the Oil Field Canals are dominated by the tidal signal so the boundary is considered valid.

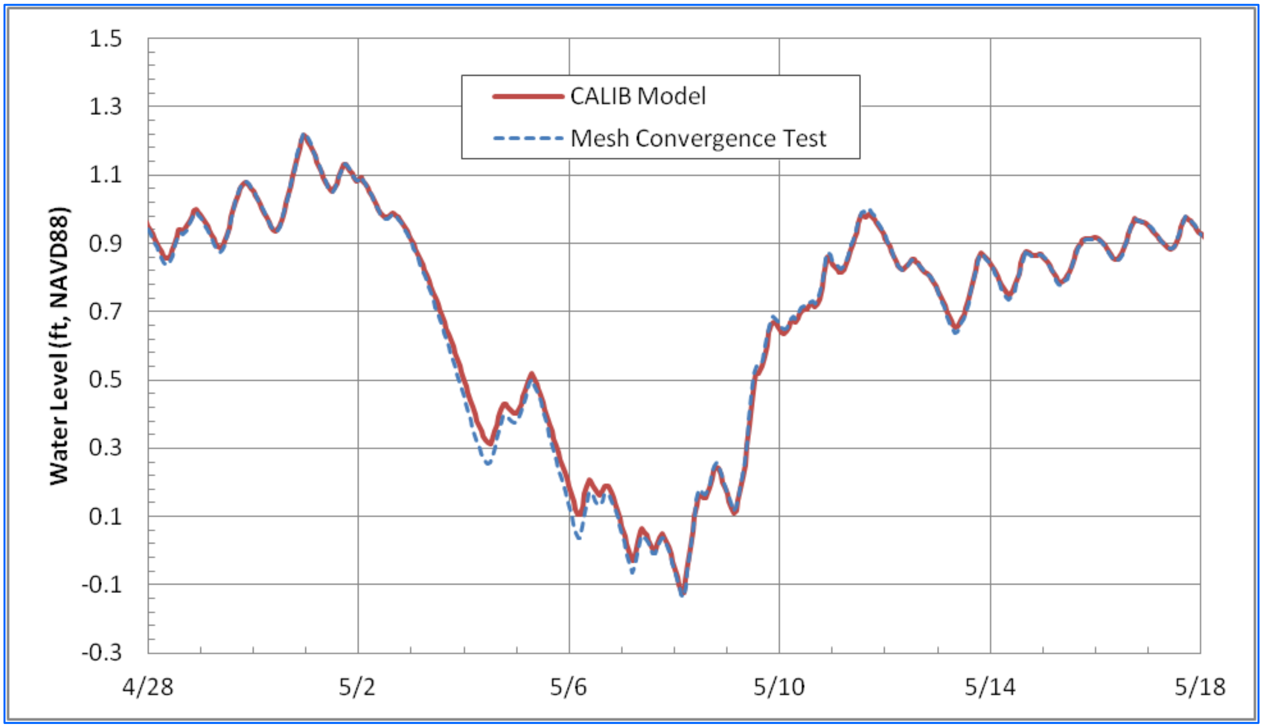

Figure 59 – Water levels for the calibrated model and for the mesh convergence test, which has a higher resolution mesh in the distributary channels

SECTION 5 MODEL SCENARIOS

The objective for scenarios is so modifications to the calibrated model representing future conditions can be tested to see how hydrodynamics within, and around, the Cole's Bayou Marsh are affected. These changes included the increase of elevation in marsh creation areas due to the introduction of sediments, closing gaps in the perimeter levee, and placing one-way flap-gated culverts at various locations in the system. The scenarios analyzed below were designed by CPRA and NOAA staff and modeled by DSLLC staff.

5.1 Scenario 1: Marsh Creation

5.1.1 Objective

This objective of Scenario 1, Marsh Creation, was to simulate the hydrodynamic response of the system to the creation of marsh within Coles Bayou. For this scenario the Existing Conditions model bathymetry was modified, setting the elevation of nodes within the marsh creation zones (shown in **Figure 60**) to the specified elevation of 1.3 feet (0.396 meters).

5.1.2 Scenario 1- Marsh Creation Results

Water Level

Median water level in the marsh did not change appreciably. The median water level for the Existing Conditions run was 0.96 feet and 0.99 feet for Scenario 1. **Figure 61** shows the inundation frequency for several points of interest within the marsh, which range from 23% to 100%. All of these points were inundated 100% of the time for the Existing Conditions run. **Figure 62** shows inundation frequency across the entire domain. **Figure 63** and **Figure 64** show water level time series at stations TV63-04 and TV63-05 for Existing Conditions and Scenario 1. At TV63-04 the water levels are quite similar once the marsh creation area is inundated. At TV63-05 there is a greater lag in water level response due to decreased connectivity with the Oil Field Canals.

Salinity

Salinity did not change appreciably at either calibration station. **Figure 65** and
Figure 66 show the salinity time series at stations at stations TV63-04 and TV63-05 for Existing Conditions and Scenario 1. Salinity values at TV63-05 are consistently marginally (typically < 0.5 ppt) higher than for the Existing Conditions model.

Flow

Flow magnitude information at each exchange (breach) on the perimeter of the marsh and where major flow pathways connect to the center of the central open water area (which are assumed to be filled for this scenario) is shown on **Figure 67.** Scenario 1 causes a 61% decrease in flow at Flow Point 1 (FP1), but typically causes approximately a 15% increase in flows through the breaches in the Oil Field Canals.

However, there is a reduction in flow by between 31% and 85% for areas near to the central marsh creation area, with the exception of FP9.

Net flow information is also shown at the exchange points and along the major flow pathways, in **Figure 68**. The largest change in net flow exists at the eastern channel where 40% less flow is exiting the system at FP7.

The average inflow was computed to be 15.9 cfs, the outflow 19.6 cfs, and consequently the net flow 3.7 cfs out of the marsh.

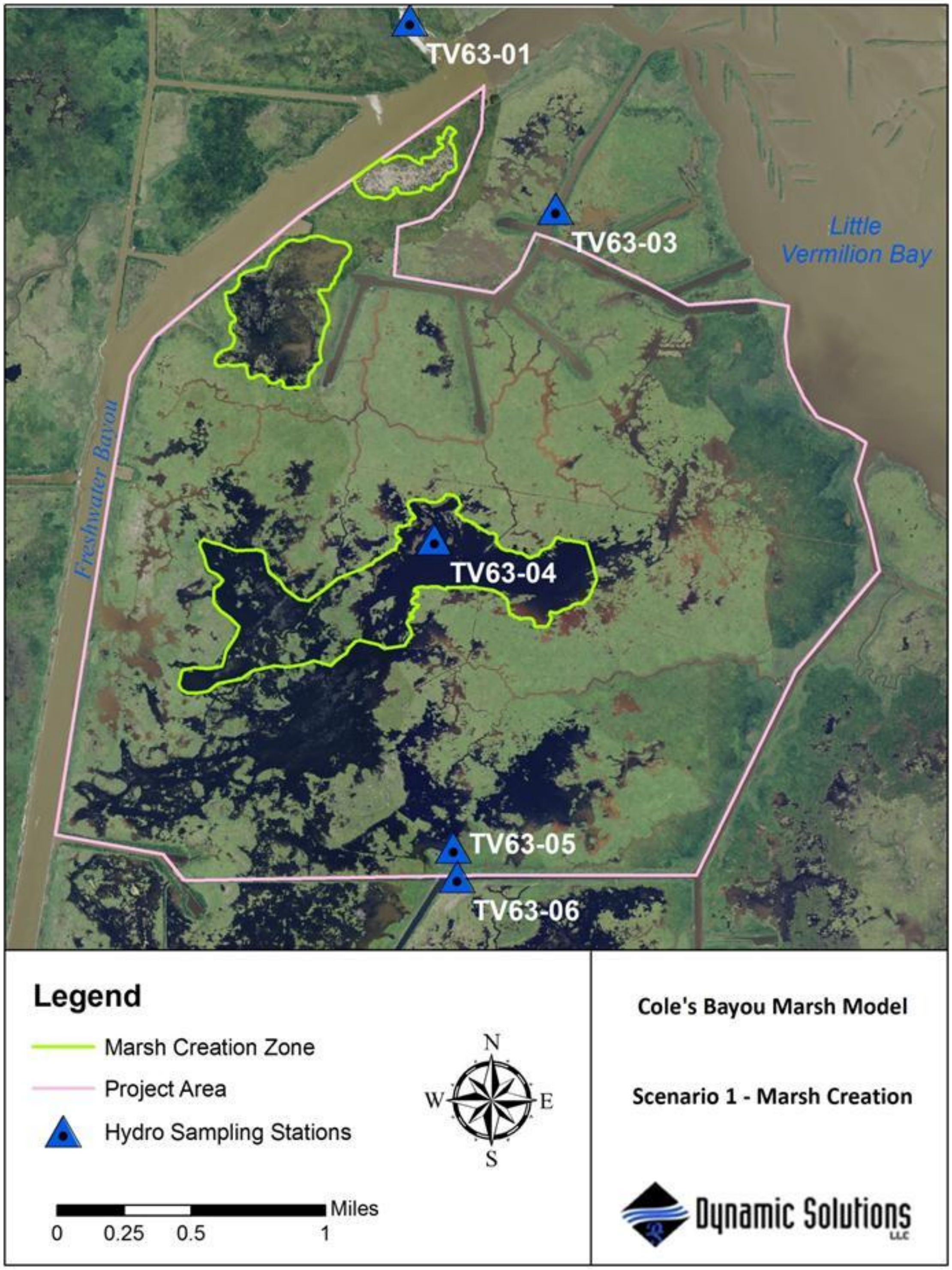

Figure 60 – Location of Marsh Creation Zones set to elevation of 1.3 feet (0.396 m), NAVD88

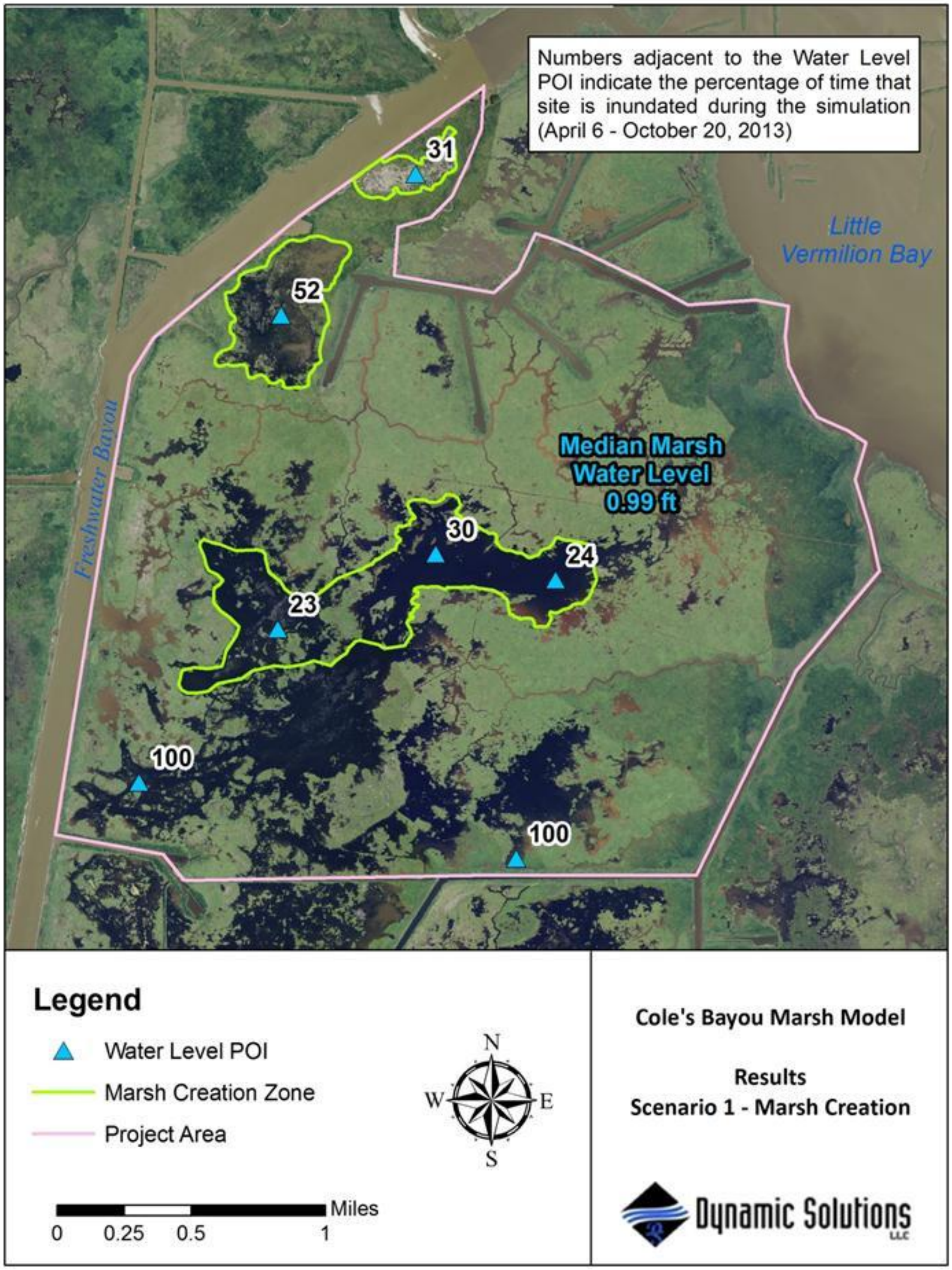

Figure 61 – Scenario 1 results for water level at points of interest (POI) in the Cole's Bayou Marsh

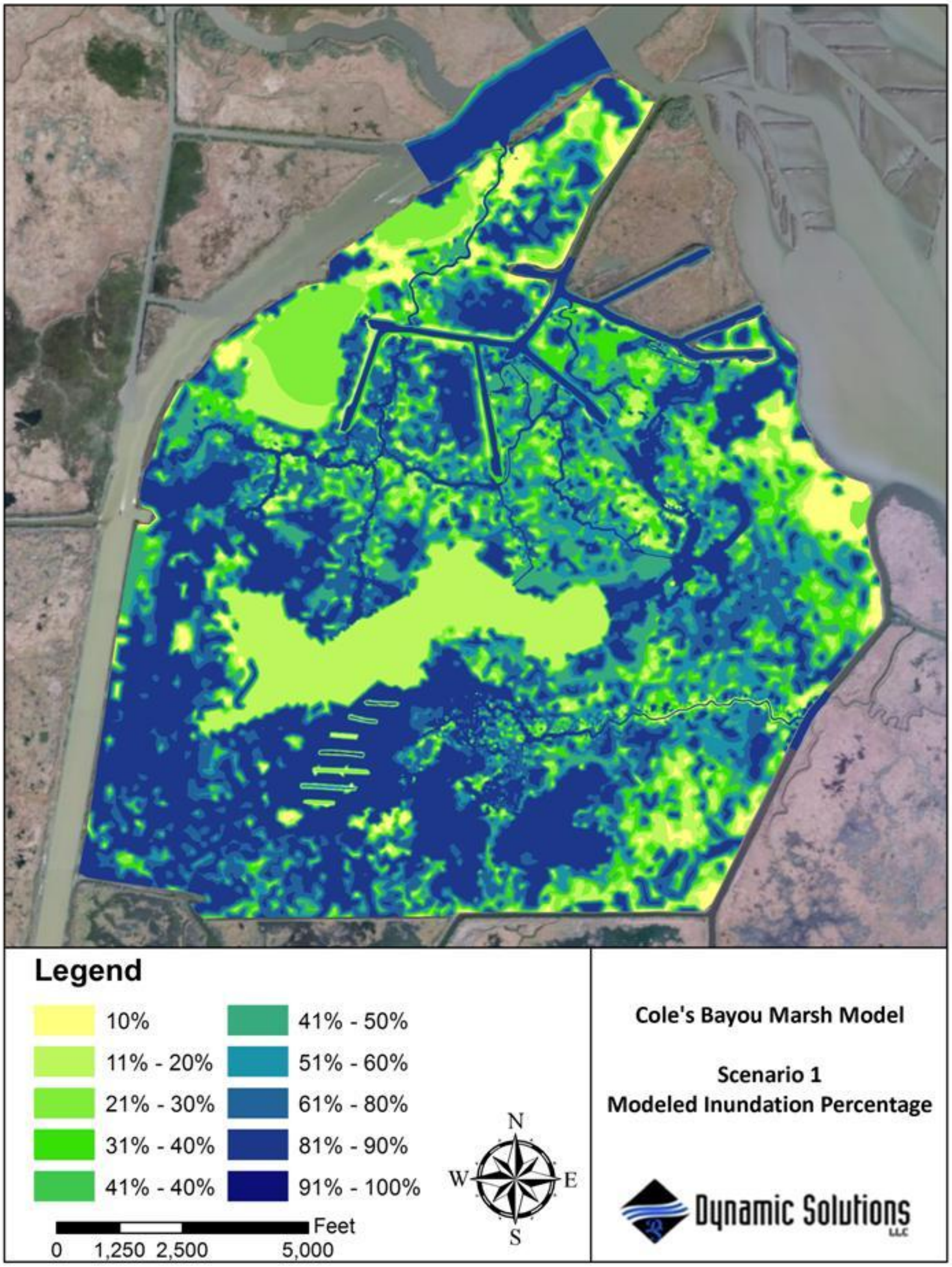

Figure 62 – Inundation percentages for Scenario 1

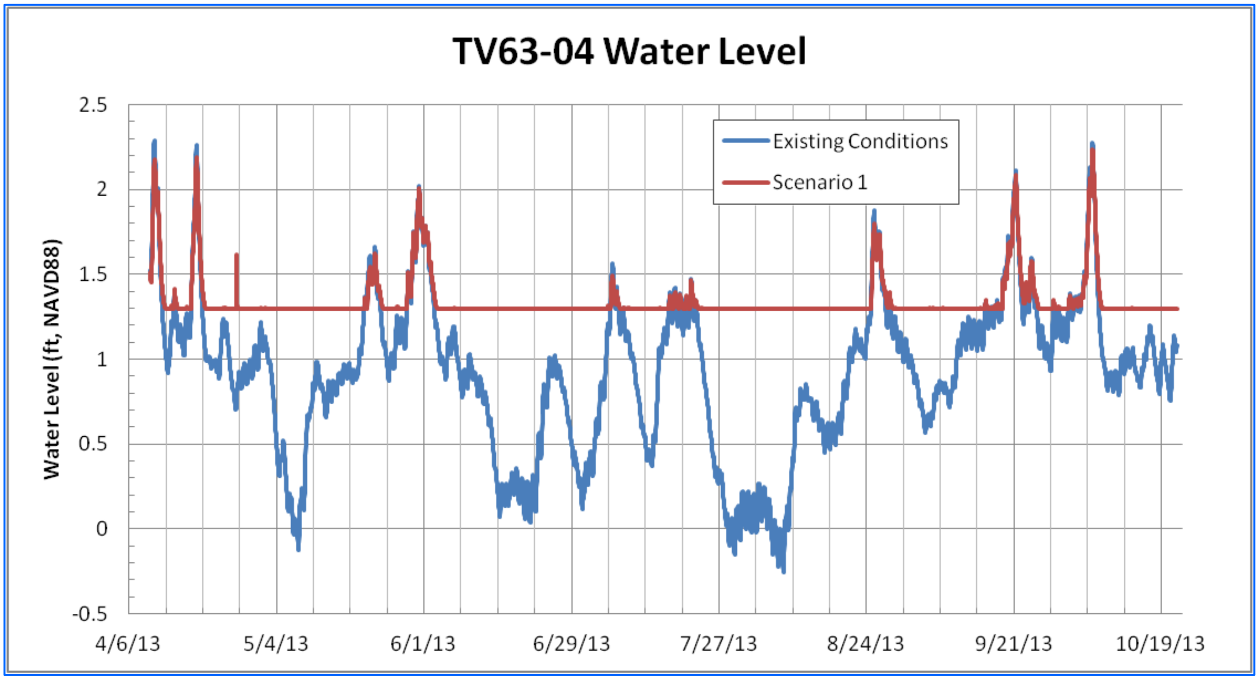

Figure 63 – Water levels at TV63-04 for Existing Conditions run and Scenario 1. The flat parts of the Scenario line indicate when the point is dry.

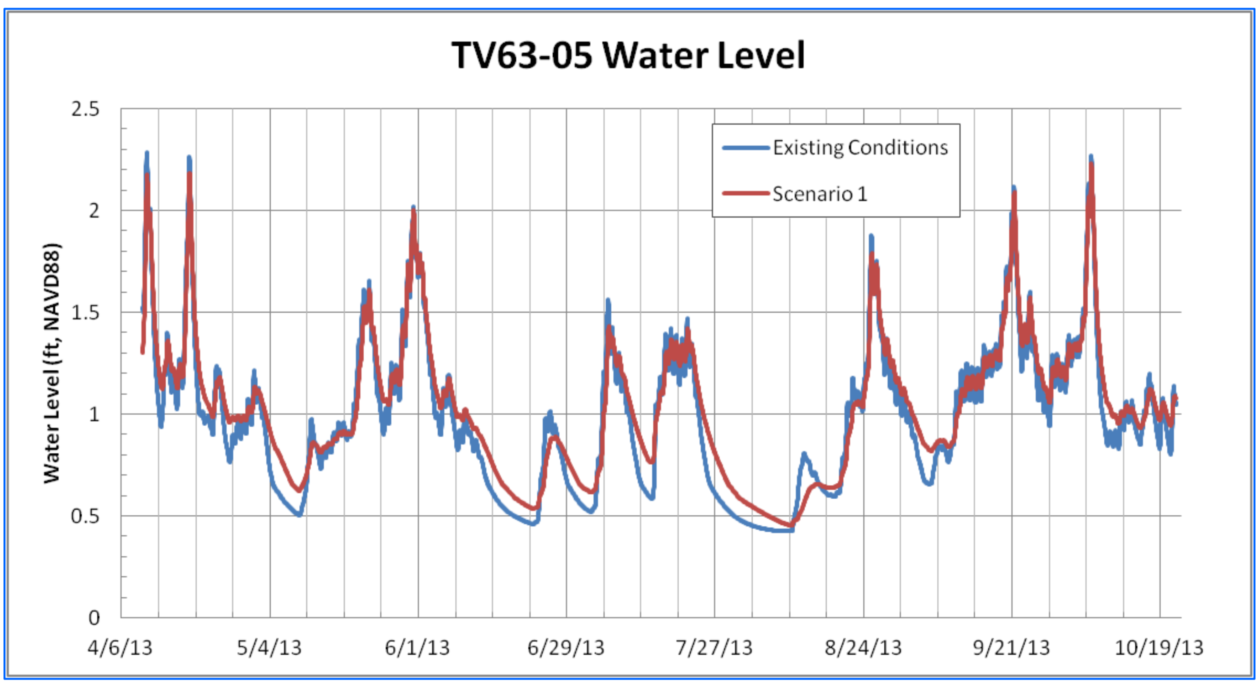

Figure 64 – Water levels at TV63-05 for Existing Conditions run and Scenario 1.

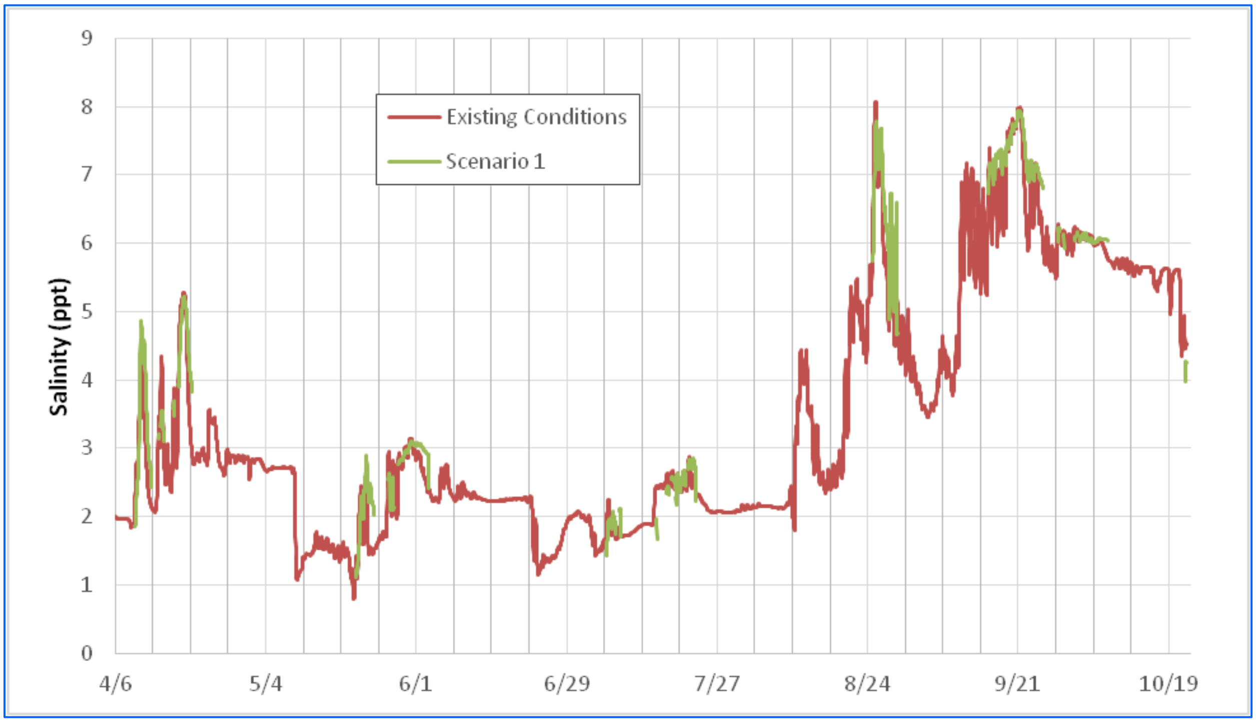

Figure 65 – Salinity at TV63-04 for Existing Conditions run and Scenario 1.

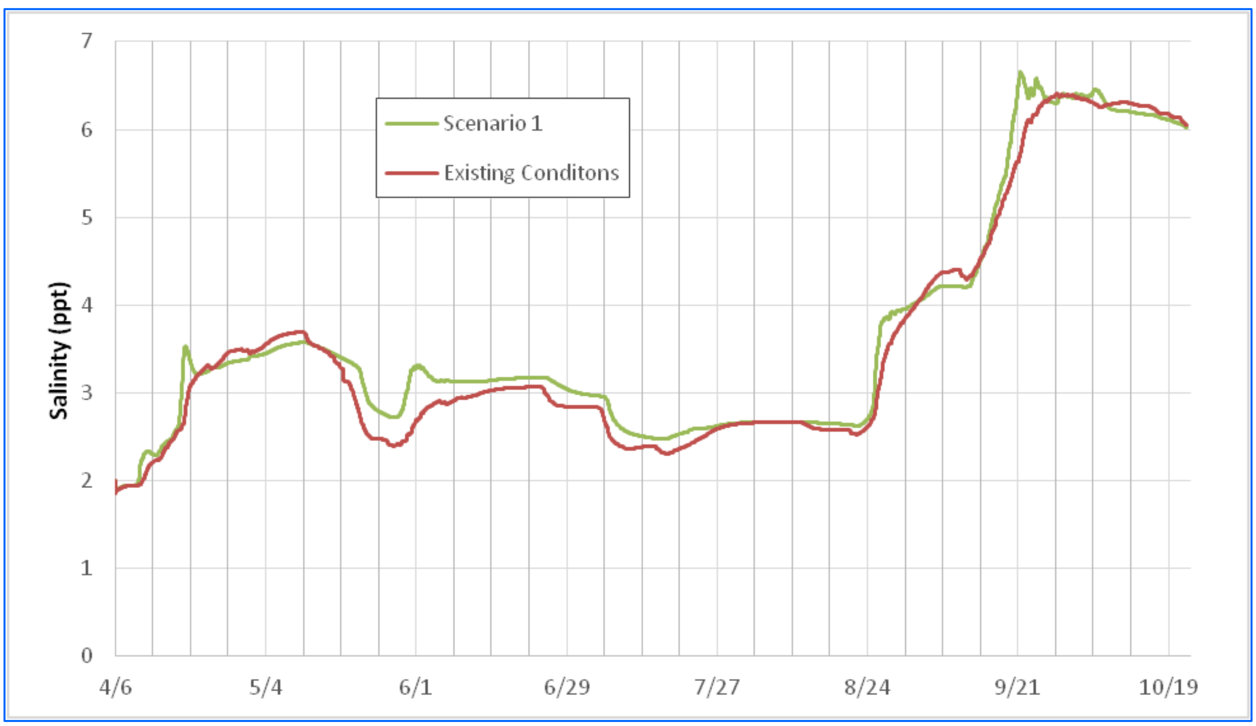

Figure 66 – Salinity at TV63-05 for Existing Conditions run and Scenario 1.

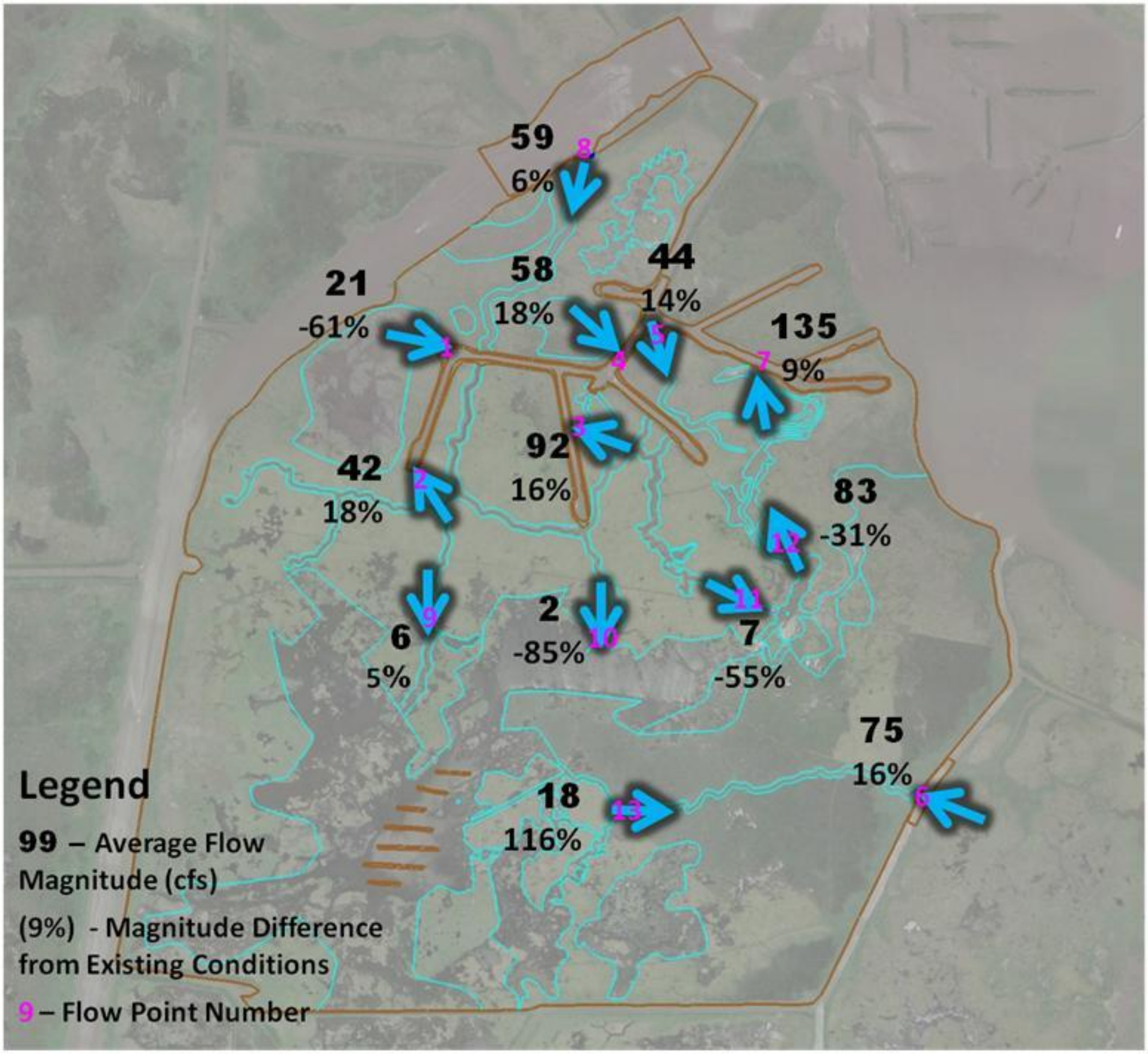

Figure 67 – Flow map for Scenario 1 showing average flow magnitude and the difference in flow magnitude compared to Existing Conditions.

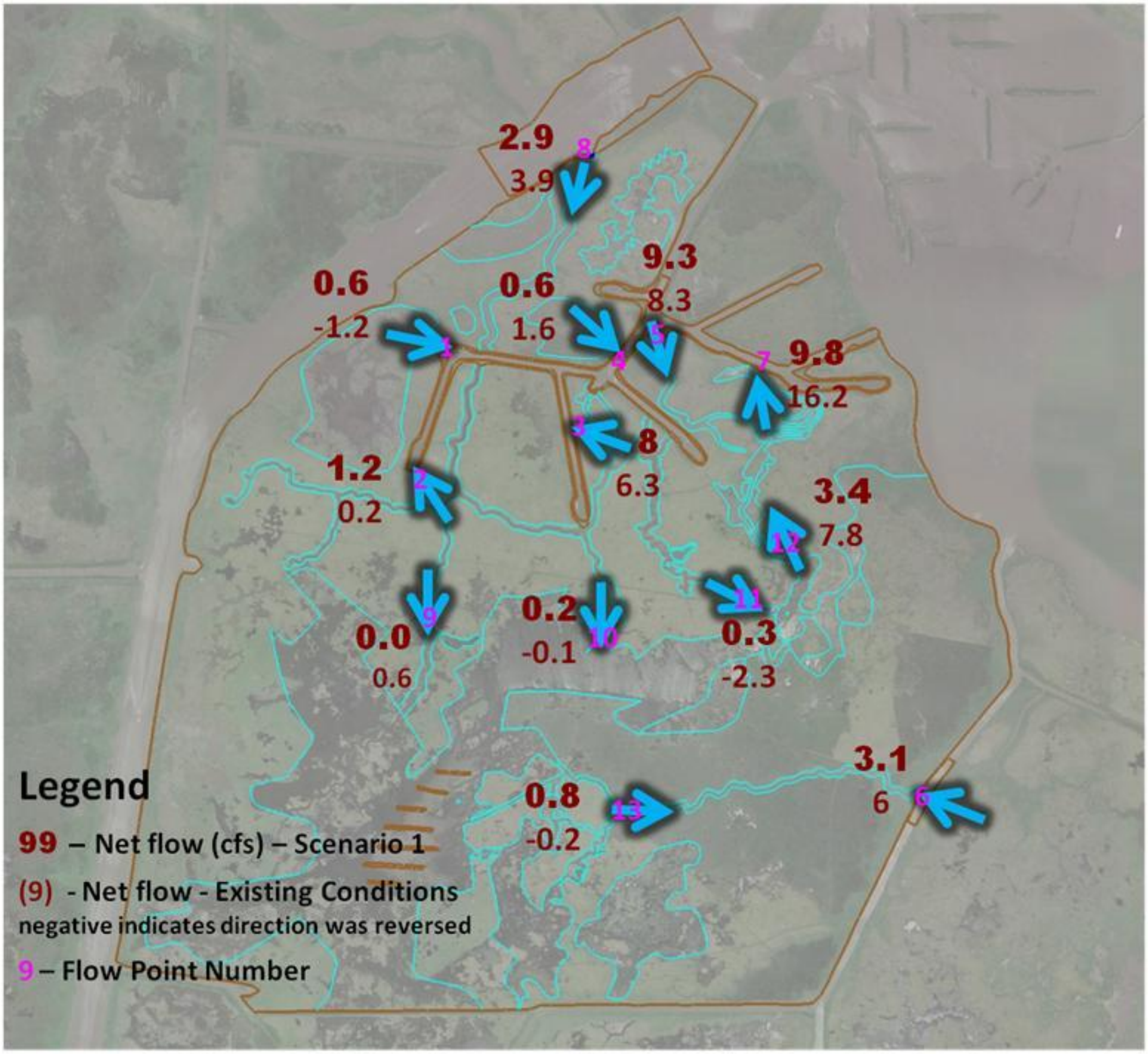

Figure 68 – Flow map for Scenario 1 showing net flow and the net flow for Existing Conditions (a negative indicates the direction of net flow changed from Existing Conditions)

5.2 Scenario 2: Marsh Creation with Culverts

5.2.1 Objective

This objective of Scenario 2, Marsh Creation with Culverts, was to simulate the hydrodynamic response of the system to the creation of marsh within Cole's Bayou Marsh Project Area. For this scenario the Scenario 1 model bathymetry was modified to place a borrow ditch around the large, central marsh creation area. The borrow ditch was constructed as a trapezoidal channel with an average flow area of 72 square feet, top width of 24 feet, and a thalweg of -3.51 feet (-1.07 meters). Also, eight flap-gate inflow culverts were inserted at specified positions on the northern Oil Field Canals and two flap-gate outflow culverts were placed on the southern McIlhenny Canal (**Figure 69**). Each culvert was specified as a 48-inch diameter corrugated HDPE pipe, 25-feet in length, with an invert of 0.0 feet.

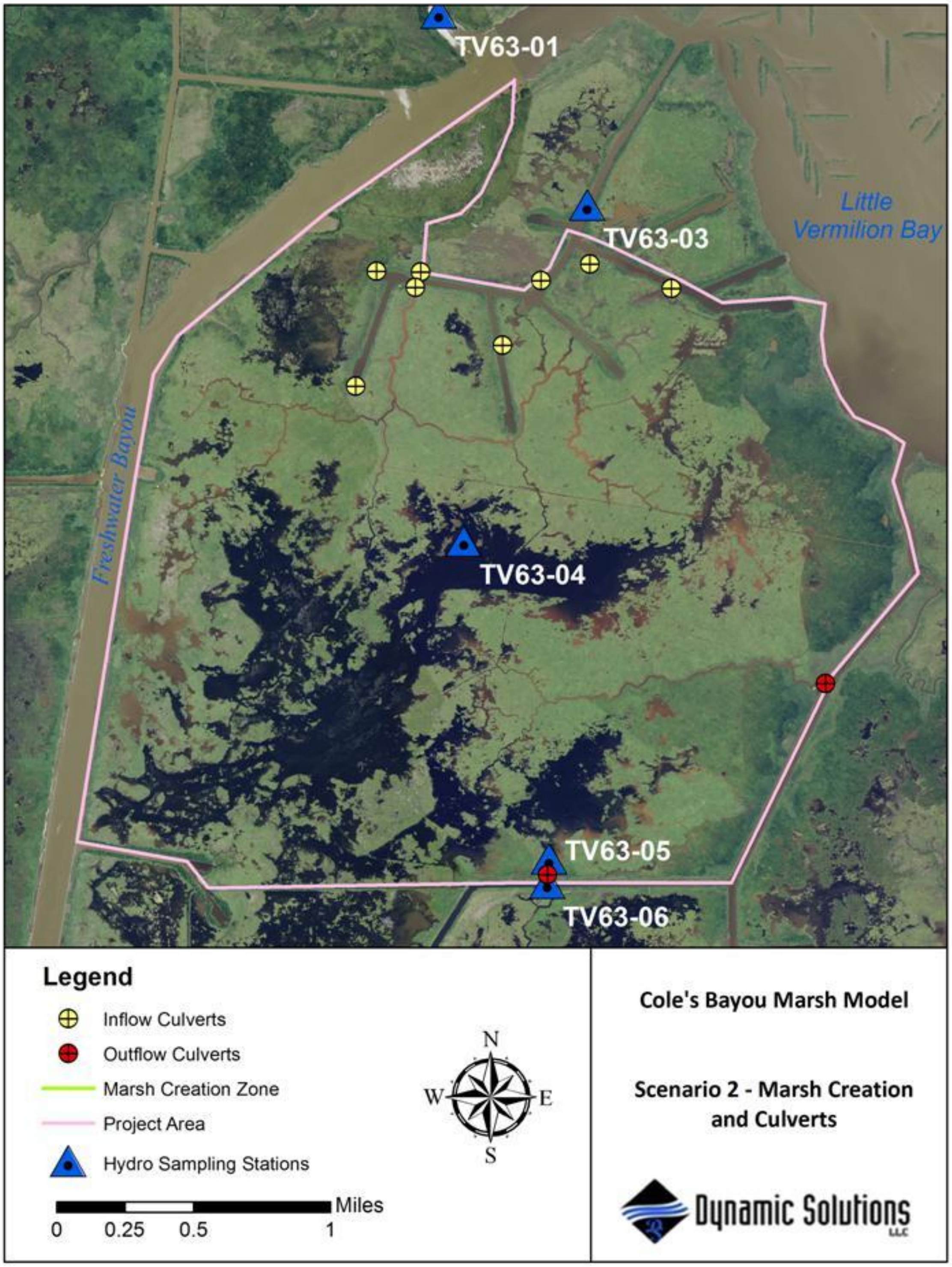

Figure 69 – Scenario 2 specifications including marsh creation areas and inlet and outlet culvert locations

5.2.2 Culvert Analysis

Curves relating head difference to discharge for these culverts was developed using the HEC-RAS model and checked using the USGS Culvert Analysis Program (CAP) model. ADH requires a head difference – discharge curve to utilize its hydraulic structure capabilities. Culvert hydraulics are very complex, and when a culvert is not submerged, the flow may be inlet controlled or outlet controlled. These conditions vary depending on inlet and outlet water surface elevations, among other factors, and the head difference – discharge curves are dependent on these conditions. A single head difference – discharge curve must be created for ADH to simulate the range of conditions which occurs in the model. The range of possible conditions was run in HEC-RAS and a family of head difference - discharge curves (**Figure 70**) was generated and adjusted to include the losses (provided by CPRA) of the duckbill flapgate. For nearly all conditions experienced, the culverts were tailwater controlled. To conservatively estimate flows, the head difference – discharge curve for 25% exceedence water level at the culvert tailwater was selected to simulate culvert flow for all stage conditions. Curves for the inflow culverts were based on a tailwater condition of 0.56 feet, the 25% exceedence elevation at TV63-04. Curves for the outflow culverts were based on a tailwater condition of 0.22 feet, the 25% exceedence elevation at TV63-06. The head difference – discharge relationship for the inflow (northern) culverts is shown in **Figure 71**, and the for the outflow (southern) culverts in **Figure 72**.

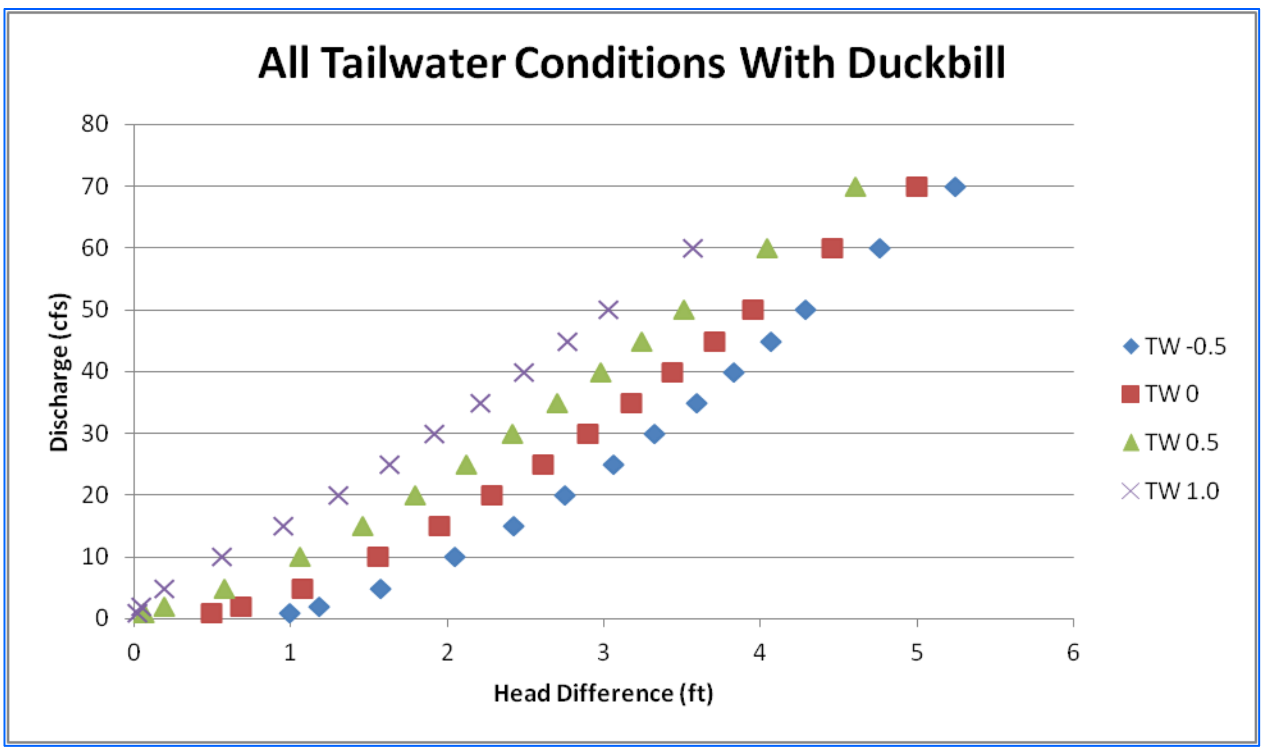

Figure 70 – Discharge as a function of head difference across the culvert for a range of tailwater conditions.

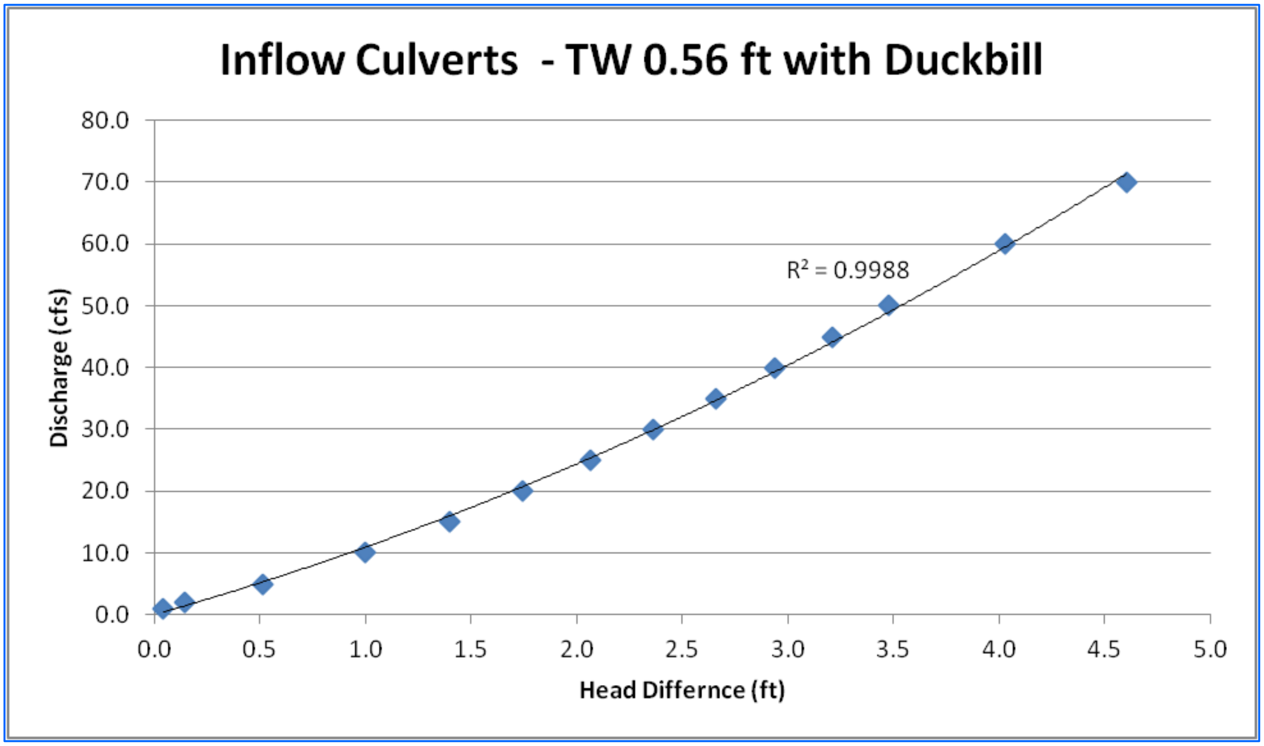

Figure 71 – Discharge as a function of head difference for the inflow culverts given a tailwater elevation of 0.56 feet.

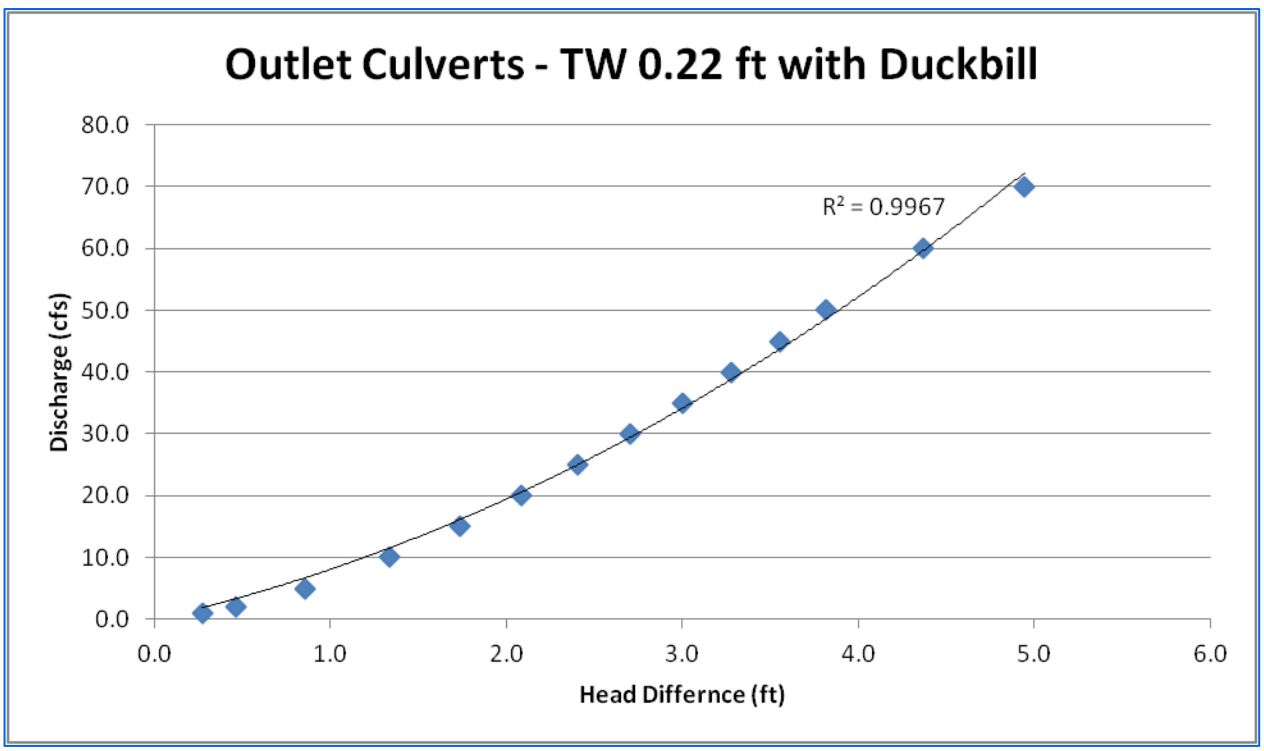

Figure 72 – Discharge as a function of head difference for the inflow culverts given a tailwater elevation of 0.22 feet.

5.2.3 Results

Water Level

Median water levels in the marsh increased from 0.99 feet to 1.22 feet. **Table 11** shows the median water level when inundated and the percentage of time each point of interest (POI) was inundated. The inundation percentages are also presented on **Figure 73.** Inundation frequency for the entire domain is shown in **Figure 74.**

Table 11 – Water level comparison for Scenario 1 and Scenario 2

		Scenario 1		**Scenario 2 - Full**	
Location	Point Elev (ft)	Median Stage (ft)	Pct Inundated	Median Stage (ft)	Pct Inundated
TV63-04	1.30	1.39	27%	1.37	35%
TV63-05	-0.92	0.99	100%	1.18	100%
Cent-East	1.30	1.47	22%	1.37	36%
Cent-West	1.30	1.45	21%	1.37	38%
NW	1.30	1.32	51%	1.30	100%
North	1.30	1.43	28%	1.37	31%
SW	-1.31	0.99	100%	1.18	100%
N-Marsh	0.98	1.31	38%	1.21	56%
CentW-Marsh	0.89	1.12	65%	1.18	100%
CentE-Marsh	0.98	1.21	46%	1.21	91%
E-Marsh	0.92	1.15	56%	1.18	97%
SE-Marsh	1.08	1.24	43%	1.22	84%
S-Marsh	0.89	1.14	62%	1.18	100%
SW-Marsh	0.62	1.03	88%	1.18	100%

Salinity

Salinity values changed very little during Scenario 2 due to the small inflows into the system. **Figure 77** and **Figure 78** show the salinity time series at stations at stations TV63-04 and TV63-05 for Existing Conditions and Scenario 2. Salinity values at TV63-04 are consistently lower and at TV63-05 salinity values change very little from the initial conditions due to a small exchange of waters.

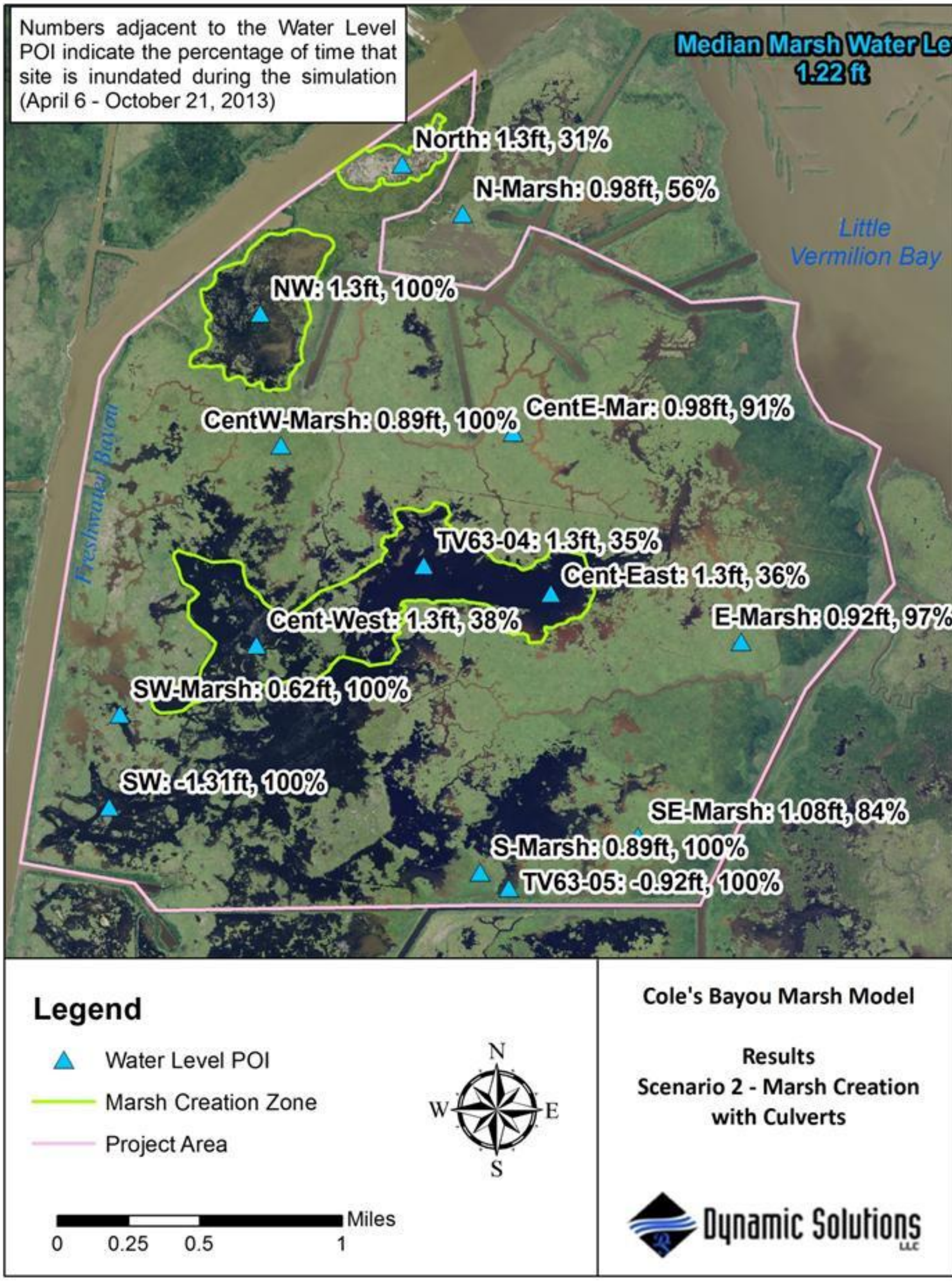

Figure 73 – Scenario 2 water level results showing greater periods of inundation in marsh areas

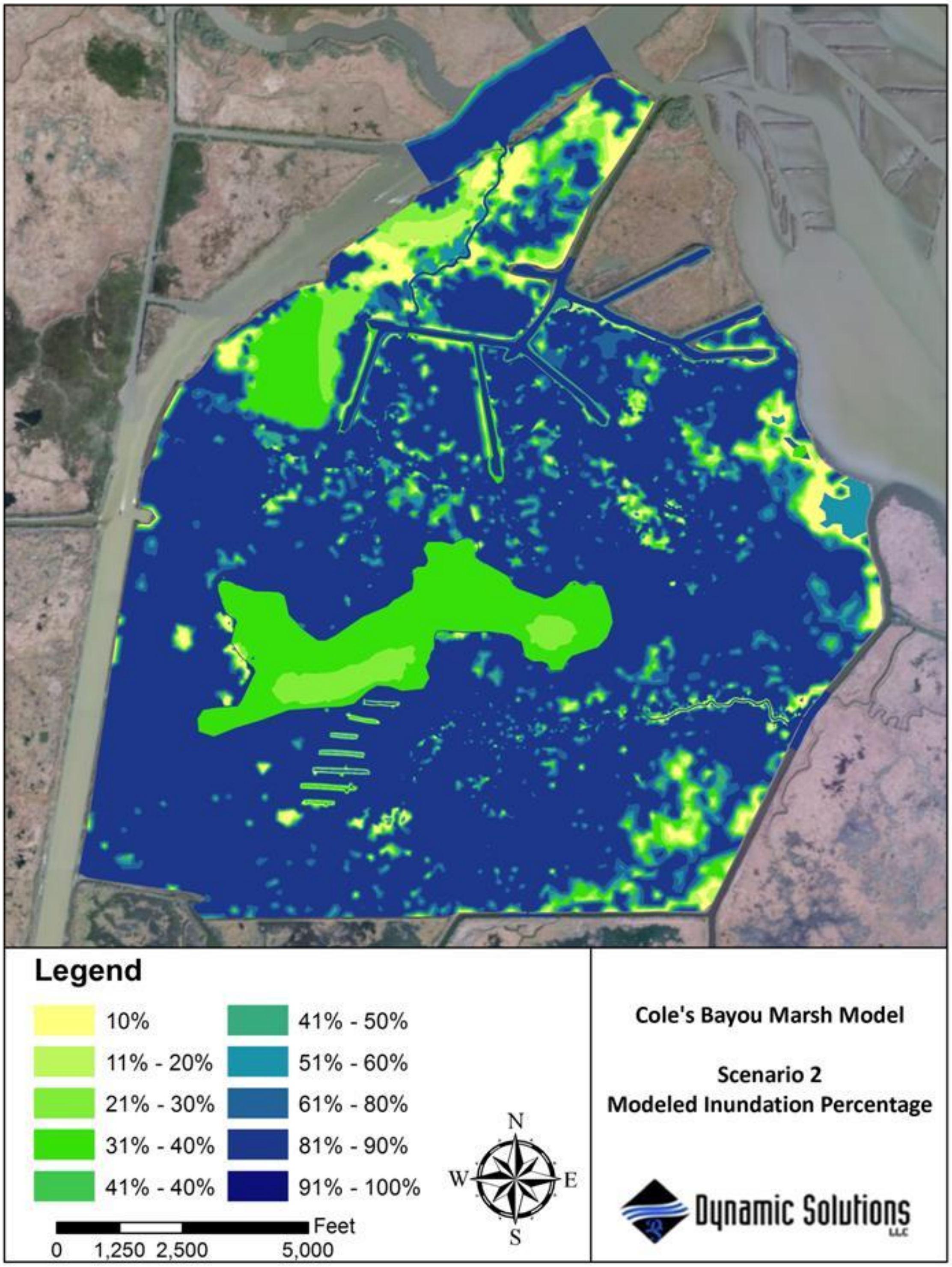

Figure 74 – Inundation frequency over the entire domain for Scenario 2

Figure 75 and **Figure 76** show the water level time series at TV63-04 and TV63-05 for existing conditions, Scenario 1, and Scenario 2. It shows that water levels vary much less in Scenario 2, with much lower peaks. At TV63-05 the water level is maintained at a higher level during periods of low water.

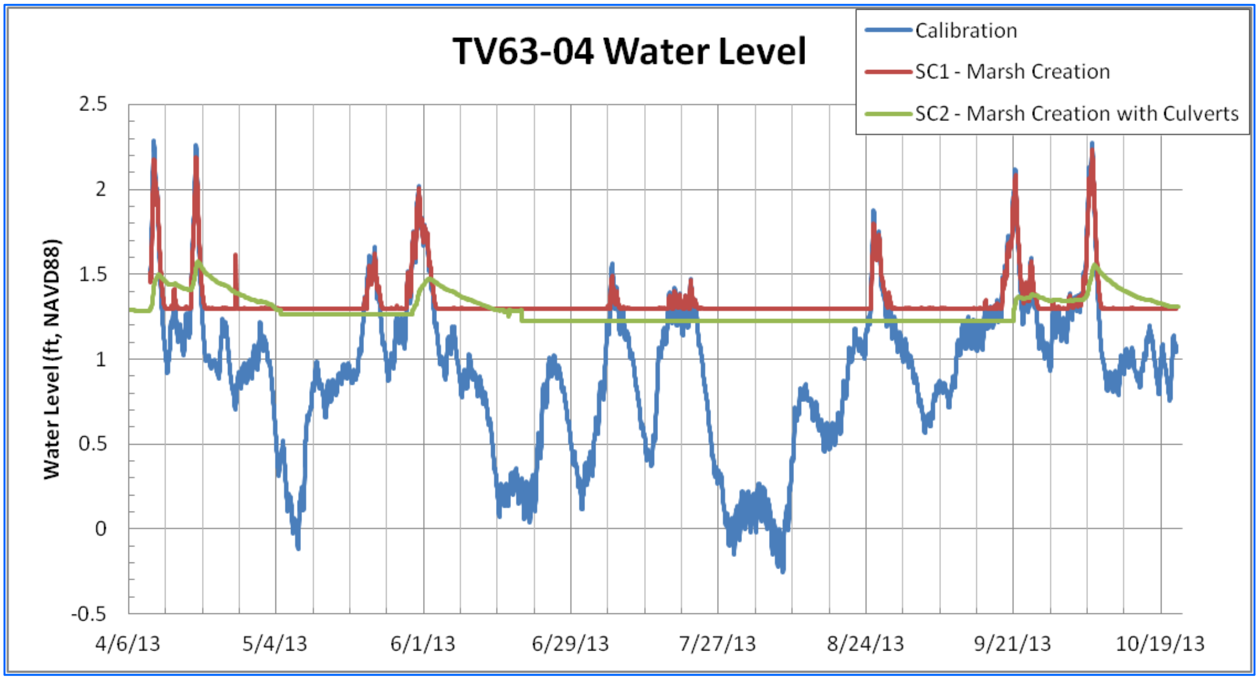

Figure 75 – Water levels at TV63-04 for Existing Conditions, Scenario 1, and Scenario 2. The flat parts of the Scenario line indicate when the point is dry.

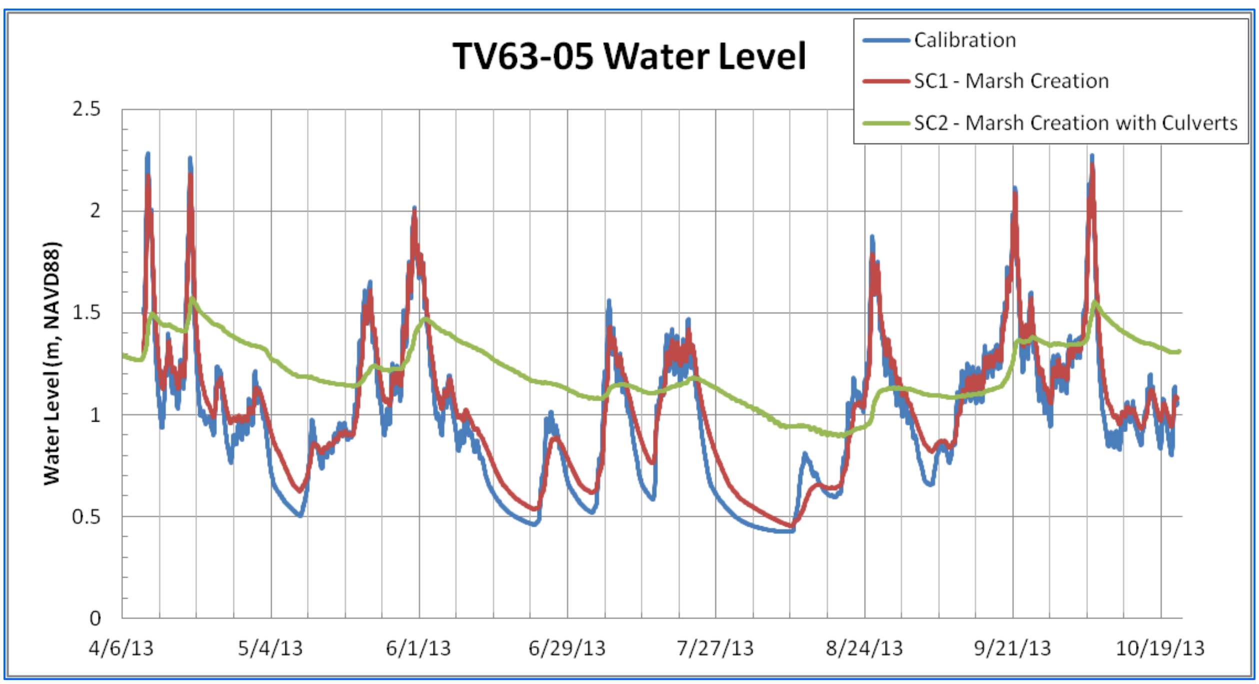

Figure 76 – Water levels at TV63-05 for Existing Conditions, Scenario 1, and Scenario 2. The flat parts of the Scenario line indicate when the point is dry.

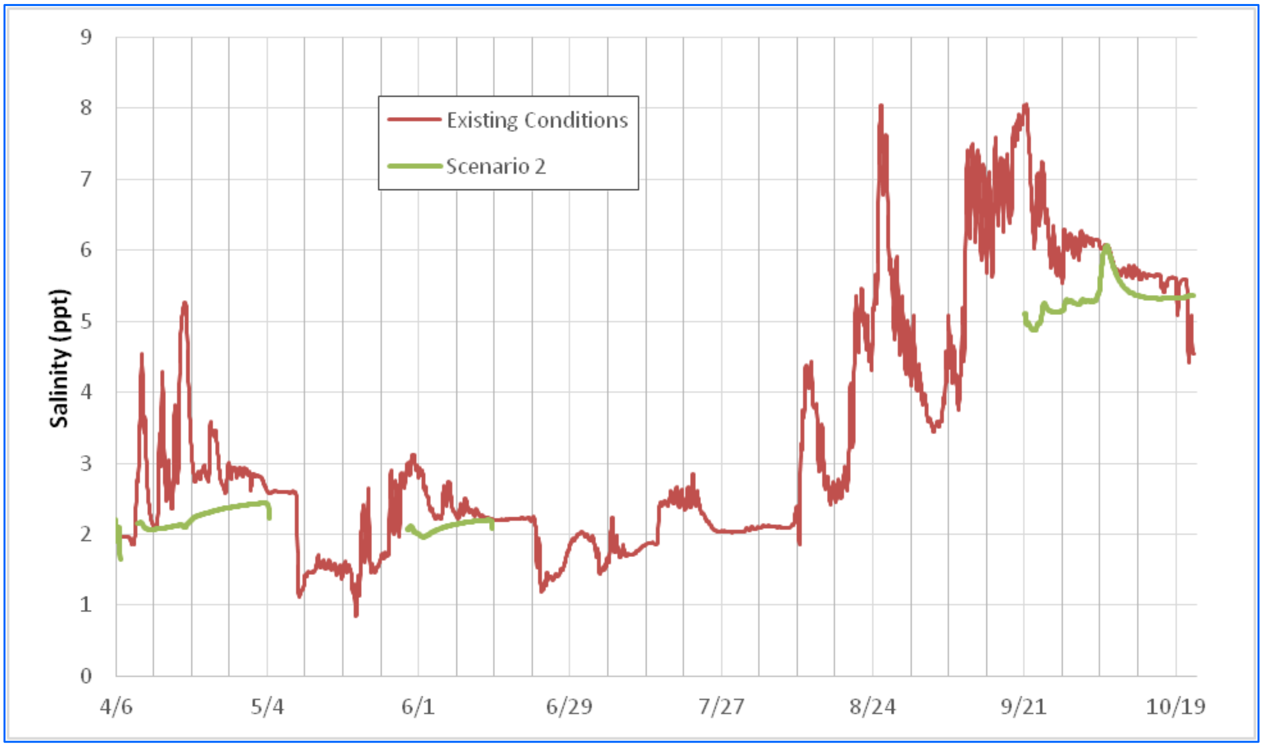

Figure 77 – Salinity at TV63-04 for Existing Conditions run and Scenario 2.

Figure 78 – Salinity at TV63-05 for Existing Conditions run and Scenario 2.

Flow

Flow into the marsh is governed by the head difference between the oil field canal water levels and the interior water levels, which is then converted to a discharge. The maximum head difference in this scenario was approximately 0.8 feet, which would lead to a flow of 8 cfs in each of the eight inflow culverts. The maximum head difference in the southern part of the model was approximately 2.9 feet, which leads to 31 cfs in each of the two outflow culverts. Average inflows are typically 0.5 -1 cfs per culvert and outflows 5.0 and 5.6 cfs in each culvert (**Table** 12). **Figure 79** shows a map of the net flow (which is also the average flow magnitude since flow is now one direction) and the percent change in flow magnitude as compared to Scenario 1 (no culverts). The magnitude of flow moving through the system is *much* less due to the comparatively small amount of flow passed through the culverts compared to the open breaches as in Scenario 1 (see culvert rating curves in figures Figure 71 and Figure 72).

The average inflow was computed to be 6.2 cfs, the outflow 10.6 cfs, and consequently the net flow 4.4 cfs out of the marsh.

Table 12 – Comparison of flows for Scenario 1 and Scenario 2. Marsh flow locations are noted, all others are breach/culvert flow locations. Note that for Scenario 1 there was no flow in arcs 14, 15, and 16 as there was no connection and that net flows for breach arcs in Scenario 2 are the same as the reported Avg. Q Mag.

	Scenario 1		**Scenario 2 - Full**		
Arc Number	Avg. Q Mag. (cfs)	Net Flow (cfs)	Avg. Q Mag. (cfs)	Net Flow (cfs)	Flow Mag. Pct. Diff.
1	21	0.1	1.0	--	-95%
2	42	-1.3	0.7	--	-98%
3	92	-9.0	0.8	--	-99%
4	58	-2.8	0.6	--	-99%
5	44	9.3	0.8	--	-98%
6	76	1.1	5.0	--	-93%
7	136	-10.9	0.8	--	-99%
8	59	5.1	68.4	--	15%
9 (marsh)	6	0.0	0.4	0.2	-93%
10 (marsh)	2	0.2	0.1	0.1	-95%
11 (marsh)	7	0.5	0.8	0.4	-89%
12 (marsh)	84	-4.1	1.8	1.8	-98%
13 (marsh)	19	-1.1	0.7	-0.7	-96%
14	N/A	N/A	0.5	--	N/A
15	N/A	N/A	1.0	--	N/A
16	N/A	N/A	5.6	--	N/A

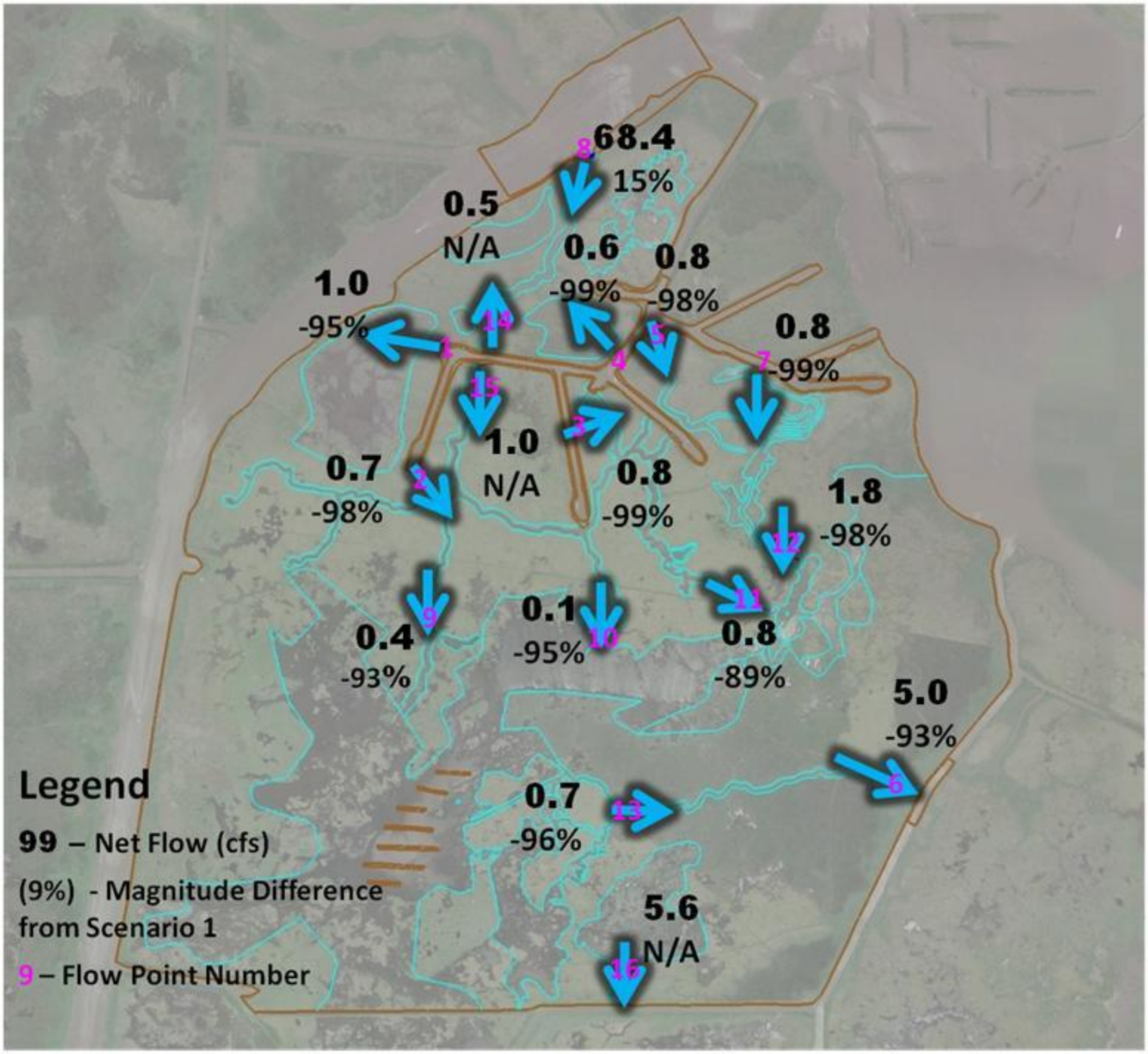

Figure 79 – Net flow (cfs) and change in flow magnitude compared to Scenario 1.

5.3 Scenario 3A: Marsh Creation with Additional Culverts

5.3.1 Objective

This objective of Scenario 3A (SC-3A), Marsh Creation with Culverts, Invert -2.0 feet, was to simulate the hydrodynamic response of the system to the creation of marsh within Cole's Bayou Marsh Project Area given 8 inflow culverts and 8 outflow culverts with inverts of -2.0 feet. The Scenario 2 model mesh (including the borrow channel surrounding the central marsh creation area) was used as the basis for this scenario. A channel connecting the open water area north of TV63-05 to the new outlet culvert complex on the McIlheny Canal was added. A new connection to Freshwater Bayou was created for the new, southwestern-most culvert complex. SC-3A has a total of eight flap-gate inflow culverts on the northern Oil Field Canals and eight flap-gate outflow culverts (four complexes of 2 culverts each) were placed on the southern boundary of the marsh model (**Figure 80**). Each culvert was specified as a 48-inch diameter corrugated HDPE pipe, 25-feet in length, with an invert of -2.0 feet. The difference between SC-3 and SC-3A is that the direction of the culvert at the northern intersection of the historic Cole's Bayou Channel and the Oil Field Canals (flow point 14 on Figure 93) has been reversed. In SC-3, the culvert allowed water to pass from the oil field canals into the Cole's Bayou Channel, from south to north. In SC-3A, water flows from the northern portion of the Cole's Bayou Channel to the oil field canals, from north to south. Results are only shown for SC-3A as this was the intended design.

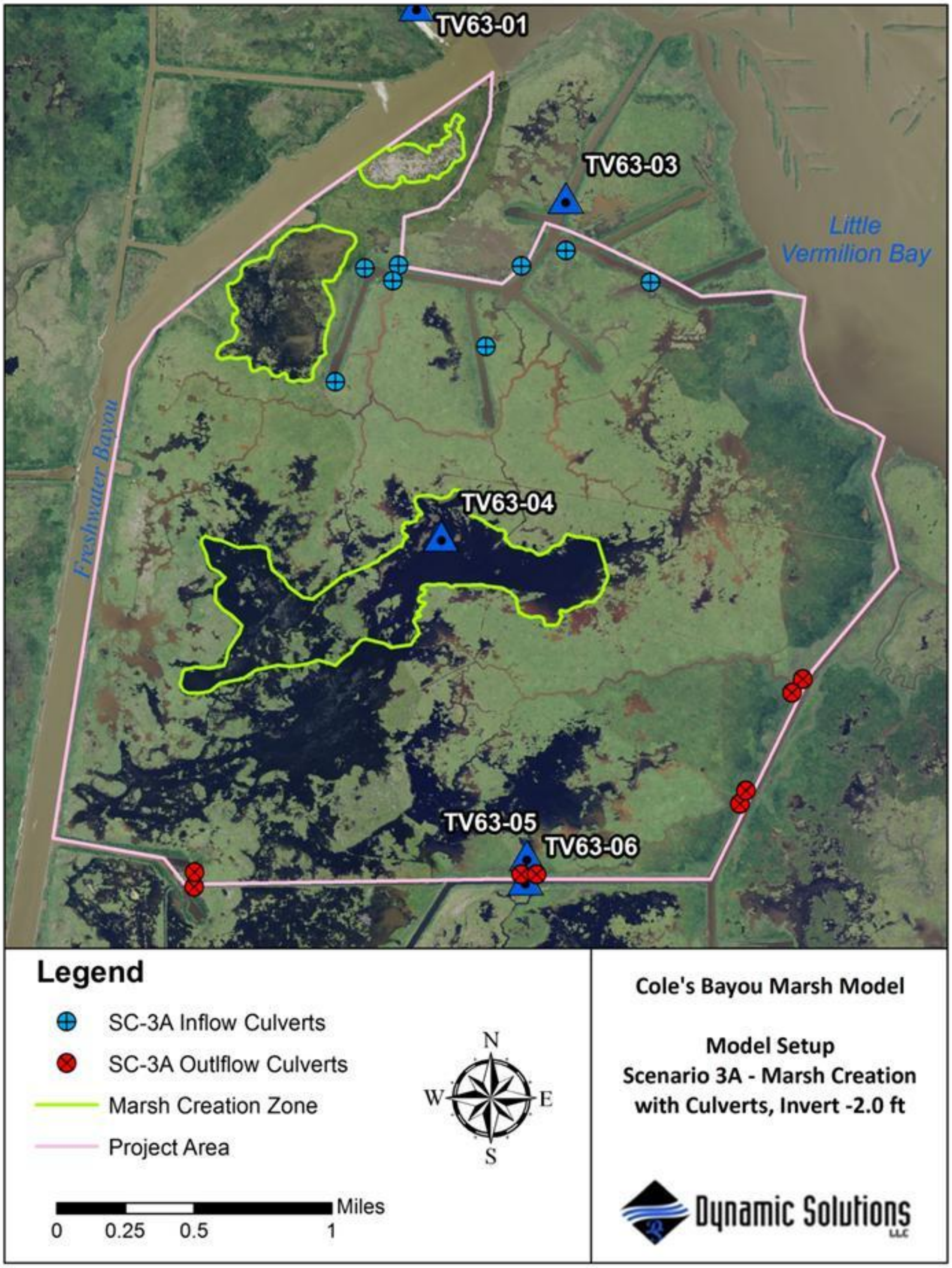

Figure 80 – Scenario 3A specifications including marsh creation areas and inlet and outlet culvert locations

5.3.2 Culvert Analysis

Curves relating head difference to discharge for these culverts was developed using the HEC-RAS model and checked using the USGS Culvert Analysis Program (CAP) model. ADH requires a head difference – discharge curve to utilize its hydraulic structure capabilities. Culvert hydraulics are very complex, and when a culvert is not submerged, the flow may be inlet controlled or outlet controlled. These conditions vary depending on inlet and outlet water surface elevations, among other factors, and the head difference – discharge curves are dependent on these conditions. A single head difference – discharge curve must be created for ADH to simulate the range of conditions which occurs in the model. The range of possible conditions was run in HEC-RAS and a family of head difference - discharge curves (**Figure 81**) was generated and adjusted to include the losses (provided by CPRA) of the duckbill flapgate. For nearly all conditions experienced, the culverts were tailwater controlled. To conservatively estimate flows, the head difference – discharge curve for 25% exceedance water level at the culvert tailwater was selected to simulate culvert flow for all stage conditions. Curves for the inflow culverts were based on a tailwater condition of 0.56 feet, the 25% exceedance elevation at TV63-04. Curves for the outflow culverts were based on a tailwater condition of 0.22 feet, the 25% exceedance elevation at TV63-06. The head difference – discharge relationship for the outflow culverts was calculated for each complex of 2 culverts (4 complexes = 8 total culverts) so any hydraulic effects of the configuration were realized. The head difference – discharge relationship for the inflow (northern) culverts is shown in **Figure 82**, and the for the outflow (southern) culverts in **Figure 83**.

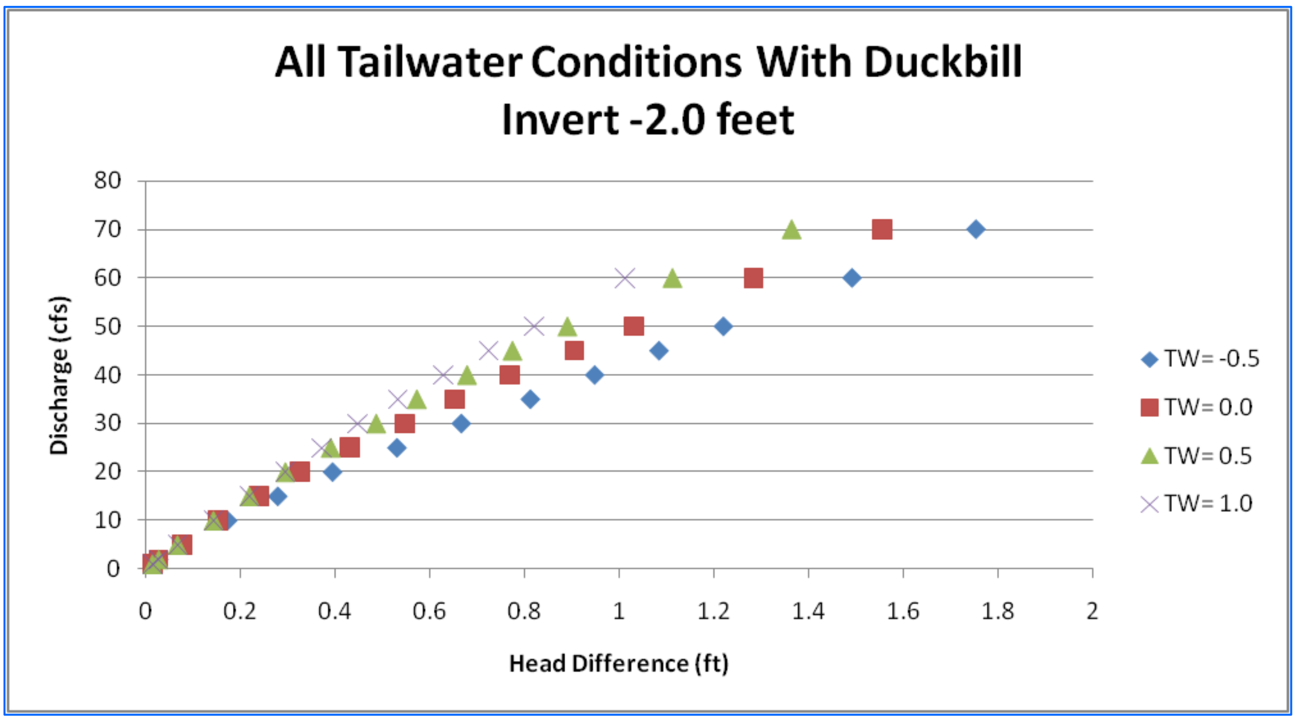

Figure 81 – Discharge as a function of head difference across the culvert for a range of tailwater conditions.

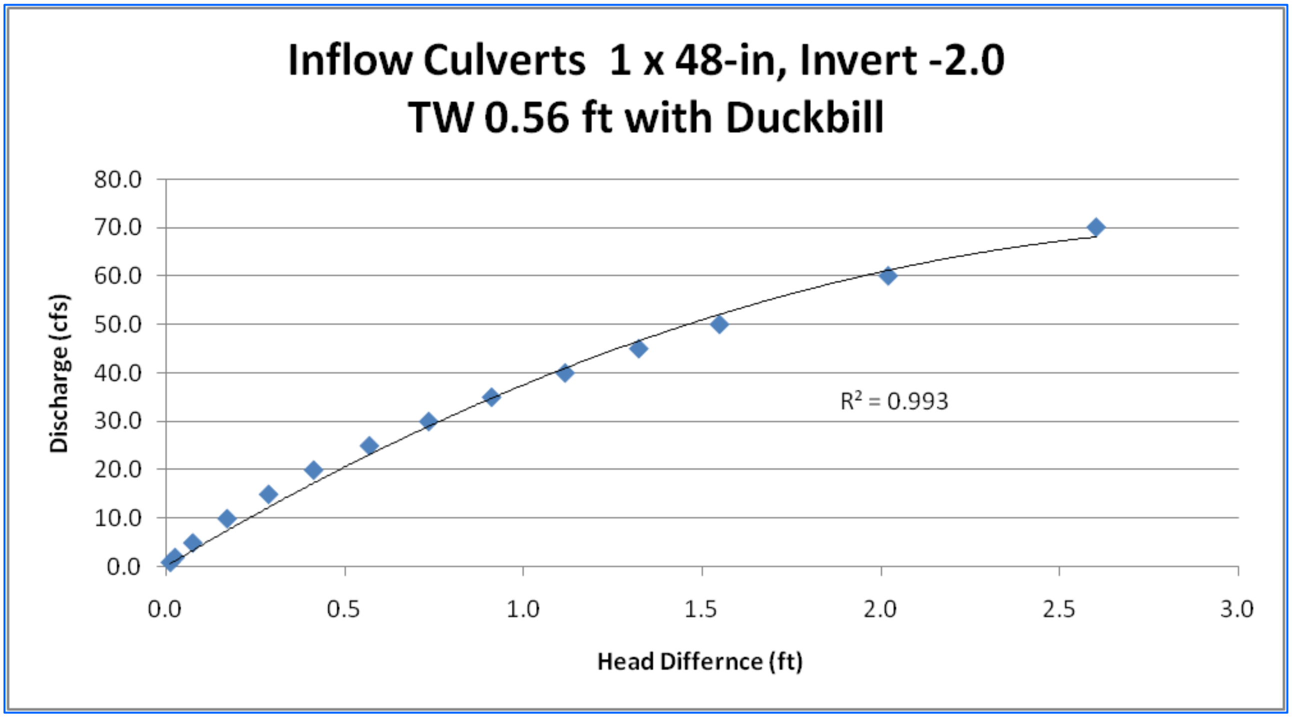

Figure 82 – Discharge as a function of head difference for the inflow culverts given a tailwater elevation of 0.56 feet.

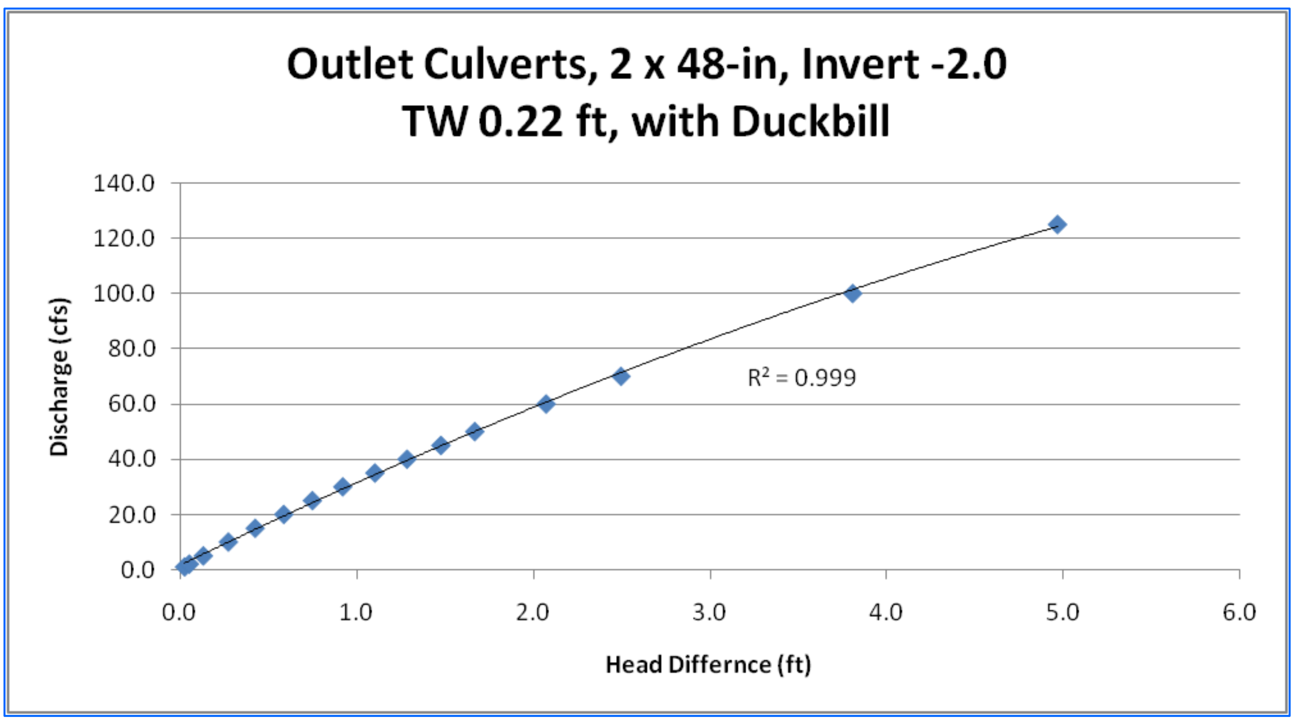

Figure 83 – Discharge as a function of head difference for each outflow culvert complex (2 culverts side-by-side) given a tailwater elevation of 0.22 feet.

5.3.3 Results

The following results are for the full simulation period, April 6 to October 21, 2013.

Water Level

Median water levels in the marsh were almost unchanged from 0.99 feet in SC-1 to 1.02 feet for SC-3A. **Table 13** shows the median water level when inundated and the percentage of time each point of interest (POI) was inundated. The inundation percentages are also presented on for selected points on **Figure 84** and for the entire marsh on **Figure 85**.

Table 13 – Water level comparison for Scenario 1, Scenario 2, and Scenario 3A

		Scenario 1		**Scenario 2 - Full**		**Scenario 3A - Full**	
Location	Point Elev (ft)	Median Stage (ft)	Pct Inundated	Median Stage (ft)	Pct Inundated	Median Stage (ft)	Pct Inundated
TV63-04	1.30	1.39	27%	1.37	35%	1.39	17%
TV63-05	-0.92	0.99	100%	1.18	100%	0.95	100%
Cent-East	1.30	1.47	22%	1.37	36%	1.37	18%
Cent-West	1.30	1.45	21%	1.37	38%	1.37	18%
NW	1.30	1.32	51%	1.30	100%	1.30	73%
North	1.30	1.43	28%	1.37	31%	1.36	31%
SW	-1.31	0.99	100%	1.18	100%	0.97	100%
N-Marsh	0.98	1.31	38%	1.21	56%	1.22	52%
CentW-Marsh	0.89	1.12	65%	1.18	100%	1.13	61%
CentE-Marsh	0.98	1.21	46%	1.21	91%	1.18	53%
E-Marsh	0.92	1.15	56%	1.18	97%	1.14	58%
SE-Marsh	1.08	1.24	43%	1.22	84%	1.29	34%
S-Marsh	0.89	1.14	62%	1.18	100%	1.14	57%
SW-Marsh	0.62	1.03	88%	1.18	100%	1.08	73%

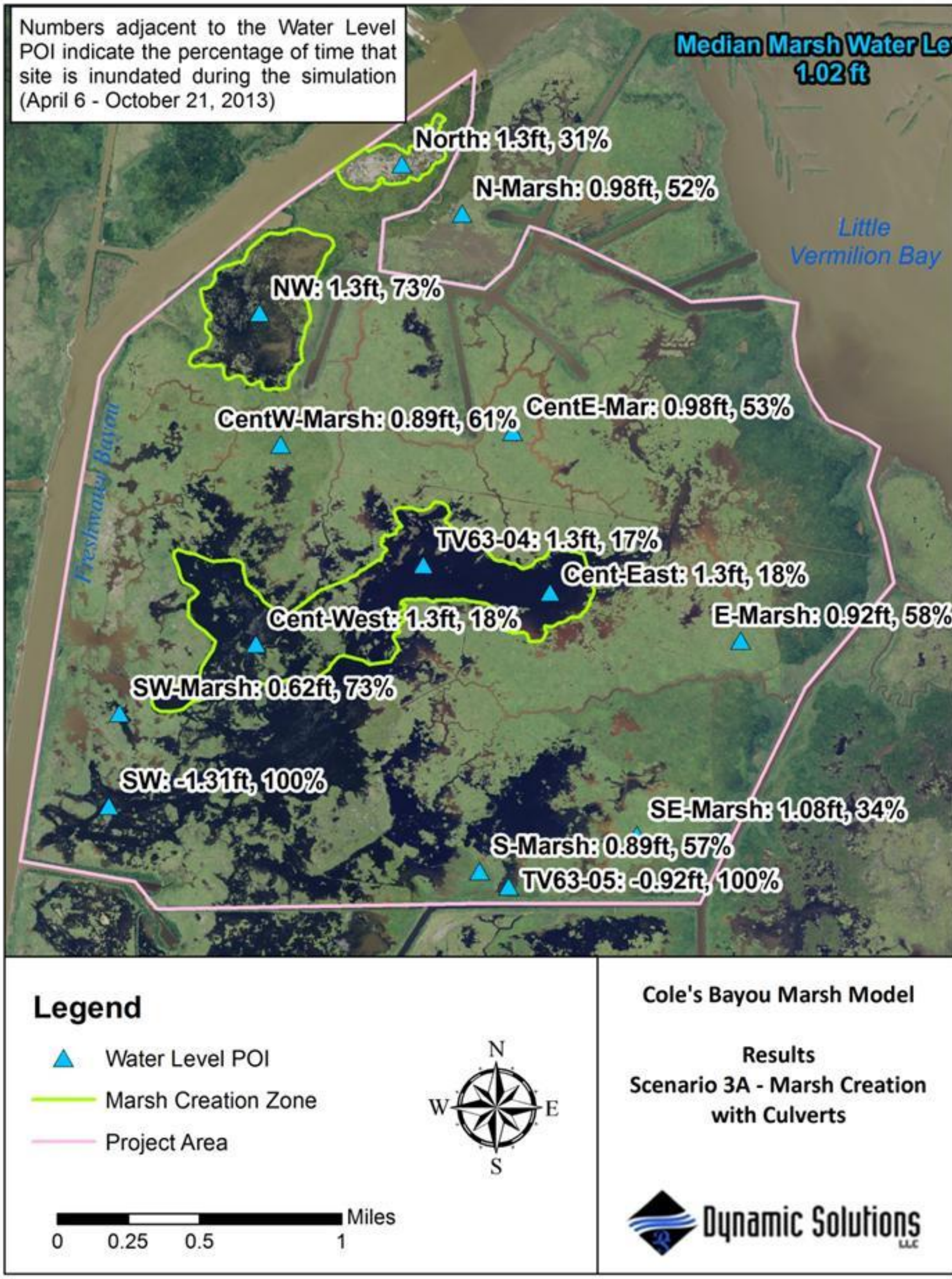

Figure 84 – Scenario 3A water level results

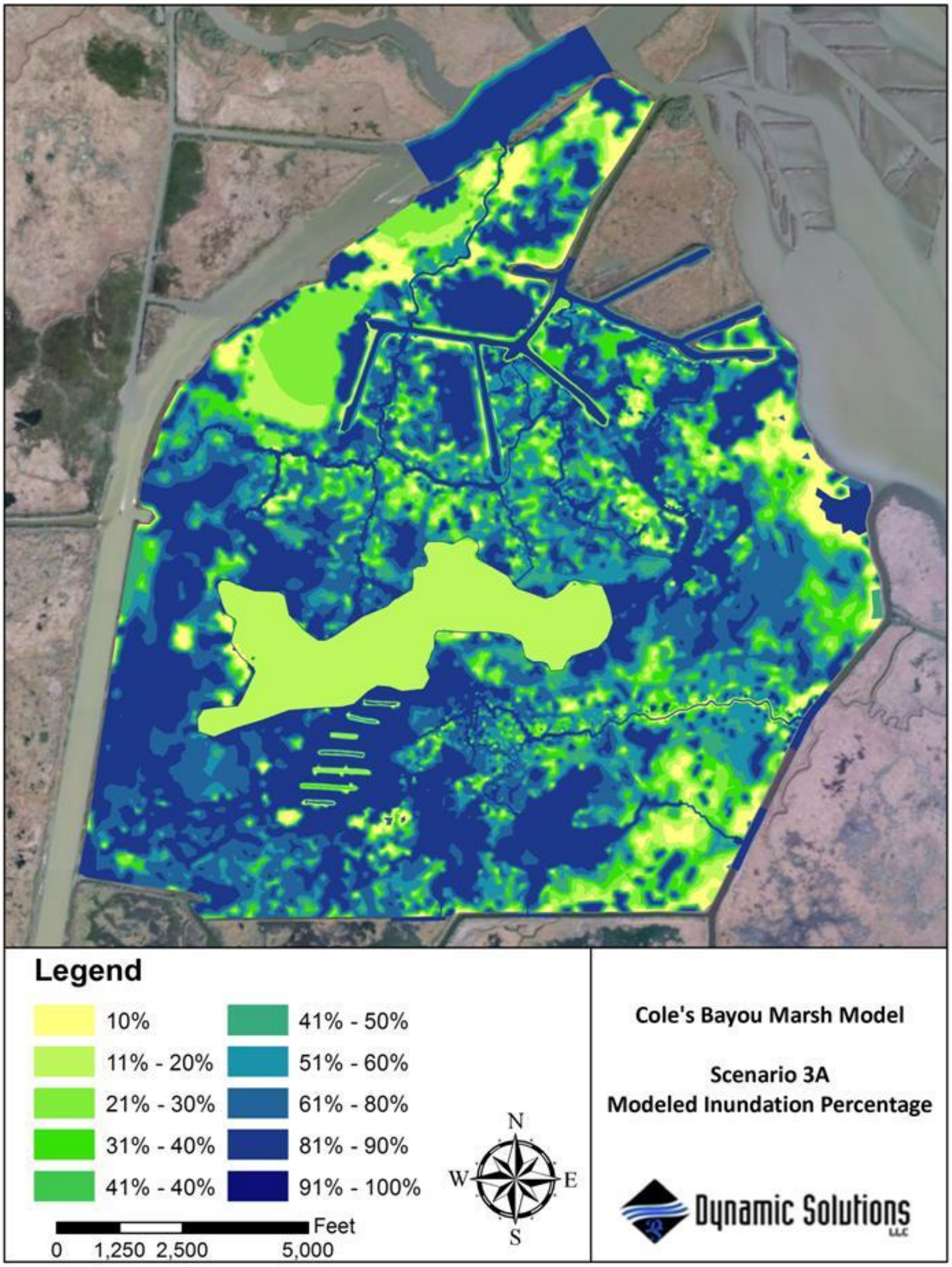

Figure 85 – Inundation frequency for Scenario 3A

Figure 86 and **Figure 87** show the water level time series at TV63-04 and TV63-05 for existing conditions, Scenario 1, Scenario 2, and Scenario 3A. It shows that water levels vary much less in Scenario 2, with much lower peaks. In Scenario 3A, the water levels rise and fall much more steeply than Scenario 2. At TV63-05, the water level falls to much lower levels in Scenario 3A than in previous models due to the increased connectivity to the open waters outside the south end of the marsh.

Figure 88, Figure 89, and **Figure 90** show the water levels at the CentW-Marsh, E-Marsh, and SW-Marsh points for existing conditions, Scenario 1, Scenario 2, and Scenario 3A. The figures show that at these locations, there is little change in water levels from the existing conditions to Scenario 1. Scenario 2 holds more water than Scenario 1 but greatly attenuates the peaks in water levels. Scenario 3A holds less water and attenuates the peaks in water level less than Scenario 2.

Salinity

Salinity values for Scenario 3A exhibit the same trend as those in the Existing Conditions model. **Figure 91** and Figure 92 show the salinity time series at stations at stations TV63-04 and TV63-05 for Existing Conditions and Scenario 2. Salinity values at TV63-04 are somewhat higher when the marsh is wet. At TV63-05 salinity values are typically with 1 ppt of those during the Existing conditions run.

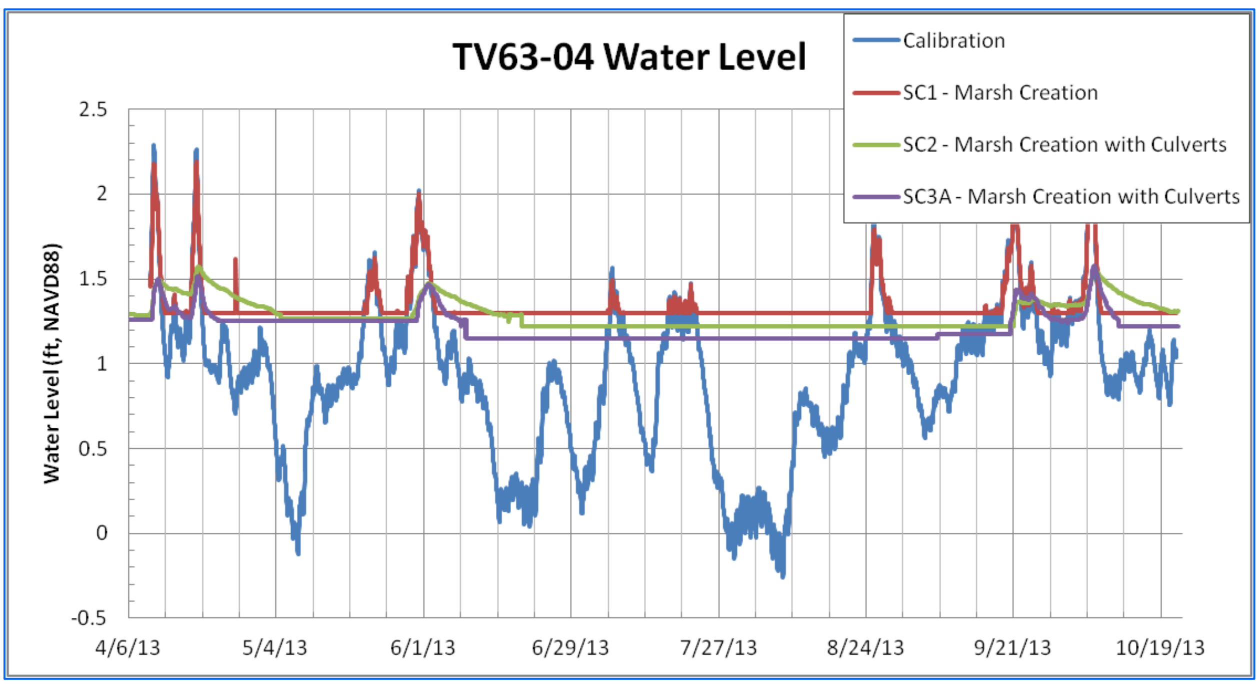

Figure 86 – Water levels at TV63-04 for Existing Conditions, Scenario 1, Scenario 2, and Scenario 3A. The flat parts of the Scenario line indicate when the point is dry.

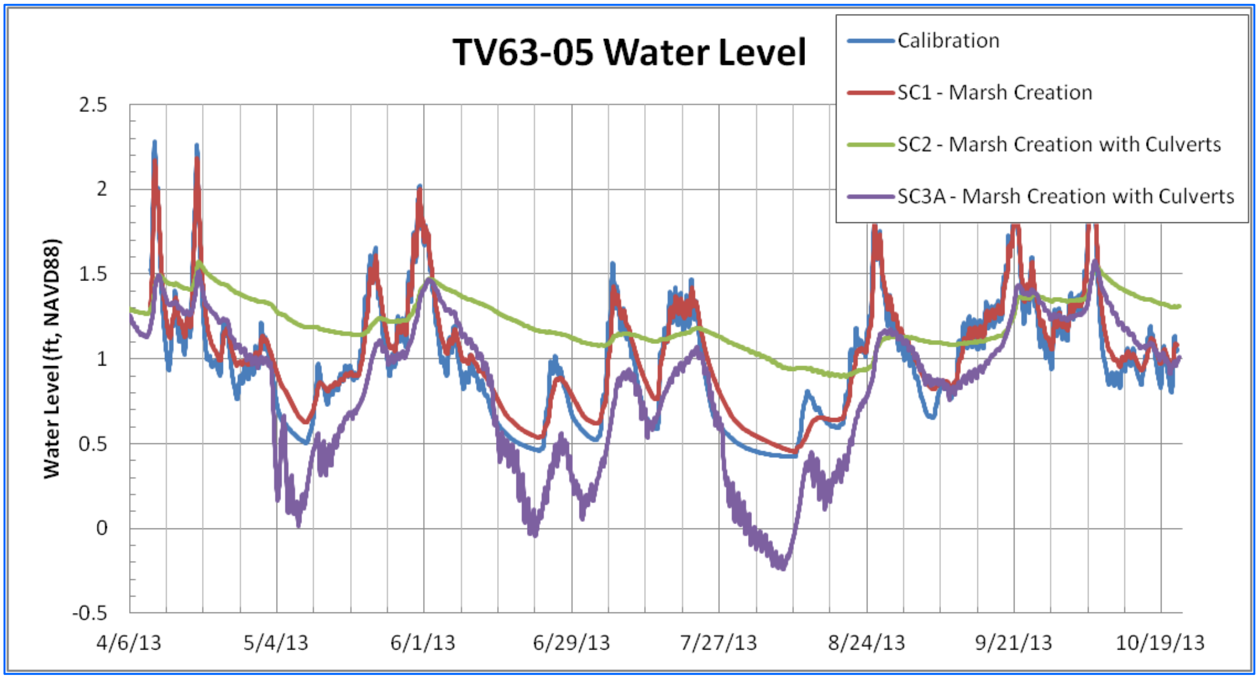

Figure 87 – Water levels at TV63-05 for Existing Conditions, Scenario 1, Scenario 2, and Scenario 3A

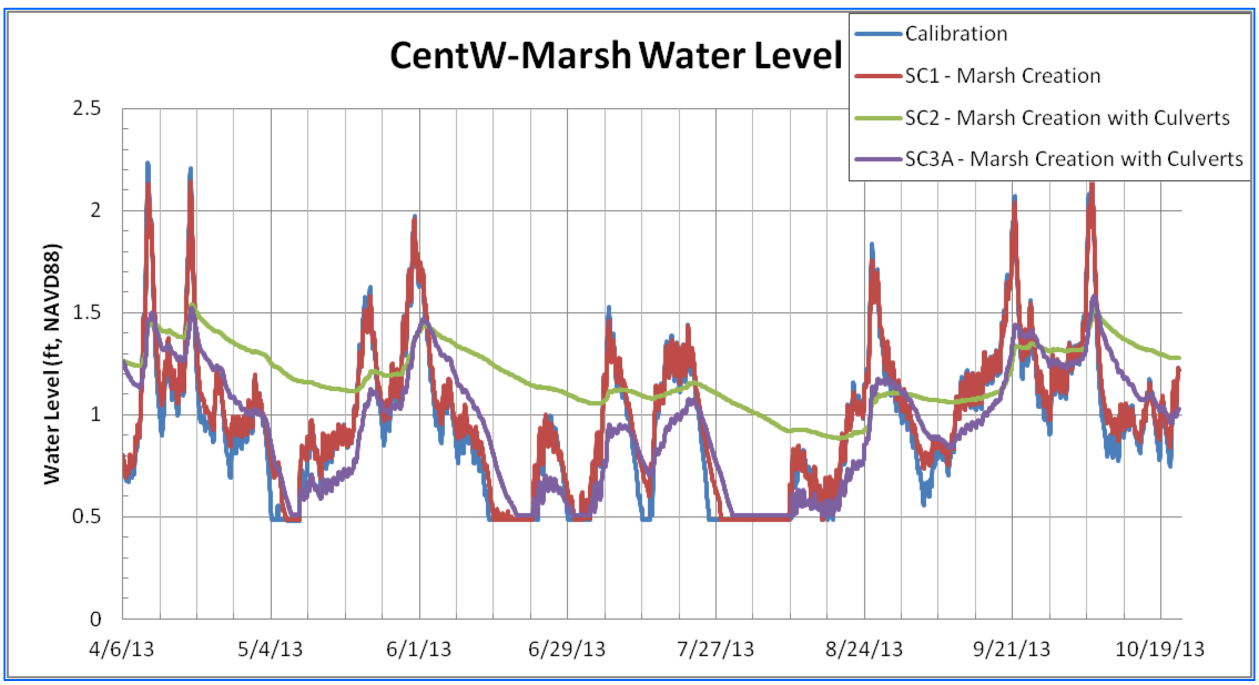

Figure 88 – Water levels at CentW-Marsh for Existing Conditions, Scenario 1, Scenario 2, and Scenario 3A. The flat parts of the Scenario line indicate when the point is dry.

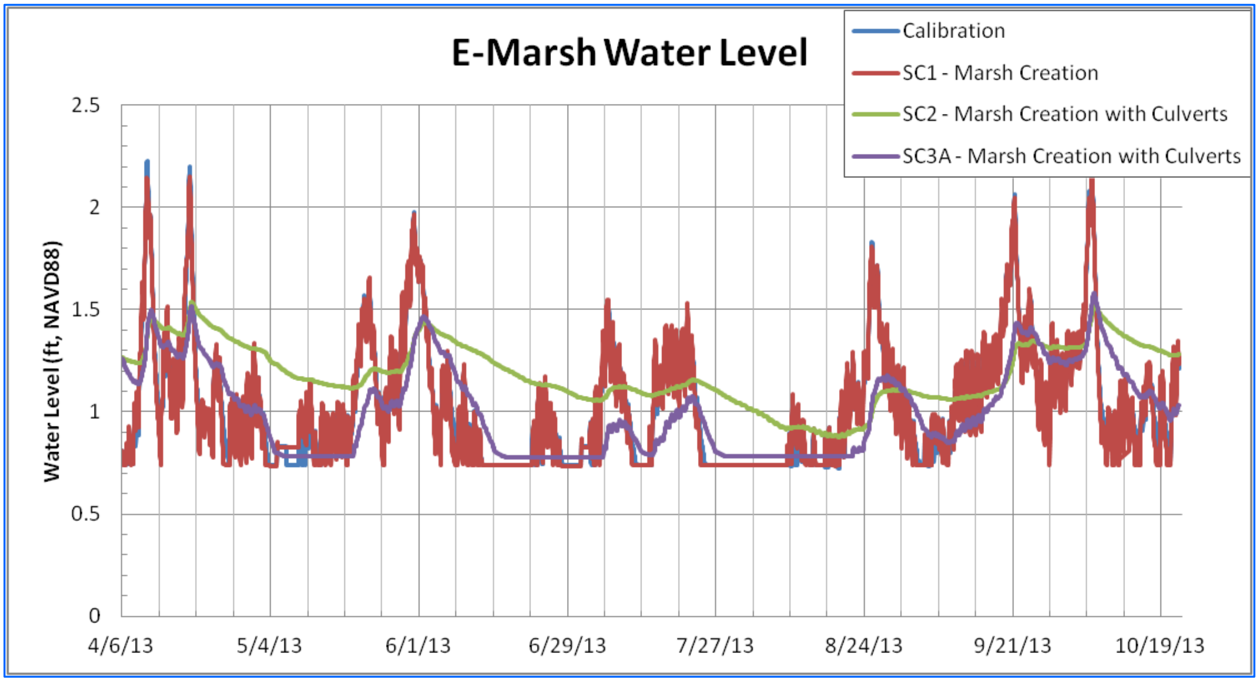

Figure 89 – Water levels at E-Marsh for Existing Conditions, Scenario 1, Scenario 2, and Scenario 3A. The flat parts of the Scenario line indicate when the point is dry.

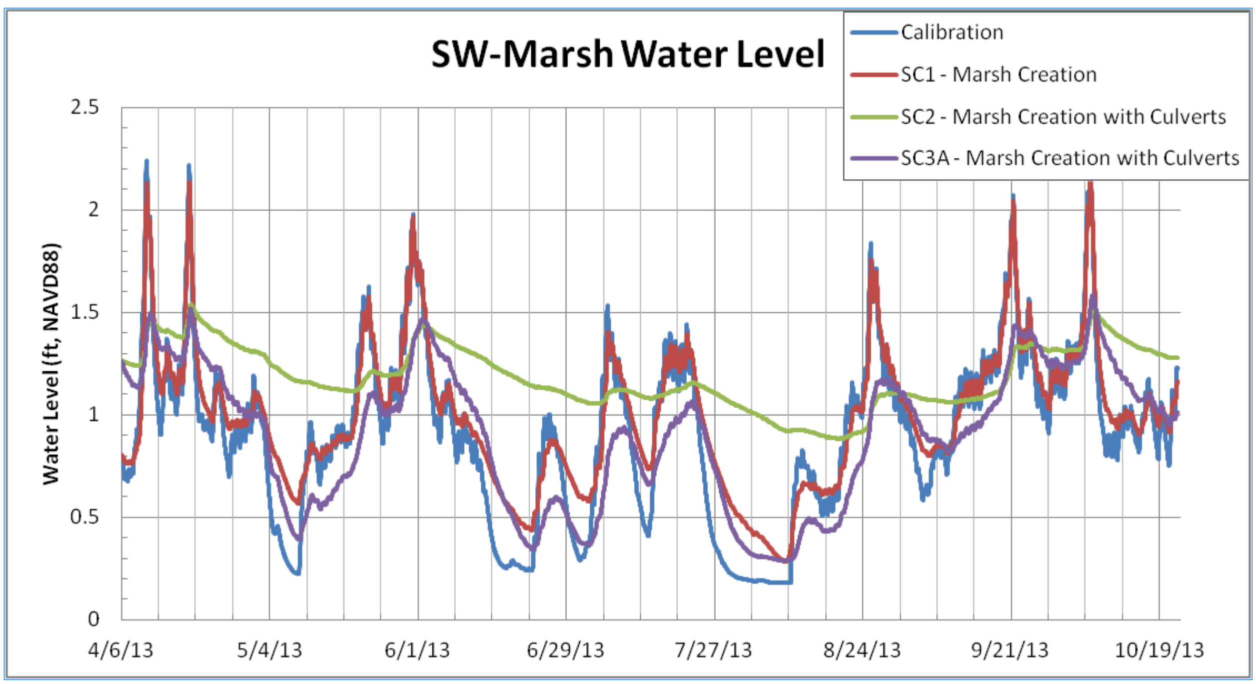

Figure 90 – Water levels at SW-Marsh for Existing Conditions, Scenario 1, Scenario 2, and Scenario 3A. The flat parts of the Scenario line indicate when the point is dry.

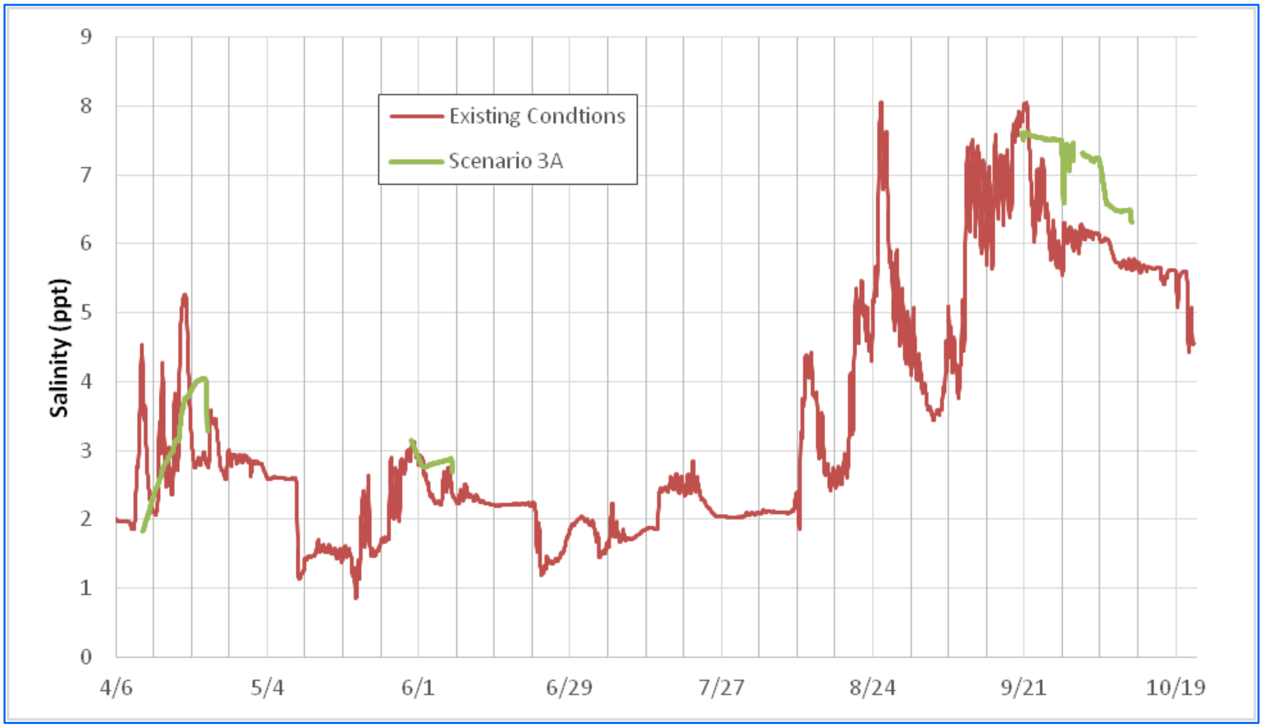

Figure 91 – Salinity at TV63-04 for Existing Conditions run and Scenario 3A.

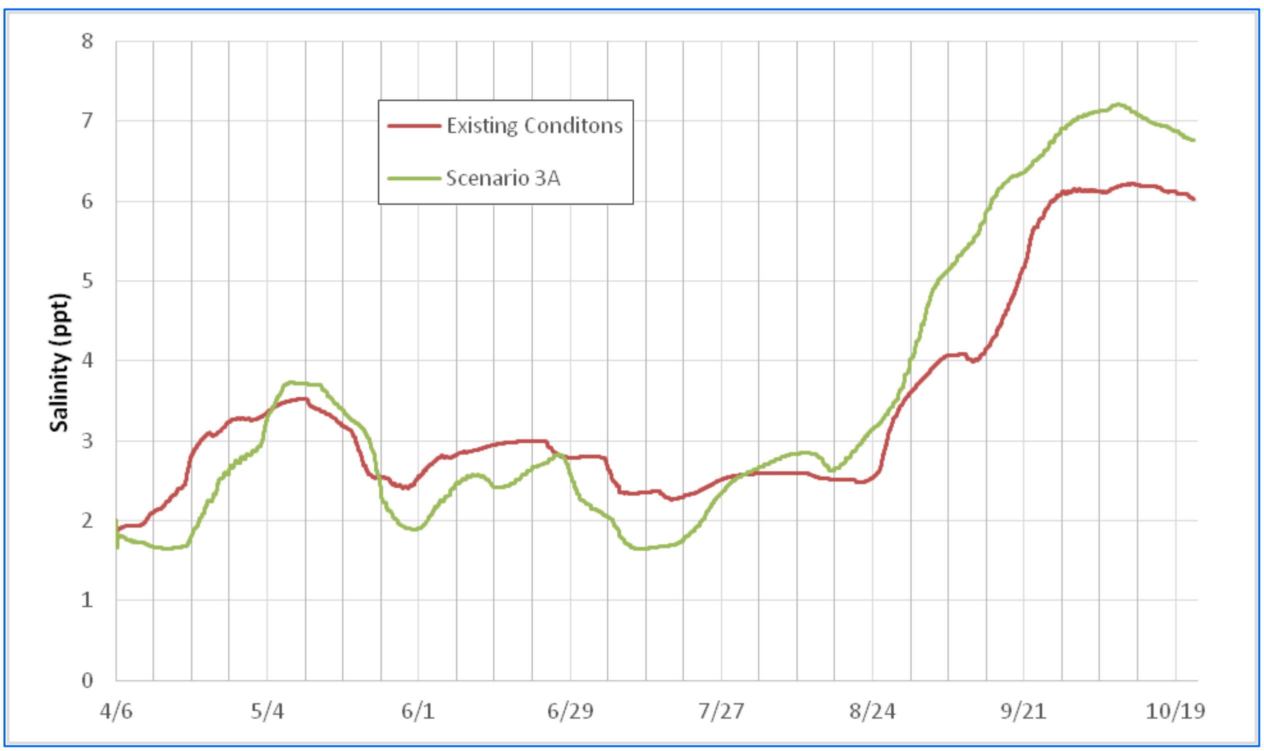

Figure 92 – Salinity at TV63-05 for Existing Conditions run and Scenario 3A.

Flow

Flow into the marsh is governed by the head difference between the oil field canal water levels and the interior water levels, which is then converted to a discharge. The maximum head difference in this scenario was approximately 0.8 feet, which would lead to a flow of 31 cfs in each of the eight inflow culverts. The maximum head difference in the southern part of the model was approximately 2.4 feet, which leads to 69 cfs in each of the four outflow culvert complexes (**Table 14**). Average inflows are typically 4.8 cfs per culvert and outflows are 4.8 cfs per culvert (9.6 cfs per complex). **Figure 93** shows a map of the average flow magnitude and the percent change in flow magnitude as compared to Scenario 1 (no culverts). The magnitude of flow moving through the system is *much* less due to the comparatively small amount of flow passed through the culverts compared to the open breaches as in Scenario 1 (see culvert rating curves in Figures 3 and 4). The new connections at the south end of the marsh in Scenario 3A increase the flows over Scenario 2 while still below Scenario 1.

The average inflow was computed to be 40.5 cfs, the outflow 43.8 cfs, and consequently the net flow 3.3 cfs out of the marsh.

Table 14 – Comparison of flows for Scenario 1, Scenario 2, and Scenario 3A. Marsh flow locations are noted, all others are breach/culvert flow locations. Note that for Scenario 1 there was no flow in arcs 14, 15, 16, 17, or 18 as there was no connection and that net flows for breach arcs in Scenario 3A are the same as the reported Avg. Q Mag.

	Scenario 1		Scenario 2 - Full		Scenario 3A - Full		SC3A
Arc Number	Avg. Q Mag. (cfs)	Net Flow (cfs)	Avg. Q Mag. (cfs)	Net Flow (cfs)	Avg. Q Mag. (cfs)	Net Flow (cfs)	Flow Mag. Pct. Diff.
1	21	0.1	1.0	--	2.7	--	-87%
2	42	-1.3	0.7	--	4.4	--	-89%
3	92	-9.0	0.8	--	5.7	--	-94%
4	58	-2.8	0.6	--	2.8	--	-95%
5	44	9.3	0.8	--	4.9	--	-89%
6	76	1.1	5.0	--	7.9	--	-90%
7	136	-10.9	0.8	--	6.4	--	-95%
8	59	5.1	68.4	--	61.1	--	3%
9 (marsh)	6	0.0	0.4	0.2	1.8	1.8	-69%
10 (marsh)	2	0.2	0.1	0.1	1.5	1.2	-39%
11 (marsh)	7	0.5	0.8	0.4	2.6	2.5	-65%
12 (marsh)	84	-4.1	1.8	1.8	10.3	10.2	-88%
13 (marsh)	19	-1.1	0.7	-0.7	3.1	-2.6	-84%
14	N/A	N/A	0.5	--	5.2	--	N/A
15	N/A	N/A	1.0	--	6.5	--	N/A
16	N/A	N/A	5.6	--	10.2	--	N/A
17	N/A	N/A	N/A	N/A	9.0	--	N/A
18	N/A	N/A	N/A	N/A	11.5	--	N/A

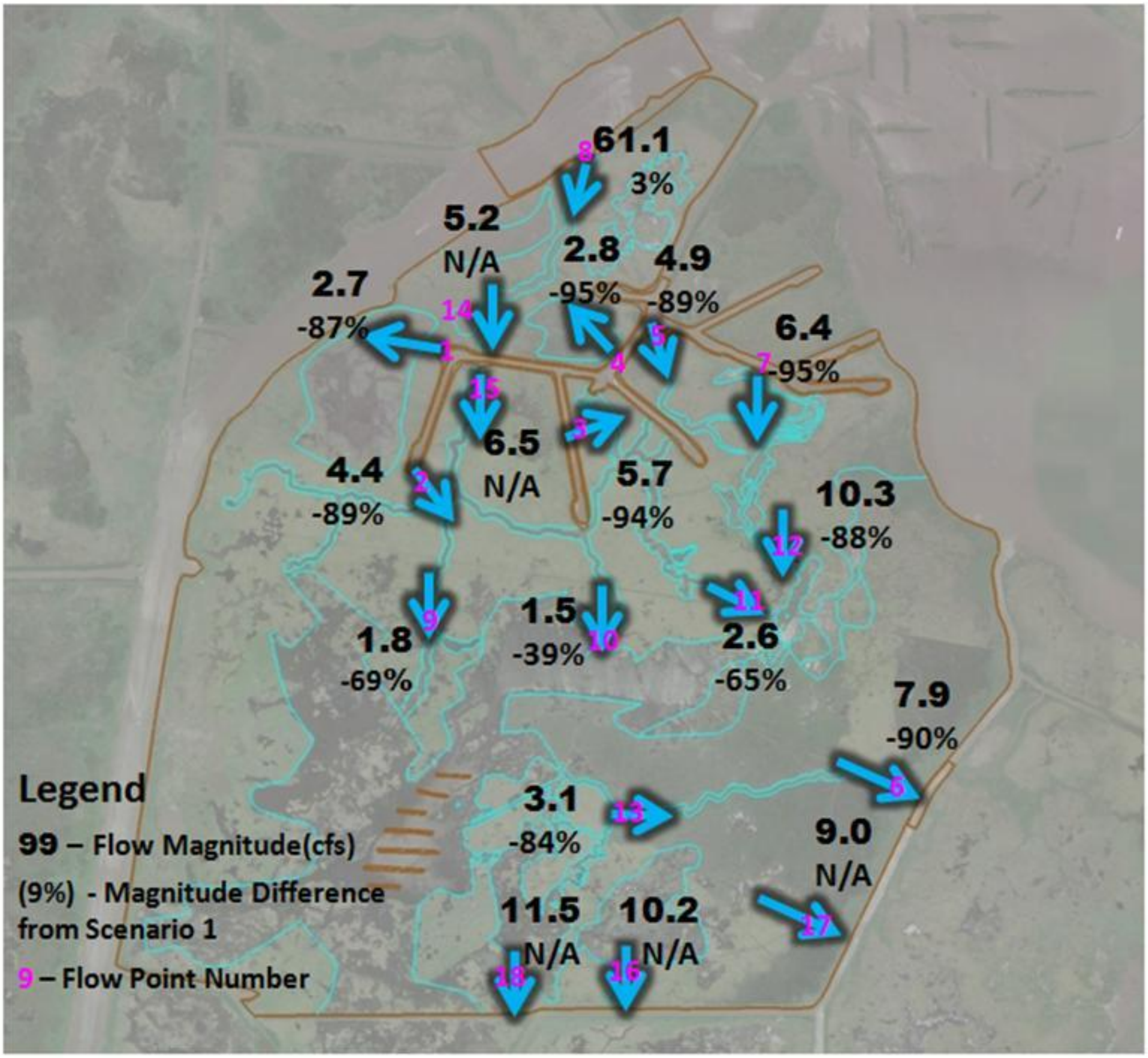

Figure 93 – Flow magnitude (cfs) and change compared to Scenario 1.

SECTION 6 CONCLUSIONS

A two-dimensional ADH hydrodynamic model of the Cole's Bayou Marsh and Vermilion Bay was developed and calibrated. A nested model framework was utilized to allow the flexibility and added understanding from the larger Vermilion Bay domain but significantly lowered the computational burden when running simulations focused on the Cole's Bayou Marsh proper. The model is valid for normal environmental conditions and care should be taken in using it for modeling extreme events.

The Vermilion Bay model was calibrated for water level and salinity at five stations. Targets for RMS error or relative RMS error were met at each station. RMS errors for the Cole's Bayou Marsh model were small at both stations and the calibration is considered very good. Flows modeled within the system were compared to those measured, and observed, during a single field study and found to match reasonably well. The models are sufficient to test how modifications to the system will affect hydrodynamics within the marsh.

As with any model, results should be used wisely. The model is calibrated for two stations within the marsh, TV63-04 in the central open water area and TV63-05 in an open water area in the southern part of the marsh. The project area is a maze of smaller channels, potholes, and rivulets which are hydraulically connected by surface and near-surface waters. The elevation survey could not account for every hydraulic connection and there are significant expanses of higher marsh areas which were not surveyed as part of this study. Caution should be used if extracting data for specific points within the domain where data is sparse.

Alterations were made to the model to test the hydrodynamic effects of potential future restoration efforts. Scenarios included the effects of marsh restoration (land building) and the installation of one-way culverts to control inflow and outflow from the project area. The culverts were modeled in HEC-RAS and a stage-discharge curve generated use in the ADH model. Scenario results can be used to evaluate **changes** in inundation, flows, and salinity within the marsh. Caution should be used when reaching for absolute prognostic values for discharge and salinity. The average inflow, outflow and net flow for the Cole's Bayou Marsh area, including flow from Freshwater Bayou into Cole's Bayou, are shown in

Table 15**.**

Table 15 – Average inflow, outflow, and net flow for the Cole's Bayou Marsh (negative numbers for net flow indicate overall outflow from the system)

Model Run	Average Inflow (cfs)	Average Outflow (cfs)	Net Flow (cfs)
Existing Conditons	19.8	23.9	-4.1
Scenario 1	15.9	19.6	-3.7
Scenario 2	6.2	10.6	-4.4
Scenario 3A	40.5	43.8	-3.3

The Vermilion Bay model offers valuable insight for hydrodynamic, ecological, or shoreline protection studies in and around the Bay. It will also be an excellent starting point for any other modeling studies in the area.

ADH was proven to be a useful tool to handle the complexities offered in this application. Great differences in scale, plenty of wetting and drying, and hydraulic structures all present challenges to two-dimensional models and were resolved with ADH. The model does a good job of representing processes in the system and can provide vital insights to the inundation and circulation patterns of water within the marsh. It also allows scientists and managers to asses potential changes to the system to accomplish the stated goals of hydrologic and marsh restoration.

SECTION 7 REFERENCES

Aquaveo (2010), Surface Water Modeling System, www.aquaveo.com

Berger, R.C; Tate, J.N.; Brown, G.L. and Savant, G (2010), Adaptive Hydraulics- USERS MANUAL: Guidelines for Solving Two Dimensional Shallow Water Problems with the Adaptive Hydraulics Modeling System, US Army Corps of Engineers – ERDC Coastal Hydraulics Lab.

Chow, V.; Maidment, D. R.; and Mays, L. W. (1988) Applied Hydrology, McGraw-Hill.

Dietrich, J.C., M. Zijlema, J.J. Westerink, L.H. Holthuijsen, C. Dawson, R.A. Luettich Jr., R.E. Jensen, J.M. Smith, G.S. Stelling, G.W. Stone (2011) Modeling hurricane waves and storm surge using integrally-coupled scalable computations, *Coastal Engineering*, 58, 45-65.

Feng, Z., 2009. Hydrodynamic Response to Cold Fronts Along the Louisiana Coast, Thesis: Louisiana State University, 120pp.

Letter, Joseph V. (1993) Grand and White Lakes Flood Control Project, US Army Corps of Engineers, Waterways Experiment Station, Technical Report HL-93-11.

LSU CADGIS Research Laboratory, "Atlas: The Louisiana Statewide GIS." *www.atlas.lsu.edu*

Morton, R.A. and Barras, J.A., 2011. Huricane impacts on coastal wetlands: a half-century record of storm-generated features from southern Louisiana. *Journal of Coastal Research*, 27(6A), 27-43.

Rodi, W. (1984) Turbulence Models and their Applications in Hydraulics – A State of the Art Review. International Association for Hydraulics Research.

Rouse, Larry J. Jr.; Wiseman, William J. Jr.; Inoue, Masamichi (2005) Aspects of the Louisiana Coastal Current, LSU Coastal Marine Institute, 50 pp.

Savant, Gaurav; Berger, Charlie; McAlpin, Tate O. and Tate, Jennifer N (2010). "An Efficient Implicit Finite Element Hydrodynamic Model for Dam and Levee Breach". Journal of Hydraulic Engineering,Vol 137, No 9, 2011, PP-1005-1018